







EX LIBRIS  
UNIVERSITATIS  
ALBERTENSIS


---

The Bruce Peel  
Special Collections  
Library









Digitized by the Internet Archive  
in 2025 with funding from  
University of Alberta Library

<https://archive.org/details/0162012647556>







UNIVERSITY OF ALBERTA

LIBRARY RELEASE FORM

Name of Author:

**William Kwesi Amenyah**

Title of Thesis:

**Interior Cracking of a Circular Inclusion with  
Imperfect Interface Under Thermal and  
Mechanical Loading**

Degree:

**Master of Science**

Year this Degree is Granted:

**2001**

Permission is hereby granted to the University of Alberta Library to reproduce single copies of this thesis and to lend or sell such copies for private, scholarly or scientific research purpose only.

The author reserves all other publication and other rights in association with the copyright in the thesis, and except as herein provided, neither the thesis nor any substantial portion thereof may be printed or otherwise reproduced in any material form whatever without the author's prior written consent.







UNIVERSITY OF ALBERTA

**INTERIOR CRACKING OF A CIRCULAR INCLUSION WITH  
IMPERFECT INTERFACE UNDER THERMAL AND  
MECHANICAL LOADING**

BY

**WILLIAM KWESI AMENYAH**



A Thesis submitted to the Faculty of Graduate Studies and Research in partial fulfillment  
of the requirements for the degree of Master of Science

Department of Mechanical Engineering

Edmonton, Alberta

Fall 2001





UNIVERSITY OF ALBERTA

FACULTY OF GRADUATE STUDIES AND RESEARCH

The undersigned certify that they have read, and recommend to the Faculty of Graduate Studies and Research for acceptance, a thesis entitled **Interior Cracking of a Circular Inclusion with Imperfect Interface Under Thermal and Mechanical Loading** submitted by William Kwesi Amenyah in partial fulfillment of the requirements for the degree of Master of Science.





This dissertation is dedicated to my son, *Gerald Selassie Amenyah*

"Any field of research contains only a few really important ideas; the remainder of the research concerns extensions and applications of these ideas" – **G. M. L. Gladwell**, 6<sup>th</sup> International Conference of IMSE, Banff, Alberta, Canada , June 12 –15, 2000.





# ABSTRACT

A semi-analytic solution is developed to determine the effect of an imperfect interface on the stress field inside a circular elastic inclusion containing a pre-existing interior radial crack, subjected to thermal or mechanical loading. The inclusion is surrounded by an infinite matrix and the inclusion-matrix interface is assumed to be homogeneously imperfect. This is characterized by continuity of tractions and discontinuity of displacements across the interface.

Using complex variable methods, series representations of the stress functions inside the circular inclusion and the surrounding matrix are derived. The governing boundary value problem is formulated in such a way that these stress functions simultaneously satisfy the traction free condition along the crack face, the imperfect interface conditions and the prescribed asymptotic conditions.

The method is illustrated for a number of crack-inclusion geometries and shear moduli ratios. Explicit values of the stress intensity factor at the crack tips are presented.





# ACKNOWLEDGEMENTS

I wish to gratefully acknowledge the guidance and unflinching support of my supervisors Dr. Peter Schiavone and Dr. Chongqing Ru and the help and advice given by Dr. Andrew Mioduchowski, as a result of which this dissertation has been accomplished.

I would also like to express my appreciation to my wife, Aretha for her love and encouragement.

William Amenyah

Edmonton, AB.

April 2001



# TABLE OF CONTENTS

<b>1</b>	<b>INTRODUCTION.....</b>	<b>1</b>
1.1	COMPOSITE MATERIALS.....	1
1.2	FIBER-REINFORCED COMPOSITES.....	3
1.3	INTERPHASE LAYER .....	3
1.3.1	<i>Perfect bonding</i> .....	6
1.3.2	<i>Imperfect bonding</i> .....	6
1.4	FIBER- CRACKING .....	8
1.5	BACKGROUND AND OUTLINE OF STUDY .....	9
<b>2</b>	<b>FORMULATION OF THE BOUNDARY VALUE PROBLEM.....</b>	<b>12</b>
2.1	INTRODUCTION .....	12
2.2	DESCRIPTION OF THE PROBLEM .....	13
2.3	INTERFACE CONDITIONS IN TERMS OF STRESS POTENTIALS .....	16
2.4	SERIES REPRESENTATION OF STRESS POTENTIALS.....	19
2.4.1	<i>Determination of <math>\phi_1(z)</math> and <math>\psi_1(z)</math></i> .....	19
2.4.2	<i>Determination of <math>\phi_2(z)</math> and <math>\psi_2(z)</math></i> .....	20
<b>3</b>	<b>ALGEBRAIC EQUATIONS AND APPLIED LOADS.....</b>	<b>29</b>
3.1	INTRODUCTION .....	29
3.2	INTERFACE CONDITIONS EXPRESSED AS INFINITE SERIES .....	29
3.3	GENERAL FORM OF ALGEBRAIC EQUATIONS.....	32
3.3.1	<i>Traction continuity condition</i> .....	33
3.3.2	<i>Displacement discontinuity condition</i> .....	36
3.4	APPLIED LOADS .....	44
3.4.1	<i>Thermal load</i> .....	44
3.4.2	<i>Mechanical load</i> .....	45
3.5	ALGEBRAIC EQUATIONS FOR SPECIFIC INTERFACE TYPES.....	46
3.5.1	<i>Case 1: Interface parameter <math>m = n</math></i> .....	47
3.5.2	<i>Case 2: Interface parameter <math>m = 3n</math></i> .....	51
3.5.3	<i>Algebraic equations for mechanical load</i> .....	54





<b>4</b>	<b>NUMERICAL PROCEDURE AND RESULTS .....</b>	<b>55</b>
4.1	INTRODUCTION .....	55
4.2	STRESS INTENSITY FACTOR.....	56
4.2.2	<i>Thermal Load</i> .....	59
4.2.2	<i>Mechanical Load</i> .....	60
4.3	RESULTS .....	62
4.3.1	<i>Thermal load</i> .....	62
4.3.1.1	Case 1 : $m = n$ .....	63
4.3.1.2	Case 2 : $m = 3n$ .....	74
4.3.2	<i>Mechanical loading</i> .....	79
4.3.2.1	Case 1 : $m = n$ .....	79
<b>5</b>	<b>CONCLUSIONS AND FUTURE WORK .....</b>	<b>86</b>
5.1	CONCLUSIONS .....	86
5.2	FUTURE WORK.....	89
	<b>REFERENCES .....</b>	<b>91</b>
	<b>APPENDIX A .....</b>	<b>97</b>
	<b>APPENDIX B .....</b>	<b>109</b>
	<b>APPENDIX C .....</b>	<b>120</b>



# LIST OF FIGURES

<b>FIGURE 1.1</b> CLASSES OF COMPOSITES .....	2
<b>FIGURE 1.2</b> SCHEMATIC REPRESENTATION OF THE INTERPHASE REGION IN POLYMERIC COMPOSITES.....	4
<b>FIGURE 2.1</b> REPRESENTATIVE VOLUME ELEMENT .....	13
<b>FIGURE 2.2</b> A CIRCULAR INCLUSION WITH AN INTERIOR RADIAL CRACK.....	14
<b>FIGURE 2.3</b> SYMMETRIC CONTINUATION .....	22
<b>FIGURE 4.1</b> DEPENDENCY OF NORMALIZED STRESS INTENSITY FACTOR ON CRACK TIP– INTERFACE DISTANCE (HARD INCLUSION) .....	67
<b>FIGURE 4.2</b> DEPENDENCY OF NORMALIZED STRESS INTENSITY FACTOR ON CRACK TIP– INTERFACE DISTANCE (SOFT INCLUSION).....	68
<b>FIGURE 4.3</b> THE EFFECT OF SHEAR MODULUS RATIO ON STRESS INTENSITY FACTOR .....	69
<b>FIGURE 4.4</b> EFFECT OF INTERFACE IMPERFECTION ON INCREASING CRACK LENGTH.....	70
<b>FIGURE 4.5</b> NORMALIZED STRESS INTENSITY FACTOR FOR A HARD INCLUSION.....	71
<b>FIGURE 4.6</b> NORMALIZED STRESS INTENSITY FACTOR FOR A SOFT INCLUSION.....	72
<b>FIGURE 4.7</b> DEPENDENCY OF NORMALIZED STRESS INTENSITY FACTOR ON CRACK TIP– INTERFACE DISTANCE (HARD INCLUSION) .....	75
<b>FIGURE 4.8</b> DEPENDENCY OF NORMALIZED STRESS INTENSITY FACTOR ON CRACK TIP– INTERFACE DISTANCE (SOFT INCLUSION).....	76
<b>FIGURE 4.9</b> NORMALIZED STRESS INTENSITY FACTOR FOR A HARD INCLUSION.....	77
<b>FIGURE 4.10</b> NORMALIZED STRESS INTENSITY FACTOR FOR A SOFT INCLUSION.....	78
<b>FIGURE 4.11</b> DEPENDENCY OF NORMALIZED STRESS INTENSITY FACTOR ON CRACK TIP– INTERFACE DISTANCE (HARD INCLUSION) .....	81
<b>FIGURE 4.12</b> DEPENDENCY OF NORMALIZED STRESS INTENSITY FACTOR ON CRACK TIP– INTERFACE DISTANCE (SOFT INCLUSION).....	82
<b>FIGURE 4.13</b> NORMALIZED STRESS INTENSITY FACTOR FOR A HARD INCLUSION.....	83
<b>FIGURE 4.14</b> NORMALIZED STRESS INTENSITY FACTOR FOR A SOFT INCLUSION.....	84





# CHAPTER 1

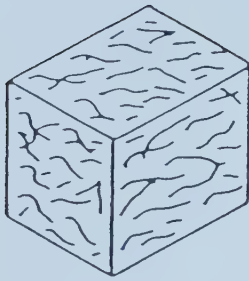
## 1 Introduction

### 1.1 Composite Materials

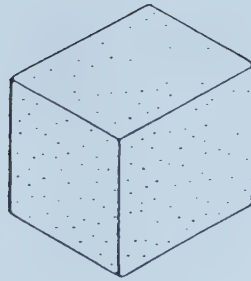
Composite materials have become one of the dominant classes of advanced materials in use in aerospace, automobile, biomedical, construction, manufacture of sporting goods and other applications, mainly as a result of the fact that conventional metals, ceramics and polymers fail to meet the performance requirements of today's technologies. A composite material is formed by combining two or more distinct materials at the macroscopic level to produce a new multiphase material. Composite materials take advantage of the combined properties of materials to produce new materials that have superior and desirable mechanical, thermal and/or electronic properties depending on specific requirements. Figure 1.1, shows the classification of composite materials based on their structural constituents. This classification leads to five classes of composite materials, namely particulate, fiber, laminate, flake and filled [1].

Particulate composites consist of particles immersed in a matrix. Fiber composites consist of a matrix phase reinforced by short (discontinuous) or long (continuous) fibers. Laminar composites are made up of two or more different constituent layers bonded together; these layers may differ in material properties and reinforcing directions [2]. Flake composites are produced when flat reinforcements are embedded inside a matrix material. Filled or skeletal composites are made up of a continuous skeletal matrix impregnated with a second-phase filler material.

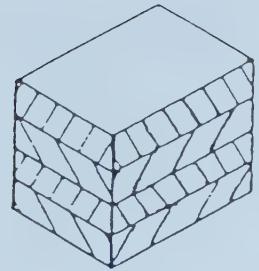




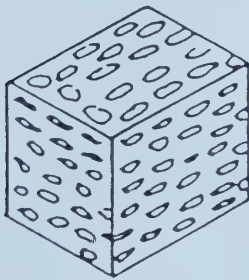
FIBER COMPOSITE



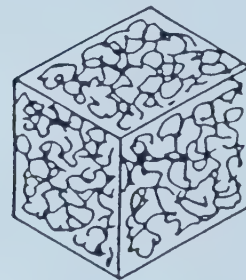
PARTICULATE COMPOSITE



LAMINAR COMPOSITE



FLAKE COMPOSITE



FILLED COMPOSITE

**Figure 1.1** Classes of Composites

(From Schwartz Mel M., "Composite Materials Handbook, Second Edition, McGraw-Hill, Inc, 1992)

Of the five types of composite materials mentioned above the fiber-reinforced composites are perhaps the most widely used and will form the basis of the investigations in this thesis.





## **1.2 Fiber-Reinforced Composites**

In most cases, the mechanical properties (stiffness, strength, fatigue, hardness and toughness) of fiber-reinforced composites can be greatly improved by embedding strong fibers into a softer matrix. The ability of fiber-reinforced composites to withstand higher stresses than can be endured by either of their constituents is mainly due to the fact that, during loading, the fiber and matrix interact, resulting in a redistribution of stresses. The transfer of stresses across one phase to the other depends largely on the effectiveness of the fiber-matrix bond (interphase layer). It is also worth noting that fibers can also serve as additives for improved performance (for example, high thermal expansion coefficient and low electrical resistivity) [60].

Fiber-reinforced composites can be classified based on the orientation of the reinforcing phase, examples of which are continuous unidirectional fibers, randomly oriented short discontinuous fibers, orthogonal fibers and multiple-ply fibers.

## **1.3 Interphase Layer**

By the mid 1960's, it became evident that the mechanical properties of certain fiber-reinforced composites depended not only on the properties of the individual fiber and matrix but also on the nature of the bond between the fiber and the surrounding matrix material [50]. In fact, it is now known that the fiber-matrix bond actually represents an interphase layer which often possesses distinct features such as a finite thickness, an independent elastic modulus, Poisson's ratio and coefficient of thermal expansion, different from those of either the fiber or matrix. This interphase layer may either be the product of a chemical interaction between the matrix and the fiber or could be introduced



deliberately. For example, in the manufacture of fiber-reinforced composite materials, a thin coating is often applied to the fiber to enhance the bonding strength as well as to control possible delamination of the fiber-matrix interface [64].

In [52], the *interphase layer* is defined as a region with distinct morphology that is formed as a result of the bonding between the fiber and the matrix. On the other hand, the *interface* is described as a one-dimensional border obtained, in the limit, as the interphase layer becomes vanishingly thin. A schematic representation of the interphase layer in a typical polymeric composite is illustrated in Figure 1.2.

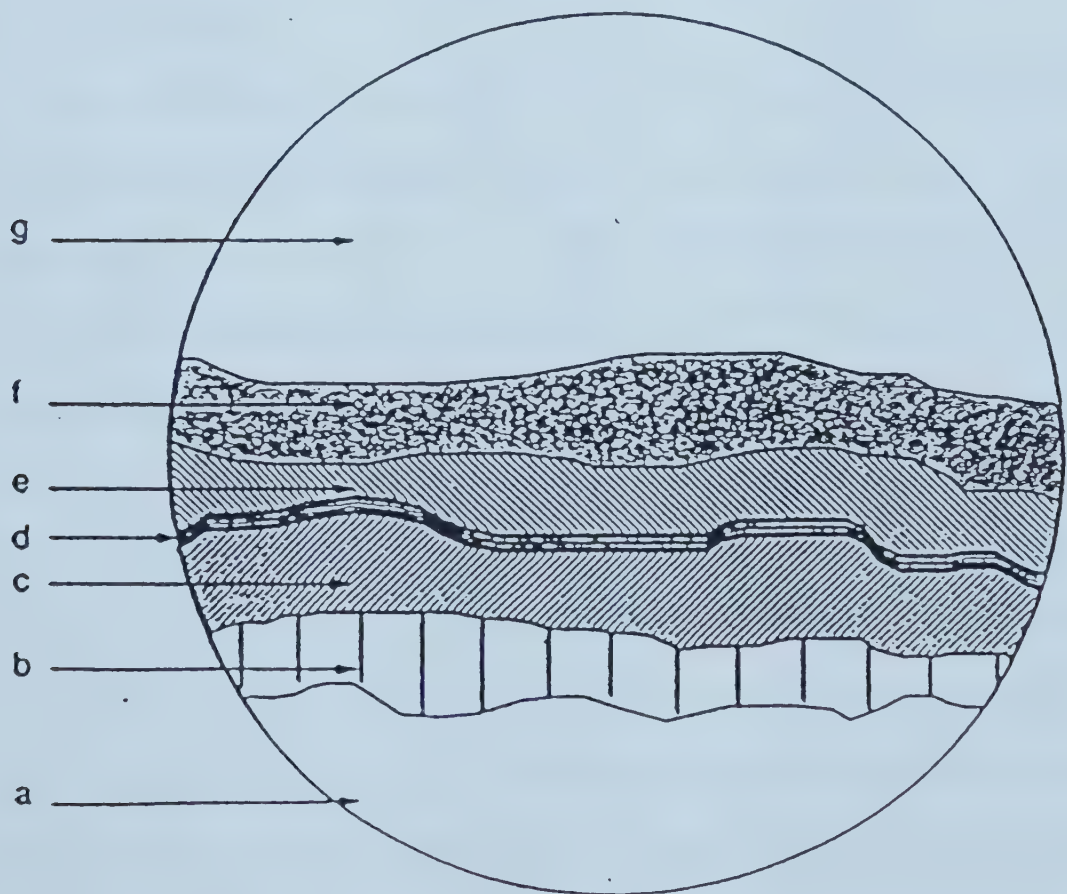


**Figure 1.2** Schematic representation of the interphase region in polymeric composites  
(From Verpoest et. al. [57])





- a**      The bulk fiber
- b**      A fiber surface layer possessing a different microstructure or chemical composition compared to the bulk fiber
- c**      An outer fiber layer altered by fiber surface treatments fiber surface.
- d**      A layer in which the fiber bonds to the sizing.
- e**      A sizing or coupling agent layer.
- f**      A layer, in which the matrix microstructure or chemical composition or both gradually changes from that of the sizing to that of the bulk matrix.
- g**      The bulk matrix.

In view of the above discussion, it is clear that the properties of the interphase layer or, more precisely, the effect of the fiber–matrix bond on stress transfer across the interface must be accounted for, since, it may significantly affect the accuracy of the micro-mechanical model and any ensuing prediction of the behavior of the composite. Consequently, several authors in the area of composites have incorporated the effect of the interphase layer into existing micromechanical models (see, for example, [20] – [45]). Walpole in [27], showed that a thin coating on an inclusion has a considerable effect on the stress fields just outside the inclusion. In [20], Ru discusses the importance of interphase layer design on thermal stresses induced within an elliptical inclusion. Ru found that if the thermal expansion coefficient of the interphase is between that of the inclusion and the matrix, it is possible to reduce the thermal stresses within the inclusion and the interphase layer. Zhong Z. et al. in [44], studied the eigenstrain problem of a spherical inclusion with an interphase region represented by a linear interfacial condition and found that the stresses inside the inclusion were not uniform. Lastly, Xiao Z. et al. in



[64] presented an analytical representation of the stress field due to an edge dislocation located near a coated inclusion. This work showed that if the coating layer is thin, both the shear modulus and the Poisson's ratio of both the inclusion and the coating could affect, and change considerably, the equilibrium position and the stability of the dislocation.

### **1.3.1 Perfect bonding**

A state of *perfect bonding* or *perfect contact* between a fiber and surrounding matrix represents an idealization of the real complex condition where an interphase layer is known to exist. In fact, the perfect bonding assumption effectively ignores the presence of interfacial damage between the fiber and matrix, damage, for example, due to weak adhesion, partial debonding, microcracks and voids. Unfortunately, the perfect bonding assumption has been used extensively in the literature dealing with the mechanical behavior of composites, for example in, [3] – [6], and in [11] – [16], concerning the interaction between a crack and inclusion.

### **1.3.2 Imperfect bonding**

The concept of imperfect bonding was developed to take into account the various degrees of damage within the interphase layer. As such, several authors have developed different models to describe the behavior of the (imperfect) interphase region (see, for example, [20] – [27]). In these models, the interphase layer is treated as a layer of specified thickness and elastic constants which characterize quantitatively the nature of the adhesion between the matrix and the fibers (see, [28] – [32] for details). The simplest



type of imperfect bonding model is one in which tractions are assumed to be continuous across the interface and displacement jumps across the interface are directly proportional to their respective interface traction components (see, for example, [24], [25] and [40] – [46]). This type of model is suitable when describing relatively 'soft' interphase layers. In some cases, the imperfect bonding condition has been modeled using finite element methods (see, for example [33] – [34] and [58]).

In this study, we adopt the established simple imperfect bonding condition mentioned above. That is, we assume that the inclusion-matrix interface is characterized by continuity of tractions and discontinuity of displacements across the interphase layer. Further, we assume that the displacement jumps across the interface are directly proportional to their respective interface traction components in terms of (two) spring-factor type interface parameters. This is the linear spring-layer model used in, for example, [35] – [45]. Here we assume that the two interface parameters are constant (the so-called *homogeneously imperfect interface*) along the entire length of the circular interface. Hashin used this model in [36] to determine the stress field in the vicinity of a spherical inclusion imperfectly bonded to the surrounding matrix. In direct contrast to the uniform stress field associated with perfect bonding, Hashin found that the stress field inside the inclusion was no longer uniform. Shen et. al. [66] – [68] have also used this model to study the stress fields associated with an elliptic inclusion subjected to anti-plane and plane deformations. Also, in [45], Amenyah W. et. al. used the spring-layer model to study interior cracking of an elastic inclusion and found that the imperfect interface has a significant effect on the stress intensity factor at the crack tips. Finally, in the study of the interaction between a matrix crack and an inclusion, Lui Y. et. al. [17],





showed that the interface imperfection (again modeled by a linear spring-layer) has a significant effect on the stress intensity factor particularly when the crack tip-interface distance is small.

It is important to mention that in the interest of incorporating fully the damage of the interphase layer, a pointwise variation of interface imperfection along the entire length of the material interface would be worth considering in a future study, since interface imperfections are almost always inhomogeneous. This type of imperfect interface condition is referred to in the literature as the *inhomogeneously imperfect interface* and has been considered in, for example, [48] – [49].

## 1.4 Fiber-Cracking

Recently, there have been significant efforts to understand the stress-induced crack growth phenomenon as one of the process variables that affects the overall fracture of fiber-reinforced composites (see, for example, [7] – [17]). In [18], the observation of high mobility dislocations inside manganese sulphide inclusions within a steel matrix prompted the study of the behavior of edge dislocations inside an inclusion [11]. Experimental investigations have shown that, in certain cases, mechanical failure, as a result of the fracture of individual components, does not occur until the fiber begins to fracture [19]. As such, the occurrence of the first fiber fracture is regarded as one of the important events in predicting crack growth behavior and the ensuing mechanical failure of the composite.

It is for this reason that this thesis seeks to investigate the effect of an imperfect interface on the direction of crack growth of a pre-existing crack inside an individual



fiber (inclusion) by calculating the stress intensity factor at the crack tips. Specifically, it is of interest to determine if the crack grows either towards the interface or away from the interface.

## 1.5 Background and Outline of Study

There are several recent examples in the literature dealing with the interaction between an inclusion and a crack or dislocation (see, for example, [11] – [17]). Crack-inclusion problems may be concerned with fiber-cracking (see, for example, [13] and [45]) or matrix-cracking (see, for example, [15] and [17]) depending on the initial location of the crack.

Most of the previous works dealing with crack-inclusion interactions have solved the problem using methods different from that used in this thesis. For example, in [11], the authors solve the problem of edge dislocation inside a circular inclusion with perfect bonding by determining the Airy's stress functions of the Burgers vector of the dislocation. These stress functions are then substituted into the elastic strain energy equation of the dislocation and the conditions under which the equilibrium position of the dislocation exists are found. There is also the integral equation method, which is perhaps considered as the most widely used procedure for solving crack-inclusion interaction problems. This method is used by Atkinson in [12] where the results of Erdogan et. al. in [14] are used to reformulate the problem and represent the crack by a distribution of dislocations with unknown dislocation density leading to a solution of the resulting integral equation. Also, using the procedure suggested in [14] for the numerical solution of the integral equation, Müller and Schmauder in [9] and [10], have represented the



radial crack by a continuous distribution of dislocations to determine the stress intensity factor at the crack tips. However, this procedure was not used in this study. This is because the determination of the solution of the integral equation for an inclusion with an imperfect interface could pose considerable computational difficulties. In this thesis and also in [17] and [45], it is shown how the difficulties associated with the integral equation method are avoided by using a relatively straightforward series method.

Most of the previous works on fiber-cracking were studied using a perfect interface model (see, for example, [11], [13] and [16]). In [13], Anlas and Santare studied the problem of an arbitrarily oriented crack inside an elliptic inclusion perfectly bonded to the surrounding matrix. In [16], Ru analyses the stresses within a perfectly bonded thermal inclusion of arbitrary shape containing voids and cracks. However, the problem concerning an interior radial crack inside a circular inclusion with imperfect interface has not yet been studied and therefore forms the subject of this thesis.

The thesis is organized as follows. Following the brief introduction in Chapter 1, Chapter 2 discusses the formulation of the plane elastic deformation of the single-inclusion model. The imperfect interface conditions are expressed solely in terms of stress potentials and the series representation of each stress potential is derived. In Chapter 3, the interface conditions are expressed as infinite series, from which, the general form of a set of algebraic equations is obtained. Further, for a single-inclusion model subjected to thermal or mechanical load and for a specific type of interface, a reduced-form of the set of algebraic equations is derived. Chapter 4 outlines the procedure for solving the set of algebraic equations and the derivation of the expressions for the stress intensity factor at the crack tips. The results for perfect and imperfect





interface models are compared. Chapter 5 provides a summary of the findings of the study and concludes that the imperfect fiber-matrix bond has a pronounced effect on the stress intensity factors at the crack tips. Finally, a brief insight into future works to be undertaken is presented.



# CHAPTER 2

## 2 Formulation of the Boundary Value Problem

### 2.1 Introduction

In 1957, the Eshelby equivalent inclusion method presented in [3] provided a closed-form solution of the resulting elastic fields in an ellipsoidal inclusion with perfect interface in terms of Eshelby's tensor. This elegant method states that the calculation of the stress perturbation caused by the inhomogeneity, in both the inhomogeneity and the surrounding matrix, can be reduced to the determination of the stress field caused by an inclusion of the same shape as the inhomogeneity, with the same material constants as the matrix. In order to guarantee that the stress and strain in both the inhomogeneity and the inclusion are equal, the inclusion must undergo a suitably chosen equivalent eigenstrain. The results of this well-known theoretical micromechanics model has had considerable effect on the development of the theory of micromechanics of solids and has been successfully adapted to solve both plane and anti-plane problems (see, for example, [53] – [55] and [66] - [68]). The model has also been used in average stiffness analysis by Jasuik I. et. al.[61].



## 2.2 Description of the Problem

In a two-phase composite material, all global geometrical characteristics are the same in any representative volume element (RVE), irrespective of its position (see, [56] for details). In a dilute fiber-reinforced composite material (with a fiber volume fraction below 20%), where the fibers are widely spaced apart, the interaction between nearby fibers can be ignored and the effective properties can be determined from the average field quantities of the RVE.



**Figure 2.1** Representative Volume Element

In this problem, by assuming a periodic configuration of fibers, the micromechanics model is taken to be a single inclusion embedded in an infinite matrix as shown in Figure 2.1. The boundary of the RVE is subjected to appropriate tractions and displacements, which satisfy the structural periodicity and the prescribed asymptotic conditions.





Consider then a circular elastic inclusion embedded in a homogeneous two – dimensional elastic matrix, infinite in extent. The inclusion (with a radial crack), with center at the origin and radius  $R$  occupies a region denoted by  $S_2$ . The region occupied by the unbounded matrix is represented by  $S_1$  and the curve  $\Gamma$  represents the inclusion – matrix interface. The subscripts 1 and 2 used on field quantities and elastic constants will refer to the matrix and inclusion, respectively. The linearly elastic materials of the matrix and inclusion are assumed to be homogeneous and isotropic.

In the analytical study of this problem, a specific geometry of crack (radial) is chosen such that it leads to the tractable derivation of the corresponding stress potentials in the inclusion by complex variable methods.

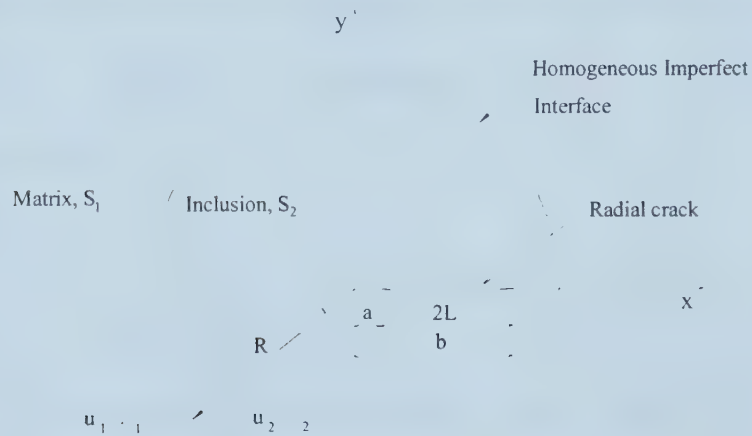


**Figure 2.2** A circular inclusion with an interior radial crack



For plane deformations, the elastic stresses and the associated displacements can be written in terms of two complex potentials,  $\phi(z)$  and  $\psi(z)$  [47] in polar coordinates as:

$$\begin{aligned} 2\mu(u_r + iu_\theta) &= e^{-i\theta} [k\phi(z) - z\overline{\phi'(z)} - \overline{\psi(z)}], \\ \sigma_{rr} + \sigma_{\theta\theta} &= 2[\phi'(z) + \overline{\phi'(z)}], \\ \sigma_{rr} - i\sigma_{r\theta} &= \phi'(z) + \overline{\phi'(z)} - e^{-2i\theta} [\overline{z}\phi''(z) + \psi'(z)], \end{aligned} \quad (2.1)$$

where  $z = x + iy = re^{i\theta}$  is the complex coordinate and  $k = 3 - 4\nu$  for plane strain and  $k = (3 - \nu) / (1 + \nu)$  for plane stress. Here,  $\mu$  and  $\nu$  are the shear modulus and Poisson's ratio, respectively.

The spring-layer type interface model representing the bond between the inclusion and the matrix is based on the assumption that tractions are continuous across the interface and displacement jumps are proportional to their respective interface tractions in terms of given interface parameters (see, for example, [35] – [45]). Hence, the interface conditions on  $\Gamma$  are given by

$$[[\sigma_{rr} - i\sigma_{r\theta}]] = 0, \quad z \in \Gamma, \quad (2.2)$$

$$\sigma_{rr} = m[[u_r]] - mu_r^o, \quad \sigma_{r\theta} = n[[u_\theta]] - nu_\theta^o, \quad z \in \Gamma, \quad (2.3)$$

where  $m$  and  $n$  are the non-negative interface parameters. Here,  $[[*]] = (*)_1 - (*)_2$  represents the jump across the interface  $\Gamma$  and  $u^o$  is the displacement induced by the uniform (stress – free) eigenstrains  $\{\varepsilon_x^o, \varepsilon_y^o, \varepsilon_{xy}^o\}$  prescribed within the inclusion.

One of the advantages of the imperfect interface model used in (2.2) and (2.3) is that it permits representation of intermediate states of bonding between the inclusion and the matrix: from perfect bonding to complete debonding. Also, in the spring-type



interface model, a linear relationship is assumed to exist between the field variables - stress and displacement and this makes the problem tractable.

### 2.3 Interface Conditions in Terms of Stress Potentials

The boundary value problem has to be formulated such that the interface conditions in (2.2) and (2.3) are satisfied by the stress potentials. Consequently, it is imperative at this stage to rewrite the interface condition solely in terms of the stress potentials,  $\phi_1$ ,  $\psi_1$ ,  $\phi_2$  and  $\psi_2$ . The traction continuity condition in (2.2) leads to the expression

$$(\sigma_{rr} - i\sigma_{r\theta})_1 = (\sigma_{rr} - i\sigma_{r\theta})_2 .$$

In view of (2.1), the above equation can be re-written as,

$$\phi_1'(z) + \overline{\phi_1'(z)} - e^{2i\theta} [z\phi_1''(z) + \psi_1'(z)] = \phi_2'(z) + \overline{\phi_2'(z)} - e^{2i\theta} [z\phi_2''(z) + \psi_2'(z)] .$$

Using  $z = Re^{i\theta}$ , on the matrix-inclusion boundary, the above equation can therefore be expressed in terms of the four stress potentials as

$$\phi_1'(z) + \overline{\phi_1'(\frac{R^2}{z})} - z\phi_1''(z) - \frac{z^2}{R^2}\psi_1'(z) = \phi_2'(z) + \overline{\phi_2'(\frac{R^2}{z})} - z\phi_2''(z) - \frac{z^2}{R^2}\psi_2'(z), \quad z \in \Gamma. \quad (2.4)$$

The normal and tangential displacement jump conditions at the interface in (2.3) can be put together into a single equation of the form

$$\sigma_{rr} - i\sigma_{r\theta} = m[[u_r]] - mu_r^0 - i(n[[u_\theta]] - nu_\theta^0), \quad z \in \Gamma. \quad (2.5)$$

The left-hand-side of (2.5) can be written as either  $(\sigma_{rr} - i\sigma_{r\theta})_1$  or  $(\sigma_{rr} - i\sigma_{r\theta})_2$  since they are equal by the assumption of continuity of tractions on the interface in (2.2).

However, owing to the presence of the crack in the inclusion, the derivation of the stress





potentials in the inclusion involves much more complicated terms than the stress potentials in the matrix. It is therefore advantageous to use  $(\sigma_{rr} - i\sigma_{r\theta})_1$ .

In anticipation of what follows, we write the displacement interface condition in (2.5) in the form (refer to Appendix A for details)

$$(\sigma_{rr} - i\sigma_{r\theta})_1 = \left(\frac{m+n}{2}\right) \left[ (u_r^1 - iu_\theta^1) - (u_r^2 - iu_\theta^2) \right] + \left(\frac{m-n}{2}\right) \left[ (u_r^1 + iu_\theta^1) - (u_r^2 + iu_\theta^2) \right] - [mu_r^0 - inu_\theta^0], \quad z \in \Gamma, \quad (2.6)$$

where

$u_r^1$  and  $u_\theta^1$  are the radial and tangential displacements in the matrix,

$u_r^2$  and  $u_\theta^2$  are the radial and tangential displacements in the inclusion and

$u_r^0$  and  $u_\theta^0$  are the displacements induced by the eigenstrain in the radial and tangential directions respectively.

The additional displacement induced by the uniform eigenstrain prescribed in the inclusion can be written using the results of [13] as:

$$u_r^0 = R(\varepsilon_x^0 \cos^2 \theta + \varepsilon_y^0 \sin^2 \theta + \varepsilon_{xy}^0 \sin 2\theta) \quad u_\theta^0 = R\left(\frac{\varepsilon_y^0 - \varepsilon_x^0}{2} \sin 2\theta + \varepsilon_{xy}^0 \cos 2\theta\right).$$

At this stage, the last term in the square bracket on the right-hand-side of (2.6) can be written in a convenient form as (refer to Appendix A for details)

$$[mu_r^0 - inu_\theta^0] = mR\varepsilon_1 + \left(\frac{m+n}{2R}\right)(\varepsilon_2 - i\varepsilon_3)z^2 + \left(\frac{m-n}{2z}\right)R^3(\varepsilon_2 + i\varepsilon_3), \quad z \in \Gamma, \quad (2.7)$$

$$\text{where } \varepsilon_1 = \frac{\varepsilon_x^0 + \varepsilon_y^0}{2}, \quad \varepsilon_2 = \frac{\varepsilon_x^0 - \varepsilon_y^0}{2}, \quad \varepsilon_3 = \varepsilon_{xy}^0.$$



Substituting (2.7) into (2.6) and then using (2.1) yields, (refer to Appendix A for derivation)

$$\begin{aligned}
\phi_1'(z) + \overline{\phi_1'}\left(\frac{R^2}{z}\right) - z\phi_1''(z) - \frac{z^2}{R^2}\psi_1'(z) &= \left(\frac{m+n}{4R}\right) \left\{ \begin{aligned} &\frac{z}{\mu_1}k_1\overline{\phi_1}\left(\frac{R^2}{z}\right) - \frac{R^2}{\mu_1}\phi_1'(z) - \frac{z}{\mu_1}\psi_1(z) \\ &-\frac{z}{\mu_2}k_2\overline{\phi_2}\left(\frac{R^2}{z}\right) + \frac{R^2}{\mu_2}\phi_2'(z) + \frac{z}{\mu_2}\psi_2(z) \end{aligned} \right\} \\
&+ R\left(\frac{m-n}{4}\right) \left\{ \begin{aligned} &\frac{1}{\mu_1 z}k_1\phi_1(z) - \frac{1}{\mu_1}\overline{\phi_1'}\left(\frac{R^2}{z}\right) - \frac{1}{\mu_1 z}\overline{\psi_1}\left(\frac{R^2}{z}\right) \\ &-\frac{1}{\mu_2 z}k_2\phi_2(z) + \frac{1}{\mu_2}\overline{\phi_2'}\left(\frac{R^2}{z}\right) + \frac{1}{\mu_2 z}\overline{\psi_2}\left(\frac{R^2}{z}\right) \end{aligned} \right\} \\
&- mR\mathcal{E}_1 - \left(\frac{m+n}{2R}\right)(\mathcal{E}_2 - i\mathcal{E}_3)z^2 \\
&-\left(\frac{m-n}{2z^2}\right)R^3(\mathcal{E}_2 + i\mathcal{E}_3), \quad z \in \Gamma.
\end{aligned} \tag{2.8}$$

At this stage, the two interface conditions in (2.2) and (2.3) have been transformed into (2.4) and (2.8) which are expressed exclusively in terms of the stress potentials  $\phi_1(z)$ ,  $\psi_1(z)$ ,  $\phi_2(z)$  and  $\psi_2(z)$ . The next step is to determine these stress potentials.



## 2.4 Series Representation of Stress Potentials

As mentioned previously in Chapter 1, for an imperfect interface model, the method of representing the crack as a distribution of dislocations cannot be used. It is envisaged that if this method is used, two difficulties could be encountered. Firstly, to our knowledge, the fundamental solution (Green's function) of a point dislocation with an imperfect interface is not available in the literature. It is of interest to point out that, to date, only the explicit analytical expression of the Green's function corresponding to a point dislocation with a *perfect* interface is available. Secondly, even if a closed-form representation of the crack as a distribution of dislocations is obtained, solving the resulting singular integral equation is highly non-trivial and poses another challenge. However, owing to the fact that the boundary of the interface is circular, a relatively simpler series method can be developed to determine the stress potentials  $\phi_1(z)$ ,  $\psi_1(z)$ ,  $\phi_2(z)$  and  $\psi_2(z)$ .

### 2.4.1 Determination of $\phi_1(z)$ and $\psi_1(z)$

The stress potentials in the matrix,  $\phi_1(z)$  and  $\psi_1(z)$  must be determined such that they satisfy the far-field loading condition. It will be assumed that the stresses at infinity are always bounded and finite. Also, at infinity, the prescribed stress is uniform and therefore we assume a linear dependency on load. This implies  $\phi_1(z)$  and  $\psi_1(z)$  are linear functions of  $z$  at infinity. Therefore the asymptotic conditions in the matrix are given by

$$\phi_1(z) \approx Az + \frac{1}{z} + \frac{1}{z^2} + \frac{1}{z^3} + \dots, \quad \psi_1(z) \approx Bz + \frac{1}{z} + \frac{1}{z^2} + \frac{1}{z^3} + \dots, \quad |z| \rightarrow \infty.$$





At infinity  $\frac{1}{z}, \frac{1}{z^2}, \frac{1}{z^3}, \dots$  are very small and hence the remote loading condition can be written as

$$\phi_1(z) \approx Az + O(1) \quad \psi_1(z) \approx Bz + O(1), \quad |z| \rightarrow \infty,$$

where  $A$  and  $B$  are known coefficients determined by the prescribed uniform stress at infinity. We choose  $A$  to be a real number and  $B$  to be a complex number for convenience. Since,  $\phi_1(z)$  and  $\psi_1(z)$  are analytic in the matrix, they admit Laurent series representations of the form

$$\phi_1(z) = Az + \sum_{k=1}^{\infty} a_k z^{-k}, \quad \psi_1(z) = Bz + \sum_{k=1}^{\infty} b_k z^{-k}, \quad z \in S_1, \quad (2.9)$$

where  $a_k$  and  $b_k$  ( $k = 1, 2, \dots$ ) are complex coefficients.

#### 2.4.2 Determination of $\phi_2(z)$ and $\psi_2(z)$

As shown in Figure 2.2, the inclusion contains a radial crack and, as such, the traction free condition assumed along the crack face must be satisfied by the derived stress potentials  $\phi_2(z)$  and  $\psi_2(z)$ . Now, since the inclusion contains a crack of length  $2L$ , it implies,  $\phi_2(z)$  and  $\psi_2(z)$  are not analytic in the entire domain  $S_2$  and hence, cannot be expanded as Taylor series in  $S_2$ . To deal with this problem, we use complex variable techniques to rewrite  $\phi_2(z)$  and  $\psi_2(z)$  in terms of two new analytic functions  $X(z)$  and  $Y(z)$  which are analytic in the circular domain  $C$ , which represents the domain occupied by the inclusion in the absence of the crack.

The cartesian components of the resultant force acting on the left of an arbitrary arc  $AB$  in an elastic body are given by [47]:



$$F_x + iF_y = -[\phi(z) + z\overline{\phi'(z)} + \overline{\psi(z)}]_A^B, \quad (2.10)$$

where  $[f(*)]_A^B = f(A) - f(B)$ . This resultant force is independent of the path and dependent only on the endpoints of the arc  $A$  and  $B$ .

The traction free condition along the crack-face in the inclusion implies that

$$\sigma_{xy} = 0, \quad \sigma_{yy} = 0 \text{ and therefore } \sigma_{yy} + i\sigma_{xy} = 0.$$

In view of (2.10) and the traction free condition, we can write that on the crack face in the upper half plane:

$$\phi_2(z)^+ + z\overline{\phi_2'(z)^+} + \overline{\psi_2(z)^+} = 0, \quad z \in 2L^+. \quad (2.11)$$

Similarly, on the crack face in the lower half plane:

$$\phi_2(z)^- + z\overline{\phi_2'(z)^-} + \overline{\psi_2(z)^-} = 0, \quad z \in 2L^-. \quad (2.12)$$

Each of (2.11) and (2.12) which can be written in a more convenient form as

$$\phi_2(z)^+ + z\overline{\phi_2'(\bar{z})^+} + \overline{\psi_2(\bar{z})^+} = 0, \quad z \in 2L^+, \quad (2.13)$$

and

$$\phi_2(z)^- + z\overline{\phi_2'(\bar{z})^-} + \overline{\psi_2(\bar{z})^-} = 0, \quad z \in 2L^-, \quad (2.14)$$

respectively.

Referring to Figure 2.3, consider a function analytic in the upper domain  $D^+$ , with one of its boundaries being the real axis, which serves as the line of symmetry. By symmetric continuation we can also define another function in the opposite domain which is also analytic. Hence, the lower domain  $D^-$ , is the analytic symmetry of the upper domain  $D^+$  about the real axis. Therefore, as a point  $\bar{z}$  (conjugate of  $z$ ) in the upper half plane of the inclusion approaches the real axis, its conjugate point  $z$  in the lower half plane also approaches the real axis and hence we can write, for example,



$\overline{\phi(\bar{z})}^+ = \overline{\phi(z)}^-$ . Again from Figure 2.3, we can also write  $\overline{\overline{\phi(\bar{z})}} = \overline{\phi(z)}$  and therefore any  $z$  in the lower domain has a conjugate  $\bar{z}$  (given by  $\bar{z}$ ) in the upper domain, which is defined. Hence, using similar arguments the conjugate of  $\phi(\bar{z})$  (given by  $\overline{\phi(\bar{z})}$ ) for any  $z$  in the lower domain is also defined.

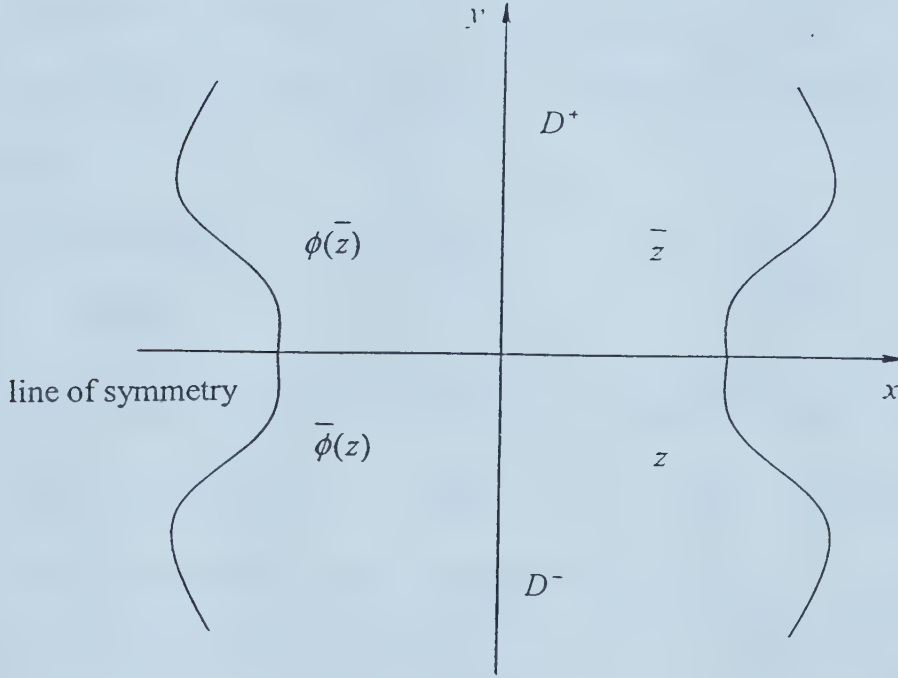


**Figure 2.3** Symmetric Continuation

In view of the above, (2.13) and (2.14) can now written as

$$\phi_2(z)^+ + z\overline{\phi_2'(z)}^- + \overline{\psi_2(z)}^- = 0, \quad z \in 2L$$

and

(2.15)

$$\phi_2(z)^- + z\overline{\phi_2'(z)}^+ + \overline{\psi_2(z)}^+ = 0, \quad z \in 2L,$$



and then rewritten in a convenient form as

$$\begin{aligned}\phi_2(z)^+ + [z\overline{\phi_2'}(z) + \overline{\psi_2}(z)]^- &= 0, & z \in 2L, \\ \phi_2(z)^- + [z\overline{\phi_2'}(z) + \overline{\psi_2}(z)]^+ &= 0, & z \in 2L.\end{aligned}\tag{2.16}$$

To this end, it follows that

$$\phi_2(z)^+ - [z\overline{\phi_2'}(z) + \overline{\psi_2}(z)]^+ = \phi_2(z)^- - [z\overline{\phi_2'}(z) + \overline{\psi_2}(z)]^-, \quad z \in 2L.\tag{2.17}$$

From (2.17) as point  $z$  approaches the real axis from either the upper or lower half planes, the above equality is satisfied which implies the function is continuous across the crack length  $2L$ .

Next, we can therefore define the function

$$X(z) \equiv \phi_2(z) - [z\overline{\phi_2'}(z) + \overline{\psi_2}(z)],\tag{2.18}$$

which is clearly analytic in the domain  $S_2$  and the continuity condition derived from (2.17) will guarantee that  $X(z)$  is continuous across the crack length  $2L$  (that is,  $X(z)^+ = X(z)^-$ ). Consequently,  $X(z)$  is continuous across the crack face and analytic inside the domain  $C$  of the inclusion without the crack and can therefore be expanded as a Taylor series:

$$X(z) = \sum_{k=0}^{\infty} c_k z^k, \quad z \in C,\tag{2.19}$$

where  $c_k$  ( $k=0,1,2,3,\dots$ ) are complex coefficients.

Further, the remaining boundary condition on the crack face in (2.16) can be written as

$$[\phi_2(z) + z\overline{\phi_2'}(z) + \overline{\psi_2}(z)]^+ + [\phi_2(z) + z\overline{\phi_2'}(z) + \overline{\psi_2}(z)]^- = 0, \quad z \in 2L.\tag{2.20}$$

Noting that each of the terms on the left-hand-side of (2.20) is always finite and using Plemelj's formula [47], we can define the second function  $Y(z)$  as





$$Y(z) \equiv \sqrt{(z-a)(z-b)} [\phi_2(z) + z\overline{\phi_2'(z)} + \overline{\psi_2(z)}]. \quad (2.21)$$

The above expression is valid as a consequence of the continuity condition given by

$$\sqrt{(z-a)(z-b)^+} = \sqrt{(z-a)(z-b)^-}, \quad z \in 2L = [a, b].$$

Hence, as for  $X(z)$ ,  $Y(z)$  is continuous across the crack face and analytic inside the domain  $C$  where it can therefore be expanded in a Taylor series:

$$Y(z) = \sum_{k=0}^{\infty} d_k z^k, \quad z \in C, \quad (2.22)$$

where  $d_k$  ( $k=0,1,2,3,\dots$ ) are complex coefficients.

We know  $\phi_2(z)$  and  $\psi_2(z)$  are analytic in  $S_2$  but not in the circle  $C$ , but they can, however, be expressed in terms  $X(z)$  and  $Y(z)$ . As a result of using (2.18) and (2.21)  $\phi_2(z)$  and  $\psi_2(z)$  defined in the inclusion with the crack can be expressed in terms of  $X(z)$  and  $Y(z)$  as

$$\phi_2(z) = \frac{Y(z)}{2\sqrt{(z-a)(z-b)}} + \frac{X(z)}{2}, \quad (2.23)$$

and

$$\psi_2(z) = \overline{\phi_2(z)} - z\overline{\phi_2'(z)} - \overline{X(z)}. \quad (2.24)$$

The term  $H(z) = \frac{1}{2\sqrt{(z-a)(z-b)}}$  in (2.23) is multi-valued across the crack face but

analytic in the domain  $S_1 \cup \Gamma$  and can therefore be expanded on the interface in a Laurent series in negative powers of  $z$  where the coefficients  $H_1, H_2, H_3, \dots$  are expressed in terms of  $a$  and  $b$ . That is,



$$H(z) \equiv \frac{1}{2\sqrt{(z-a)(z-b)}} = \frac{1}{z} \left(1 - \frac{a}{z}\right)^{-\frac{1}{2}} \left(1 - \frac{b}{z}\right)^{-\frac{1}{2}}, \quad (2.25)$$

$$H(z) = \frac{1}{z} \left( 1 + \frac{a}{2z} + \frac{3a^2}{8z^2} + \frac{5a^3}{16z^3} + \frac{35a^4}{128z^4} + \frac{63a^5}{256z^5} + \frac{231a^6}{1024z^6} + \frac{429a^7}{2048z^7} + \frac{6435a^8}{32768z^8} + \dots \right) \\ \left( 1 + \frac{b}{2z} + \frac{3b^2}{8z^2} + \frac{5b^3}{16z^3} + \frac{35b^4}{128z^4} + \frac{63b^5}{256z^5} + \frac{231b^6}{1024z^6} + \frac{429b^7}{2048z^7} + \frac{6435b^8}{32768z^8} + \dots \right),$$

and can be written as

$$H(z) = \frac{H_1}{z} + \frac{H_2}{z^2} + \frac{H_3}{z^3} + \frac{H_4}{z^4} + \frac{H_5}{z^5} + \frac{H_6}{z^6} + \frac{H_7}{z^7} + \frac{H_8}{z^8} + \frac{H_9}{z^9} + \frac{H_{10}}{z^{10}} + \dots, \quad (2.26)$$

where

$$H_1 = 1, \quad H_2 = \frac{1}{2}(a+b), \quad H_3 = \frac{3a^2}{8} + \frac{ab}{4} + \frac{3b^2}{8},$$

$$H_4 = \frac{5a^3}{16} + \frac{3a^2b}{16} + \frac{3ab^2}{16} + \frac{5b^3}{16}, \quad H_5 = \frac{35a^4}{128} + \frac{5a^3b}{32} + \frac{9a^2b^2}{64} + \frac{5ab^3}{32} + \frac{35b^4}{128},$$

$$H_6 = \frac{63a^5}{256} + \frac{35a^4b}{256} + \frac{15a^3b^2}{128} + \frac{15a^2b^3}{128} + \frac{35ab^4}{256} + \frac{63b^5}{256},$$

$$H_7 = \frac{231a^6}{1024} + \frac{63a^5b}{512} + \frac{105a^4b^2}{1024} + \frac{25a^3b^3}{256} + \frac{105a^2b^4}{1024} + \frac{63ab^5}{512} + \frac{231b^6}{1024},$$

$$H_8 = \frac{429a^7}{2048} + \frac{231a^6b}{2048} + \frac{189a^5b^2}{2048} + \frac{175a^4b^3}{2048} + \frac{175a^3b^4}{2048} + \frac{189a^2b^5}{2048} + \frac{231ab^6}{2048} + \frac{429b^7}{2048},$$

$$H_9 = \frac{6435a^8}{32768} + \frac{429a^8b}{4096} + \frac{693a^6b^2}{8192} + \frac{315a^5b^3}{4096} + \frac{1225a^4b^4}{16384} + \frac{315a^3b^5}{4096} + \frac{693a^2b^6}{8192} \\ + \frac{429ab^7}{4096} + \frac{6435b^8}{32768}.$$



Further, using the expansion of  $H(z)$ , we can expand  $\phi_2(z)$  and  $\psi_2(z)$  at the interface as infinite Laurent series in positive and negative powers of  $z$  from (2.23) and (2.24) as follows (see Appendix A for details)

$$\begin{aligned}
\phi_2(z) = & \frac{c_5}{2}z^5 + \frac{1}{2}(c_4 + H_1d_5)z^4 + \frac{1}{2}(c_3 + H_2d_5 + H_1d_4)z^3 \\
& + \frac{1}{2}(c_2 + H_3d_5 + H_2d_4 + H_1d_3)z^2 + \frac{1}{2}(c_1 + H_4d_5 + H_3d_4 + H_2d_3 + H_1d_2)z \\
& + \frac{1}{2}(c_0 + H_5d_5 + H_4d_4 + H_3d_3 + H_2d_2 + H_1d_1) \\
& + \frac{1}{2}(H_6d_5 + H_5d_4 + H_4d_3 + H_3d_2 + H_2d_1 + H_1d_0)\frac{1}{z} \\
& + \frac{1}{2}(H_7d_5 + H_6d_4 + H_5d_3 + H_4d_2 + H_3d_1 + H_2d_0)\frac{1}{z^2} \\
& + \frac{1}{2}(H_8d_5 + H_7d_4 + H_6d_3 + H_5d_2 + H_4d_1 + H_3d_0)\frac{1}{z^3} \\
& + \frac{1}{2}(H_9d_5 + H_8d_4 + H_7d_3 + H_6d_2 + H_5d_1 + H_4d_0)\frac{1}{z^4} \\
& + \frac{1}{2}(H_{10}d_5 + H_9d_4 + H_8d_3 + H_7d_2 + H_6d_1 + H_5d_0)\frac{1}{z^5} \\
& + \frac{1}{2}(H_{11}d_5 + H_{10}d_4 + H_9d_3 + H_8d_2 + H_7d_1 + H_6d_0)\frac{1}{z^6} \\
& + \frac{1}{2}(H_{12}d_5 + H_{11}d_4 + H_{10}d_3 + H_9d_2 + H_8d_1 + H_7d_0)\frac{1}{z^7},
\end{aligned} \tag{2.27}$$

and





$$\begin{aligned}
\psi_2 = & -\frac{1}{2}(\overline{c_5} + 5c_5)z^5 - \frac{1}{2}(\overline{c_4} - H_1\overline{d_5} + 4c_4 + 4H_1d_5)z^4 \\
& - \frac{1}{2}(\overline{c_3} - H_2\overline{d_5} - H_1\overline{d_4} + 3c_3 + 3H_2d_5 + 3H_1d_4)z^3 \\
& + \left( -\frac{\overline{c_2}}{2} + \frac{H_3\overline{d_5}}{2} + \frac{H_2\overline{d_4}}{2} + \frac{H_1\overline{d_3}}{2} - c_2 - H_3d_5 - H_2d_4 - H_1d_3 \right) z^2 \\
& + \left( -\frac{\overline{c_1}}{2} + \frac{H_4\overline{d_5}}{2} + \frac{H_3\overline{d_4}}{2} + \frac{H_2\overline{d_3}}{2} + \frac{H_1\overline{d_2}}{2} - \frac{c_1}{2} - \frac{H_4d_5}{2} - \frac{H_3d_4}{2} - \frac{H_2d_3}{2} - \frac{H_1d_2}{2} \right) z \\
& + \left( -\frac{c_0}{2} + \frac{H_5\overline{d_5}}{2} + \frac{H_4\overline{d_4}}{2} + \frac{H_3\overline{d_3}}{2} + \frac{H_2\overline{d_2}}{2} + \frac{H_1\overline{d_1}}{2} \right) \\
& + \left( \frac{H_6\overline{d_5}}{2} + \frac{H_5\overline{d_4}}{2} + \frac{H_4\overline{d_3}}{2} + \frac{H_3\overline{d_2}}{2} + \frac{H_2\overline{d_1}}{2} + \frac{H_1d_0}{2} + \frac{H_6d_5}{2} + \frac{H_5d_4}{2} + \frac{H_4d_3}{2} \right. \\
& \quad \left. + \frac{H_3d_2}{2} + \frac{H_2d_1}{2} + \frac{H_1d_0}{2} \right) \frac{1}{z} \\
& + \left( \frac{H_7\overline{d_5}}{2} + \frac{H_6\overline{d_4}}{2} + \frac{H_5\overline{d_3}}{2} + \frac{H_4\overline{d_2}}{2} + \frac{H_3\overline{d_1}}{2} + \frac{H_2d_0}{2} + H_7d_5 + H_6d_4 + H_5d_3 \right. \\
& \quad \left. + H_4d_2 + H_3d_1 + H_2d_0 \right) \frac{1}{z^2} \\
& + \left( \frac{H_8\overline{d_5}}{2} + \frac{H_7\overline{d_4}}{2} + \frac{H_6\overline{d_3}}{2} + \frac{H_5\overline{d_2}}{2} + \frac{H_4\overline{d_1}}{2} + \frac{H_3d_0}{2} + \frac{3H_8d_5}{2} + \frac{3H_7d_4}{2} + \frac{3H_6d_3}{2} \right. \\
& \quad \left. + \frac{3H_5d_2}{2} + \frac{3H_4d_1}{2} + \frac{3H_3d_0}{2} \right) \frac{1}{z^3}
\end{aligned}$$



$$\begin{aligned}
& + \left( \frac{H_9 \overline{d_5}}{2} + \frac{H_8 \overline{d_4}}{2} + \frac{H_7 \overline{d_3}}{2} + \frac{H_6 \overline{d_2}}{2} + \frac{H_5 \overline{d_1}}{2} + \frac{H_4 d_0}{2} + 2H_9 d_5 + 2H_8 d_4 + 2H_7 d_3 \right. \\
& \quad \left. + 2H_6 d_2 + 2H_5 d_1 + 2H_4 d_0 \right) \frac{1}{z^4} \\
& + \left( \frac{H_{10} \overline{d_5}}{2} + \frac{H_9 \overline{d_4}}{2} + \frac{H_8 \overline{d_3}}{2} + \frac{H_7 \overline{d_2}}{2} + \frac{H_6 \overline{d_1}}{2} + \frac{H_5 d_0}{2} + \frac{5H_{10} d_5}{2} + \frac{5H_9 d_4}{2} + \frac{5H_8 d_3}{2} \right. \\
& \quad \left. + \frac{5H_7 d_2}{2} + \frac{5H_6 d_1}{2} + \frac{5H_5 d_0}{2} \right) \frac{1}{z^5} \\
& + \left( \frac{H_{11} \overline{d_5}}{2} + \frac{H_{10} \overline{d_4}}{2} + \frac{H_9 \overline{d_3}}{2} + \frac{H_8 \overline{d_2}}{2} + \frac{H_7 \overline{d_1}}{2} + \frac{H_6 d_0}{2} + 3H_{11} d_5 + 3H_{10} d_4 + 3H_9 d_3 \right. \\
& \quad \left. + 3H_8 d_2 + 3H_7 d_1 + 3H_6 d_0 \right) \frac{1}{z^6} \\
& + \left( \frac{H_{12} \overline{d_5}}{2} + \frac{H_{11} \overline{d_4}}{2} + \frac{H_{10} \overline{d_3}}{2} + \frac{H_9 \overline{d_2}}{2} + \frac{H_8 \overline{d_1}}{2} + \frac{H_7 d_0}{2} + \frac{7H_{12} d_5}{2} + \frac{7H_{11} d_4}{2} + \frac{7H_{10} d_3}{2} \right. \\
& \quad \left. + \frac{7H_9 d_2}{2} + \frac{7H_8 d_1}{2} + \frac{7H_7 d_0}{2} \right) \frac{1}{z^7}.
\end{aligned} \tag{2.28}$$

Finally, for a given thermal or mechanical loading condition, having expressed all four complex potentials in series form, the problem is reduced to determining the unknown coefficients  $a_k, b_k, c_k$  and  $d_k$  such that the interface conditions (2.3) and (2.8) are satisfied. When these unknown coefficients are found, the real form of these stress potentials can be determined completely and further the elastic stresses, displacements and ultimately the stress intensity factor at the crack tips can be calculated.



# CHAPTER 3

## 3 Algebraic Equations and Applied Loads

### 3.1 Introduction

This chapter presents the general form and specific examples of the set of linear algebraic equations to be solved numerically to determine the unknown coefficients of the stress potentials. The two examples presented for the case of a homogeneously imperfect inclusion-matrix interface are based on interface parameters taking the values  $m = n$  and  $m = 3n$  (see sections 3.5.1 and 3.5.2). The RVE is subjected to pure thermal or mechanical loads. The thermal load is modeled by a prescribed uniform volume expansion, which represents a stress-free thermal strain of the inclusion. The mechanical load, which is a uniaxial tensile load, is modeled by a prescribed remote load normal to the face of the crack. This type of tensile load was considered because it is known to have a significant effect on the magnitude of the mode I stress intensity factor of a radial crack.

By substituting the truncated series representations of the stress potentials derived in Chapter 2 into the interface conditions, infinite series are obtained.

### 3.2 Interface Conditions Expressed as Infinite Series

When the stress potentials are substituted into the interface conditions in (2.4) and (2.8), the traction continuity and the displacement discontinuity relationships both yield two infinite series when terms on the left-hand and right-hand sides are considered. The



left-hand-side of the traction continuity condition in (2.4) leads to the expression (see Appendix B for details)

$$\begin{aligned}
\phi_1'(z) + \overline{\phi_1'} \left( \frac{R^2}{z} \right) - z \phi_1''(z) - \frac{z^2}{R^2} \psi_1'(z) = & -\frac{5\overline{a_5}}{R^{12}} z^6 - \frac{4\overline{a_4}}{R^{10}} z^5 - \frac{3\overline{a_3}}{R^8} z^4 - \frac{2\overline{a_2}}{R^6} z^3 \\
& - \left( \frac{\overline{a_1}}{R^4} + \frac{B}{R^2} \right) z^2 + 2A + \frac{b_1}{R^2} + \frac{2b_2}{R^2} \frac{1}{z} + 3 \left( \frac{b_3}{R^2} - a_1 \right) \frac{1}{z^2} \quad (3.1) \\
& + 4 \left( \frac{b_4}{R^2} - 2a_2 \right) \frac{1}{z^3} + 5 \left( \frac{b_5}{R^2} - 3a_3 \right) \frac{1}{z^4} - 24a_4 \frac{1}{z^5}.
\end{aligned}$$

The right-hand-side of the traction continuity condition in (2.4) yields (see Appendix B for details)

$$\begin{aligned}
\phi_2'(z) + \overline{\phi_2'} \left( \frac{R^2}{z} \right) - z \phi_2''(z) - \frac{z^2}{R^2} \psi_2'(z) = & \left[ \frac{5}{2R^2} (\overline{c_5} + 5c_5) - \frac{5}{2R^{12}} (H_{10}d_5 + H_9d_4 + H_8d_3 + H_7d_2 + H_6d_1 + H_5d_0) \right] z^6 \\
& + \left[ \frac{2}{R^2} (\overline{c_4} - H_1\overline{d_5} + 4c_4 + 4H_1d_5) - \frac{2}{R^{10}} \left( \begin{aligned} & H_9\overline{d_5} + H_8\overline{d_4} + H_7\overline{d_3} \\ & + H_6\overline{d_2} + H_5\overline{d_1} + H_4d_0 \end{aligned} \right) \right] z^5 \\
& + \left[ \begin{aligned} & -\frac{15}{2}c_5 - \frac{2}{R^2} (\overline{c_4} - H_1\overline{d_5} + 4c_4 + 4H_1d_5) \\ & -\frac{3}{2R^8} (H_8\overline{d_5} + H_7\overline{d_4} + H_6\overline{d_3} + H_5\overline{d_2} + H_4\overline{d_1} + H_3d_0) \\ & +\frac{3}{2R^2} (\overline{c_3} - H_2\overline{d_5} - H_1\overline{d_4} + 3c_3 + 3H_2d_5 + 3H_1d_4) \end{aligned} \right] z^4
\end{aligned}$$





$$\begin{aligned}
& + \left[ -4(c_4 + H_1 d_5) - \frac{1}{R^6} (H_7 \bar{d}_5 + H_6 \bar{d}_4 + H_5 \bar{d}_3 + H_4 \bar{d}_2 + H_3 \bar{d}_1 + H_2 d_0) \right. \\
& \quad \left. - \frac{2}{R^2} \left( -\frac{\bar{c}_2}{2} + \frac{H_3 \bar{d}_5}{2} + \frac{H_2 \bar{d}_4}{2} + \frac{H_1 \bar{d}_3}{2} - c_2 - H_3 d_5 - H_2 d_4 - H_1 d_3 \right) \right] z^3 \\
& + \left[ -\frac{3}{2} (c_3 + H_2 d_5 + H_1 d_4) - \frac{1}{2R^4} (H_6 \bar{d}_5 + H_5 \bar{d}_4 + H_4 \bar{d}_3 + H_3 \bar{d}_2 + H_2 \bar{d}_1 + H_1 d_0) \right. \\
& \quad \left. - \frac{1}{R^2} \left( -\frac{\bar{c}_1}{2} + \frac{H_4 \bar{d}_5}{2} + \frac{H_3 \bar{d}_4}{2} + \frac{H_2 \bar{d}_3}{2} + \frac{H_1 \bar{d}_2}{2} \right) \right. \\
& \quad \left. - \frac{1}{R^2} \left( -\frac{c_1}{2} - \frac{H_4 d_5}{2} - \frac{H_3 d_4}{2} - \frac{H_2 d_3}{2} - \frac{H_1 d_2}{2} \right) \right] z^2 \\
& + \left[ \frac{1}{2} (c_1 + H_4 d_5 + H_3 d_4 + H_2 d_3 + H_1 d_2) + \frac{1}{2} (\bar{c}_1 + H_4 \bar{d}_5 + H_3 \bar{d}_4 + H_2 \bar{d}_3 + H_1 \bar{d}_2) \right. \\
& \quad \left. + \frac{1}{R^2} \left( \frac{H_6 \bar{d}_5}{2} + \frac{H_5 \bar{d}_4}{2} + \frac{H_4 \bar{d}_3}{2} + \frac{H_3 \bar{d}_2}{2} + \frac{H_2 \bar{d}_1}{2} + \frac{H_1 d_0}{2} \right) \right. \\
& \quad \left. + \frac{1}{R^2} \left( \frac{H_6 d_5}{2} + \frac{H_5 d_4}{2} + \frac{H_4 d_3}{2} + \frac{H_3 d_2}{2} + \frac{H_2 d_1}{2} + \frac{H_1 d_0}{2} \right) \right] \\
& + \left[ R^2 (\bar{c}_2 + H_3 \bar{d}_5 + H_2 \bar{d}_4 + H_1 \bar{d}_3) \right. \\
& \quad \left. + \frac{2}{R^2} \left( \frac{H_7 \bar{d}_5}{2} + \frac{H_6 \bar{d}_4}{2} + \frac{H_5 \bar{d}_3}{2} + \frac{H_4 \bar{d}_2}{2} + \frac{H_3 \bar{d}_1}{2} + \frac{H_2 d_0}{2} \right) \right. \\
& \quad \left. + \frac{2}{R^2} (H_7 d_5 + H_6 d_4 + H_5 d_3 + H_4 d_2 + H_3 d_1 + H_2 d_0) \right] \frac{1}{z} \\
& + \left[ -\frac{3}{2} (H_6 d_5 + H_5 d_4 + H_4 d_3 + H_3 d_2 + H_2 d_1 + H_1 d_0) + \frac{3R^4}{2} (\bar{c}_3 + H_2 \bar{d}_5 + H_1 \bar{d}_4) \right. \\
& \quad \left. + \frac{3}{R^2} \left( \frac{H_8 \bar{d}_5}{2} + \frac{H_7 \bar{d}_4}{2} + \frac{H_6 \bar{d}_3}{2} + \frac{H_5 \bar{d}_2}{2} + \frac{H_4 \bar{d}_1}{2} + \frac{H_3 d_0}{2} \right) \right. \\
& \quad \left. + \frac{3}{R^2} \left( \frac{3H_8 d_5}{2} + \frac{3H_7 d_4}{2} + \frac{3H_6 d_3}{2} + \frac{3H_5 d_2}{2} + \frac{3H_4 d_1}{2} + \frac{3H_3 d_0}{2} \right) \right] \frac{1}{z^2}
\end{aligned}$$



$$\begin{aligned}
& + \left[ \begin{aligned} & -4(H_7 d_5 + H_6 d_4 + H_5 d_3 + H_4 d_2 + H_3 d_1 + H_2 d_0) + 2R^6(\bar{c}_4 + H_1 \bar{d}_5) \\ & + \frac{4}{R^2} \left( \frac{H_9 \bar{d}_5}{2} + \frac{H_8 \bar{d}_4}{2} + \frac{H_7 \bar{d}_3}{2} + \frac{H_6 \bar{d}_2}{2} + \frac{H_5 \bar{d}_1}{2} + \frac{H_4 d_0}{2} \right) \\ & 2H_9 d_5 + 2H_8 d_4 + 2H_7 d_3 + 2H_6 d_2 + 2H_5 d_1 + 2H_4 d_0 \end{aligned} \right] \frac{1}{z^3} \\
& + \left[ \begin{aligned} & -\frac{15}{2}(H_8 d_5 + H_7 d_4 + H_6 d_3 + H_5 d_2 + H_4 d_1 + H_3 d_0) + \frac{5}{2}R^8 \bar{c}_5 \\ & + \frac{5}{R^2} \left( \frac{H_{10} \bar{d}_5}{2} + \frac{H_9 \bar{d}_4}{2} + \frac{H_8 \bar{d}_3}{2} + \frac{H_7 \bar{d}_2}{2} + \frac{H_6 \bar{d}_1}{2} + \frac{H_5 d_0}{2} \right) \\ & \frac{5H_{10} d_5}{2} + \frac{5H_9 d_4}{2} + \frac{5H_8 d_3}{2} + \frac{5H_7 d_2}{2} + \frac{5H_6 d_1}{2} + \frac{5H_5 d_0}{2} \end{aligned} \right] \frac{1}{z^4}. \quad (3.2)
\end{aligned}$$

The first two infinite series from the traction continuity equation are as in (3.1) and (3.2). The third infinite series to be obtained from the left-hand-side of the displacement discontinuity condition in (2.8) is the same as in (3.1). In order to avoid lengthy succession of equations in this section of the dissertation, the expansions required to obtain the fourth infinite series from the right-hand-side of (2.8) are presented in Appendix B.

### 3.3 General form of algebraic equations

A power series converges uniformly for any point  $z$  inside and on any circle about the origin, which lies entirely inside its circle of convergence [59]. Knowing that the above series are uniformly convergent, we can conveniently (with negligible loss of accuracy) truncate the infinite series for a given number of terms in order to be able to carry out a numerical analysis. In this study, the set of linear algebraic equations is



obtained by equating the coefficients of powers of  $z$  from  $z^4$  to  $z^{-4}$  of the four infinite series. Equating coefficients of  $z$  in (3.1) and (3.2), we get the following set of equations

### 3.3.1 Traction continuity condition

For  $z^4$ :

$$\begin{aligned} -\frac{3\overline{a_3}}{R^8} = & -\frac{15}{2}c_5 - \frac{2}{R^2}(\overline{c_4} - H_1\overline{d_5} + 4c_4 + 4H_1d_5) \\ & - \frac{3}{2R^8}(H_8\overline{d_5} + H_7\overline{d_4} + H_6\overline{d_3} + H_5\overline{d_2} + H_4\overline{d_1} + H_3d_0) \\ & + \frac{3}{2R^2}(\overline{c_3} - H_2\overline{d_5} - H_1\overline{d_4} + 3c_3 + 3H_2d_5 + 3H_1d_4). \end{aligned} \quad (3.3)$$

For  $z^3$ :

$$\begin{aligned} -\frac{2\overline{a_2}}{R^6} = & -4(c_4 + H_1d_5) - \frac{1}{R^6}(H_7\overline{d_5} + H_6\overline{d_4} + H_5\overline{d_3} + H_4\overline{d_2} + H_3\overline{d_1} + H_2d_0) \\ & - \frac{2}{R^2}\left(-\frac{\overline{c_2}}{2} + \frac{H_3\overline{d_5}}{2} + \frac{H_2\overline{d_4}}{2} + \frac{H_1\overline{d_3}}{2} - c_2 - H_3d_5 - H_2d_4 - H_1d_3\right). \end{aligned} \quad (3.4)$$

For  $z^2$ :

$$\begin{aligned} -\left(\frac{\overline{a_1}}{R^4} + \frac{B}{R^2}\right) = & -\frac{3}{2}(c_3 + H_2d_5 + H_1d_4) - \frac{1}{2R^4}\left(\begin{aligned} & H_6\overline{d_5} + H_5\overline{d_4} + H_4\overline{d_3} \\ & + H_3\overline{d_2} + H_2\overline{d_1} + H_1d_0 \end{aligned}\right) \\ & - \frac{1}{R^2}\left(\begin{aligned} & -\frac{\overline{c_1}}{2} + \frac{H_4\overline{d_5}}{2} + \frac{H_3\overline{d_4}}{2} + \frac{H_2\overline{d_3}}{2} + \frac{H_1\overline{d_2}}{2} \\ & -\frac{c_1}{2} - \frac{H_4d_5}{2} - \frac{H_3d_4}{2} - \frac{H_2d_3}{2} - \frac{H_1d_2}{2} \end{aligned}\right). \end{aligned} \quad (3.5)$$





For  $z$  :

The comparison of coefficients for  $z$  yields no equation since the left-hand-side of (3.1) and the right-hand-side of (3.2) are automatically satisfied and therefore does not provide any new information.

For constant term ( $z^0$ ):

$$2A + \frac{b_1}{R^2} = \frac{1}{2}(c_1 + H_4 d_5 + H_3 d_4 + H_2 d_3 + H_1 d_2) + \frac{1}{2} \begin{pmatrix} \overline{c_1} + H_4 \overline{d_5} \\ + H_3 \overline{d_4} + H_2 \overline{d_3} + H_1 \overline{d_2} \end{pmatrix} \quad (3.6)$$

$$+ \frac{1}{R^2} \begin{pmatrix} \frac{H_6 \overline{d_5}}{2} + \frac{H_5 \overline{d_4}}{2} + \frac{H_4 \overline{d_3}}{2} + \frac{H_3 \overline{d_2}}{2} + \frac{H_2 \overline{d_1}}{2} + \frac{H_1 d_0}{2} \\ + \frac{H_6 d_5}{2} + \frac{H_5 d_4}{2} + \frac{H_4 d_3}{2} + \frac{H_3 d_2}{2} + \frac{H_2 d_1}{2} + \frac{H_1 d_0}{2} \end{pmatrix}.$$

For  $\frac{1}{z}$  :

$$\frac{2b_2}{R^2} = R^2 (\overline{c_2} + H_3 \overline{d_5} + H_2 \overline{d_4} + H_1 \overline{d_3}) \quad (3.7)$$

$$+ \frac{2}{R^2} \begin{pmatrix} \frac{H_7 \overline{d_5}}{2} + \frac{H_6 \overline{d_4}}{2} + \frac{H_5 \overline{d_3}}{2} + \frac{H_4 \overline{d_2}}{2} + \frac{H_3 \overline{d_1}}{2} + \frac{H_2 d_0}{2} \\ + H_7 d_5 + H_6 d_4 + H_5 d_3 + H_4 d_2 + H_3 d_1 + H_2 d_0 \end{pmatrix}.$$



For  $\frac{1}{z^2}$ :

$$3\left(\frac{b_3}{R^2} - a_1\right) = -\frac{3}{2}\left(\frac{H_6 d_5 + H_5 d_4}{+ H_4 d_3 + H_3 d_2 + H_2 d_1 + H_1 d_0}\right) + \frac{3R^4}{2}(\overline{c_3} + H_2 \overline{d_5} + H_1 \overline{d_4})$$

$$+ \frac{3}{R^2}\left(\frac{\frac{H_8 \overline{d_5}}{2} + \frac{H_7 \overline{d_4}}{2} + \frac{H_6 \overline{d_3}}{2} + \frac{H_5 \overline{d_2}}{2} + \frac{H_4 \overline{d_1}}{2} + \frac{H_3 d_0}{2}}{+ \frac{3H_8 d_5}{2} + \frac{3H_7 d_4}{2} + \frac{3H_6 d_3}{2} + \frac{3H_5 d_2}{2} + \frac{3H_4 d_1}{2} + \frac{3H_3 d_0}{2}}\right).$$
(3.8)

For  $\frac{1}{z^3}$ :

$$4\left(\frac{b_4}{R^2} - 2a_2\right) = -4\left(\frac{H_7 d_5 + H_6 d_4 + H_5 d_3}{+ H_4 d_2 + H_3 d_1 + H_2 d_0}\right) + 2R^6(\overline{c_4} + H_1 \overline{d_5})$$

$$+ \frac{4}{R^2}\left(\frac{\frac{H_9 \overline{d_5}}{2} + \frac{H_8 \overline{d_4}}{2} + \frac{H_7 \overline{d_3}}{2} + \frac{H_6 \overline{d_2}}{2} + \frac{H_5 \overline{d_1}}{2} + \frac{H_4 d_0}{2}}{+ 2H_9 d_5 + 2H_8 d_4 + 2H_7 d_3 + 2H_6 d_2 + 2H_5 d_1 + 2H_4 d_0}\right).$$
(3.9)



For  $\frac{1}{z^4}$ :

$$5\left(\frac{b_5}{R^2} - 3a_3\right) = -\frac{15}{2}\left(\frac{H_8 d_5 + H_7 d_4 + H_6 d_3}{+ H_5 d_2 + H_4 d_1 + H_3 d_0}\right) + \frac{5R^8}{2}\overline{c_5} \\ + \frac{5}{R^2}\left(\frac{\frac{H_{10}\overline{d_5}}{2} + \frac{H_9\overline{d_4}}{2} + \frac{H_8\overline{d_3}}{2} + \frac{H_7\overline{d_2}}{2} + \frac{H_6\overline{d_1}}{2} + \frac{H_5 d_0}{2}}{+ \frac{5H_{10}d_5}{2} + \frac{5H_9d_4}{2} + \frac{5H_8d_3}{2} + \frac{5H_7d_2}{2} + \frac{5H_6d_1}{2} + \frac{5H_5d_0}{2}}\right). \quad (3.10)$$

The traction continuity condition therefore yields a total of eight equations, (3.3) – (3.10).

### 3.3.2 Displacement discontinuity condition

Details of the expansions required to enable comparison of the coefficients of  $z$  can be found in Appendix B. In order to simplify the derived expressions, we introduce two new variables  $F$  and  $G$  which are given by  $F = \frac{m+n}{4R}$  and  $G = R\left(\frac{m-n}{4}\right)$ . Upon equating coefficients of  $z$ , we get the following set of equations:

For  $z^4$ :

$$-\frac{3\overline{a_3}}{R^8} = \frac{Fk_1\overline{a_3}}{\mu_1 R^6} - \frac{Fk_2}{2\mu_2 R^6}\left(\frac{H_8\overline{d_5} + H_7\overline{d_4} + H_6\overline{d_3}}{+ H_5\overline{d_2} + H_4\overline{d_1} + H_3 d_0}\right) \\ + \frac{5FR^2\overline{c_5}}{2\mu_2} - \frac{F}{2\mu_2}\left(\frac{\overline{c_3} - H_2\overline{d_5} - H_1\overline{d_4}}{+ 3\overline{c_3} + 3H_2d_5 + 3H_1d_4}\right) + \frac{3G\overline{a_3}}{\mu_1 R^8}$$



$$\begin{aligned}
& -\frac{G\overline{b_5}}{\mu_1 R^{10}} - \frac{Gk_2 c_5}{2\mu_2} - \frac{3G}{2\mu_2 R^8} \left( \begin{aligned} & H_8 \overline{d_5} + H_7 \overline{d_4} + H_6 \overline{d_3} \\ & + H_5 \overline{d_2} + H_4 \overline{d_1} + H_3 d_0 \end{aligned} \right) \\
& + \frac{G}{\mu_2 R^{10}} \left( \begin{aligned} & \frac{H_{10} \overline{d_5}}{2} + \frac{H_9 \overline{d_4}}{2} + \frac{H_8 \overline{d_3}}{2} + \frac{H_7 \overline{d_2}}{2} + \frac{H_6 \overline{d_1}}{2} + \frac{H_5 d_0}{2} \\ & + \frac{5H_{10} d_5}{2} + \frac{5H_9 d_4}{2} + \frac{5H_8 d_3}{2} + \frac{5H_7 d_2}{2} + \frac{5H_6 d_1}{2} + \frac{5H_5 d_0}{2} \end{aligned} \right).
\end{aligned} \tag{3.11}$$

For  $z^3$ :

$$\begin{aligned}
& -\frac{2\overline{a_2}}{R^6} = \frac{Fk_1 \overline{a_2}}{\mu_1 R^4} - \frac{Fk_2}{2\mu_2 R^4} (H_7 \overline{d_5} + H_6 \overline{d_4} + H_5 \overline{d_3} + H_4 \overline{d_2} + H_3 \overline{d_1} + H_2 d_0) \\
& + \frac{2FR^2}{\mu_2} (c_5 + H_1 d_5) + \frac{F}{\mu_2} \left( \begin{aligned} & -\frac{\overline{c_2}}{2} + \frac{H_3 \overline{d_5}}{2} + \frac{H_2 \overline{d_4}}{2} + \frac{H_1 \overline{d_3}}{2} \\ & -c_2 - H_3 d_5 - H_2 d_4 - H_1 d_3 \end{aligned} \right) \\
& + \frac{2G\overline{a_2}}{\mu_1 R^6} - \frac{G\overline{b_4}}{\mu_1 R^8} - \frac{Gk_2}{2\mu_2} (c_4 + H_1 d_5) \\
& - \frac{G}{\mu_2 R^6} (H_7 \overline{d_5} + H_6 \overline{d_4} + H_5 \overline{d_3} + H_4 \overline{d_2} + H_3 \overline{d_1} + H_2 d_0) \\
& + \frac{G}{\mu_2 R^8} \left( \begin{aligned} & \frac{H_9 \overline{d_5}}{2} + \frac{H_8 \overline{d_4}}{2} + \frac{H_7 \overline{d_3}}{2} + \frac{H_6 \overline{d_2}}{2} + \frac{H_5 \overline{d_1}}{2} + \frac{H_4 d_0}{2} \\ & + 2H_{10} d_5 + 2H_9 d_4 + 2H_8 d_3 + 2H_7 d_2 + 2H_6 d_1 + 2H_5 d_0 \end{aligned} \right).
\end{aligned} \tag{3.12}$$





For  $z^2$ :

$$\begin{aligned}
& -\left(\frac{\overline{a_1}}{R^6} + \frac{B}{R^2}\right) = \frac{Fk_1\overline{a_1}}{\mu_1 R^2} - \frac{FB}{\mu_1} - \frac{Fk_2}{2\mu_2 R^2} \left( \begin{aligned} & H_6\overline{d_5} + H_5\overline{d_4} + H_4\overline{d_3} \\ & + H_3\overline{d_2} + H_2\overline{d_1} + H_1d_0 \end{aligned} \right) \\
& + \frac{3FR^2}{2\mu_2} (c_3 + H_2d_5 + H_1d_4) + \frac{F}{\mu_2} \left( \begin{aligned} & -\frac{\overline{c_1}}{2} + \frac{H_4\overline{d_5}}{2} + \frac{H_3\overline{d_4}}{2} + \frac{H_2\overline{d_3}}{2} + \frac{H_1\overline{d_2}}{2} \\ & -\frac{c_1}{2} - \frac{H_4d_5}{2} - \frac{H_3d_4}{2} - \frac{H_2d_3}{2} - \frac{H_1d_2}{2} \end{aligned} \right) \\
& + \frac{G\overline{a_1}}{\mu_1 R^4} - \frac{G\overline{b_3}}{\mu_1 R^6} - \frac{Gk_2}{2\mu_2} (c_3 + H_2d_5 + H_1d_4) \\
& - \frac{G}{2\mu_2 R^4} (H_6\overline{d_5} + H_5\overline{d_4} + H_4\overline{d_3} + H_3\overline{d_2} + H_2\overline{d_1} + H_1d_0) \\
& + \frac{G}{\mu_2 R^6} \left( \begin{aligned} & \frac{H_8d_5}{2} + \frac{H_7d_4}{2} + \frac{H_6d_3}{2} + \frac{H_5d_2}{2} + \frac{H_4d_1}{2} + \frac{H_3d_0}{2} \\ & \frac{3H_8\overline{d_5}}{2} + \frac{3H_7\overline{d_4}}{2} + \frac{3H_6\overline{d_3}}{2} + \frac{3H_5\overline{d_2}}{2} + \frac{3H_4\overline{d_1}}{2} + \frac{3H_3d_0}{2} + \end{aligned} \right) \quad (3.13) \\
& - 2F(\varepsilon_2 - i\varepsilon_3).
\end{aligned}$$



For  $z$  :

$$\begin{aligned}
0 = & -\frac{Fk_2}{2\mu_2} \left( c_0 + H_5 \overline{d_5} + H_4 \overline{d_4} + H_3 \overline{d_3} + H_2 \overline{d_2} + H_1 \overline{d_1} \right) \\
& + \frac{FR^2}{\mu_2} (c_2 + H_3 d_5 + H_2 d_4 + H_1 d_3) \\
& + \frac{F}{\mu_2} \left( -\frac{\overline{c_0}}{2} + \frac{H_5 \overline{d_5}}{2} + \frac{H_4 \overline{d_4}}{2} + \frac{H_3 \overline{d_3}}{2} + \frac{H_2 \overline{d_2}}{2} + \frac{H_1 \overline{d_1}}{2} \right) \\
& - \frac{G\overline{b_2}}{\mu_1 R^4} - \frac{Gk_2}{2\mu_2} (c_2 + H_3 d_5 + H_2 d_4 + H_1 d_3) \\
& + \frac{G}{\mu_2 R^4} \left( \frac{H_7 d_5}{2} + \frac{H_6 d_4}{2} + \frac{H_5 d_3}{2} + \frac{H_4 d_2}{2} + \frac{H_3 d_1}{2} + \frac{H_2 d_0}{2} \right. \\
& \left. H_7 \overline{d_5} + H_6 \overline{d_4} + H_5 \overline{d_3} + H_4 \overline{d_2} + H_3 \overline{d_1} + H_2 d_0 \right).
\end{aligned} \tag{3.14}$$

For constant term ( $z^0$ ):

$$\begin{aligned}
\left( 2A + \frac{b_1}{R^2} \right) = & \frac{Fk_1 AR^2}{\mu_1} - \frac{FAR^2}{\mu_1} - \frac{Fb_1}{\mu_1} - \frac{Fk_2 R^2}{2\mu_2} \left( \overline{c_1} + H_4 \overline{d_5} + H_3 \overline{d_4} + H_2 \overline{d_3} + H_1 \overline{d_2} \right) \\
& + \frac{FR^2}{2\mu_2} (c_1 + H_4 d_5 + H_3 d_4 + H_2 d_3 + H_1 d_2) \\
& + \frac{F}{\mu_2} \left( \frac{H_6 \overline{d_5}}{2} + \frac{H_5 \overline{d_4}}{2} + \frac{H_4 \overline{d_3}}{2} + \frac{H_3 \overline{d_2}}{2} + \frac{H_2 \overline{d_1}}{2} + \frac{H_1 d_0}{2} \right. \\
& \left. \frac{H_6 d_5}{2} + \frac{H_5 d_4}{2} + \frac{H_4 d_3}{2} + \frac{H_3 d_2}{2} + \frac{H_2 d_1}{2} + \frac{H_1 d_0}{2} \right)
\end{aligned}$$



$$\begin{aligned}
& + \frac{Gk_1 A}{\mu_1} - \frac{GA}{\mu_1} - \frac{G\bar{b}_1}{\mu_1 R^2} - \frac{Gk_2}{2\mu_2} (c_1 + H_4 d_5 + H_3 d_4 + H_2 d_3 + H_1 d_2) \\
& + \frac{G}{2\mu_2} (\bar{c}_1 + H_4 \bar{d}_5 + H_3 \bar{d}_4 + H_2 \bar{d}_3 + H_1 \bar{d}_2)
\end{aligned} \tag{3.15}$$

$$+ \frac{G}{\mu_2 R^2} \left( \begin{aligned} & \frac{H_6 d_5}{2} + \frac{H_5 d_4}{2} + \frac{H_4 d_3}{2} + \frac{H_3 d_2}{2} + \frac{H_2 d_1}{2} + \frac{H_1 d_0}{2} \\ & + \frac{H_6 \bar{d}_5}{2} + \frac{H_5 \bar{d}_4}{2} + \frac{H_4 \bar{d}_3}{2} + \frac{H_3 \bar{d}_2}{2} + \frac{H_2 \bar{d}_1}{2} + \frac{H_1 \bar{d}_0}{2} \end{aligned} \right) - mR\epsilon_1 .$$

For  $\frac{1}{z}$ :

$$\begin{aligned}
\frac{2b_2}{R^2} = & -\frac{Fb_2}{\mu_1} - \frac{Fk_2 R^4}{2\mu_2} (\bar{c}_2 + H_3 \bar{d}_5 + H_2 \bar{d}_4 + H_1 \bar{d}_3) \\
& + \frac{F}{\mu_2} \left( \begin{aligned} & \frac{H_7 \bar{d}_5}{2} + \frac{H_6 \bar{d}_4}{2} + \frac{H_5 \bar{d}_3}{2} + \frac{H_4 \bar{d}_2}{2} + \frac{H_3 \bar{d}_1}{2} + \frac{H_2 \bar{d}_0}{2} \\ & + H_7 d_5 + H_6 d_4 + H_5 d_3 + H_4 d_2 + H_3 d_1 + H_2 d_0 \end{aligned} \right) \\
& - \frac{Gk_2}{2\mu_2} (c_0 + H_5 d_5 + H_4 d_4 + H_3 d_3 + H_2 d_2 + H_1 d_1) \\
& + \frac{GR^2}{\mu_2} (\bar{c}_2 + H_3 \bar{d}_5 + H_2 \bar{d}_4 + H_1 \bar{d}_3) \\
& + \frac{G}{\mu_2} \left( -\frac{c_0}{2} + \frac{H_5 d_5}{2} + \frac{H_4 d_4}{2} + \frac{H_3 d_3}{2} + \frac{H_2 d_2}{2} + \frac{H_1 d_1}{2} \right).
\end{aligned} \tag{3.16}$$



For  $\frac{1}{z^2}$ :

$$\begin{aligned}
3\left(\frac{b_3}{R^2} - a_1\right) &= \frac{Fa_1R^2}{\mu_1} - \frac{Fb_3}{\mu_1} - \frac{Fk_2R^6}{2\mu_2}(\overline{c_3} + H_2\overline{d_5} + H_1\overline{d_4}) \\
&\quad - \frac{FR^2}{2\mu_2}(H_6d_5 + H_5d_4 + H_4d_3 + H_3d_2 + H_2d_1 + H_1d_0) \\
&\quad + \frac{F}{\mu_2}\left(\frac{H_8\overline{d_5}}{2} + \frac{H_7\overline{d_4}}{2} + \frac{H_6\overline{d_3}}{2} + \frac{H_5\overline{d_2}}{2} + \frac{H_4\overline{d_1}}{2} + \frac{H_3d_0}{2}\right. \\
&\quad \left. + \frac{3H_8d_5}{2} + \frac{3H_7d_4}{2} + \frac{3H_6d_3}{2} + \frac{3H_5d_2}{2} + \frac{3H_4d_1}{2} + \frac{3H_3d_0}{2}\right) \\
&\quad + \frac{Gk_1a_1}{\mu_1} - \frac{G\overline{B}R^2}{\mu_1} - \frac{Gk_2}{2\mu_2}(H_6d_5 + H_5d_4 + H_4d_3 + H_3d_2 + H_2d_1 + H_1d_0) \\
&\quad + \frac{3GR^4}{2\mu_2}(\overline{c_3} + H_2\overline{d_5} + H_1\overline{d_4}) \\
&\quad + \frac{GR^2}{\mu_2}\left(-\frac{c_1}{2} + \frac{H_4d_5}{2} + \frac{H_3d_4}{2} + \frac{H_2d_3}{2} + \frac{H_1d_2}{2}\right. \\
&\quad \left.- \frac{\overline{c_1}}{2} - \frac{H_4\overline{d_5}}{2} - \frac{H_3\overline{d_4}}{2} - \frac{H_2\overline{d_3}}{2} - \frac{H_1\overline{d_2}}{2}\right) - 2GR^2(\varepsilon_2 + i\varepsilon_3).
\end{aligned} \tag{3.17}$$





For  $\frac{1}{z^3}$ :

$$\begin{aligned}
4\left(\frac{b_4}{R^2} - 2a_2\right) &= \frac{2Fa_2R^2}{\mu_1} - \frac{Fb_4}{\mu_1} - \frac{Fk_2R^8}{2\mu_2}(\overline{c_4} + H_1\overline{d_5}) \\
&\quad - \frac{FR^2}{\mu_2}(H_7d_5 + H_6d_4 + H_5d_3 + H_4d_2 + H_3d_1 + H_2d_0) \\
&\quad + \frac{F}{\mu_2} \left( \frac{H_9\overline{d_5}}{2} + \frac{H_8\overline{d_4}}{2} + \frac{H_7\overline{d_3}}{2} + \frac{H_6\overline{d_2}}{2} + \frac{H_5\overline{d_1}}{2} + \frac{H_4d_0}{2} \right. \\
&\quad \left. + 2H_9d_5 + 2H_8d_4 + 2H_7d_3 + 2H_6d_2 + 2H_5d_1 + 2H_4d_0 \right) \\
&\quad + \frac{Gk_1a_2}{\mu_1} - \frac{Gk_2}{2\mu_2}(H_7d_5 + H_6d_4 + H_5d_3 + H_4d_2 + H_3d_1 + H_2d_0) \\
&\quad + \frac{2GR^6}{\mu_2}(\overline{c_4} + H_1\overline{d_5}) + \frac{GR^4}{\mu_2} \left( \begin{aligned} &-\frac{\overline{c_2}}{2} + \frac{H_3\overline{d_5}}{2} + \frac{H_2\overline{d_4}}{2} + \frac{H_1\overline{d_3}}{2} \\ &-c_2 - \frac{H_3d_5}{2} - \frac{H_2d_4}{2} - \frac{H_1d_3}{2} \end{aligned} \right). \tag{3.18}
\end{aligned}$$



For  $\frac{1}{z^4}$  :

$$\begin{aligned}
5\left(\frac{b_5}{R^2} - 3a_3\right) &= \frac{3Fa_3R^2}{\mu_1} - \frac{Fb_5}{\mu_1} - \frac{Fk_2R^{10}}{2\mu_2}\overline{c_5} + \frac{5GR^8}{2\mu_2}\overline{c_5} \\
&\quad - \frac{3FR^2}{2\mu_2}(H_8d_5 + H_7d_4 + H_6d_3 + H_5d_2 + H_4d_1 + H_3d_0) \\
&\quad + \frac{F}{\mu_2} \left( \frac{H_{10}\overline{d_5}}{2} + \frac{H_9\overline{d_4}}{2} + \frac{H_8\overline{d_3}}{2} + \frac{H_7\overline{d_2}}{2} + \frac{H_6\overline{d_1}}{2} + \frac{H_5d_0}{2} \right. \\
&\quad \left. + \frac{5H_{10}d_5}{2} + \frac{5H_9d_4}{2} + \frac{5H_8d_3}{2} + \frac{5H_7d_2}{2} + \frac{5H_6d_1}{2} + \frac{5H_5d_0}{2} \right) \\
&\quad + \frac{Gk_1a_3}{\mu_1} - \frac{Gk_2}{2\mu_2}(H_8d_5 + H_7d_4 + H_6d_3 + H_5d_2 + H_4d_1 + H_3d_0) \\
&\quad - \frac{GR^6}{2\mu_2} \left( \overline{c_3} - H_2d_5 - H_1d_4 + 3\overline{c_3} - \frac{3H_2\overline{d_5}}{2} + \frac{3H_1\overline{d_4}}{2} - \frac{H_1d_3}{2} \right).
\end{aligned} \tag{3.19}$$

The displacement discontinuity condition yields a total of nine equations (3.11) – (3.19) and in all, a total of 17 equations (3.3) – (3.19) were obtained after equating coefficients of  $z$ . This provides the general form of the set of equations, out of which, reduced forms can be derived, based on the interface parameter chosen.



### 3.4 Applied Loads

The induced stresses within an inclusion containing an interior radial crack imperfectly bonded to the surrounding matrix are studied by the application of a thermal or mechanical load. With the application of these loads, the magnitude of the elastic stress fields in the neighborhood of the crack tips - the stress intensity factor can be calculated. Knowledge of the stress intensity factor at the crack tips is useful information in estimating the load-bearing capabilities of fiber-reinforced composite devices and also in ascertaining the direction of crack growth under such loads.

#### 3.4.1 Thermal load

It is well known that, to a certain extent, fracture of many fibrous materials is temperature dependent within a certain temperature range. Consequently, failure caused by thermal-stress-induced fiber cracking is of major importance in the manufacture of fiber-reinforced composites and in, for example, components subjected to thermal loading in microelectronic packaging. The thermal stresses, which induce fiber cracking, are known to be caused by thermal mismatch between the fiber and the surrounding matrix as the result of a uniform change in temperature [16].

In [13], an inclusion is defined as a subdomain  $S_2$  in a domain  $S_1$  where an eigenstrain (also known as a stress-free transformation strain, misfit strain or a nonelastic strain) is prescribed. The eigenstrains  $\epsilon_x^o, \epsilon_y^o, \epsilon_{xy}^o$  are introduced into the matrix domain  $S_1$  and the inclusion  $S_2$  as a result of the thermal loading. These eigenstrains are proportional to the change in temperature and the difference between the thermal



expansion coefficients of the matrix and the inclusion. An example of an eigenstrain, which is referred to as a stress-free displacement (no external load applied) is the contraction of a heated rod during cooling from an elevated temperature down to room temperature. To determine the internal thermal stress field within the inclusion, a uniform volume eigenstrain, which is proportional to the uniform change in temperature, is prescribed inside the inclusion. In this part of the study, a purely thermal load is applied and under this condition only eigenstrains make up the entire external loading, all stresses vanish at infinity, so that  $A = B = 0$  in (2.9) and the uniform volume expansion assumption leads to  $\varepsilon_x^o = \varepsilon_y^o \neq 0$  and  $\varepsilon_{xy}^o = 0$ . Therefore, from

$$\varepsilon_1 = \frac{\varepsilon_x^o + \varepsilon_y^o}{2}, \quad \varepsilon_2 = \frac{\varepsilon_x^o - \varepsilon_y^o}{2}, \quad \varepsilon_3 = \varepsilon_{xy}^o \quad \text{we obtain, for uniform volume expansion,}$$

$$\varepsilon_1 = \varepsilon_x^o, \quad \varepsilon_2 = 0, \quad \varepsilon_3 = 0.$$

### 3.4.2 Mechanical load

For plane deformations, the elastic stresses and the associated displacements introduced in polar form in (2.1) can be written in terms of two complex potentials,  $\phi(z)$  and  $\psi(z)$  [47] in cartesian form as:

$$2\mu(u + iv) = k\phi(z) - z\overline{\phi'(z)} - \overline{\psi(z)}, \quad (3.20)$$

$$\sigma_{xx} + \sigma_{yy} = 2[\phi'(z) + \overline{\phi'(z)}], \quad (3.21)$$

$$\sigma_{xx} - i\sigma_{xy} = \phi'(z) + \overline{\phi'(z)} - z\overline{\phi''(z)} - \psi'(z), \quad (3.22)$$

The remote loading condition can again be written as

$$\phi_1(z) \approx Az + \text{constant} \quad \text{and} \quad \psi_1(z) \approx Bz + \text{constant} \quad |z| \rightarrow \infty.$$





The constants in the above expression are taken to be zero since they have negligible effect on the stress potentials at infinity. Therefore  $\phi_1(z) \approx Az$  and  $\psi_1(z) \approx Bz$  and hence we can write  $\phi_1'(z) = A$  and  $\psi_1'(z) = B$ ,  $|z| \rightarrow \infty$ .

If  $\sigma_{xx}^\infty$  and  $\sigma_{yy}^\infty$  represents the remote stresses in the  $x$  and  $y$  directions respectively, then by substituting the above into (3.21) and (3.22) we obtain

$\sigma_{xx}^\infty + \sigma_{yy}^\infty = 2[A + A] = 4A$  and  $\sigma_{xx}^\infty - i\sigma_{xy}^\infty = 2A - B$ , from which we can determine  $A$  and  $B$  from the expressions

$$A = \frac{\sigma_{xx}^\infty + \sigma_{yy}^\infty}{4} \text{ and } B = \frac{\sigma_{yy}^\infty - \sigma_{xx}^\infty}{2} + i\sigma_{xy}^\infty.$$

The uniaxial tensile load applied is represented by  $\sigma_{xx}^\infty = 0$ ,  $\sigma_{yy}^\infty = \sigma^\infty$ ,  $\sigma_{xy}^\infty = 0$ ,

and we obtain  $A = \frac{\sigma^\infty}{4}$  and  $B = \bar{B} = 2A = \frac{\sigma^\infty}{2}$ .

By the application of this tensile load, since  $A$  and  $B$  are both real, it is expected that all the derived equations and coefficients and subsequently all calculations deals with real numbers only.

### 3.5 Algebraic Equations for Specific Interface Types

In order to be able to relate this study to a practical problem of fiber-cracking of thin composite devices, a plane-stress formulation is analyzed. Assuming that the Poisson's ratio  $\nu$ , of both the matrix and inclusion materials are identical, with a value of  $\nu = 1/3$  and using the expression  $k = (3 - \nu) / (1 + \nu)$  we obtain  $k_1 = k_2 = 2$ . Two non-dimensional parameters, which represent the extent of inclusion-matrix adhesion for the



two cases of interface parameters, are varied to simulate different interfacial bond conditions.

### 3.5.1 Case 1: Interface parameter $m = n$

First, we consider the case where the homogeneously imperfect inclusion–matrix interface is represented by the condition where normal and tangential spring - factor type interface parameters are equal ( $m = n$ ). This means that the same degree of imperfection is assumed in both the normal and tangential directions on the interface  $\Gamma$ . This condition corresponds to the case where the jump in the displacement vector across the interface is in the same direction as the corresponding interface tractions. Further, to derive a solution that takes into account various degrees of imperfection, a convenient non-dimensional parameter,  $M = mR/\mu_2$  is introduced into the set of equations. Here,  $M$  characterizes the effectiveness of the bonding at the interface in transferring load between the inclusion and the matrix. Physically, a very small value of  $M$  ( $M = 0.01$ ) corresponds to a completely debonded inclusion and values of  $M$  between 1 and 100 are assumed to correspond to an imperfect bonding condition. In this study, a value of  $M = 1$  is chosen to represent imperfect bonding and a large value of  $M$  (eg.  $M > 100$ ) corresponds to the case of perfect bonding between the matrix and inclusion.

Given that  $m = n$  we can compute  $F$  and  $G$ .

From  $F = \frac{m+n}{4R}$  we obtain  $F = \frac{m}{2R}$  and from  $G = R\left(\frac{m-n}{4}\right)$  we obtain  $G = 0$ .

Substituting the above into (3.3) – (3.19), the reduced-form of the general set of algebraic equations are obtained below:



$$-a_3 - 2c_3 + 2.5c_5 + \frac{H_3}{2}d_0 + \frac{H_4}{2}d_1 + \frac{H_5}{2}d_2 + \frac{H_6}{2}d_3 + \left(\frac{H_7}{2} - H_1\right)d_4 = 0, \quad (3.23)$$

$$-a_2 - 1.5c_2 + 2c_4 + \frac{H_2}{2}d_0 + \frac{H_3}{2}d_1 + \frac{H_4}{2}d_2 + \left(\frac{H_5}{2} - \frac{H_1}{2}\right)d_3 + \left(\frac{H_6}{2} - \frac{H_2}{2}\right)d_4 = 0, \quad (3.24)$$

$$-a_1 - c_1 + 1.5c_3 + \frac{H_1}{2}d_0 + \frac{H_2}{2}d_1 + \frac{H_3}{2}d_2 + \frac{H_4}{2}d_3 + \left(\frac{H_5}{2} + 1.5H_1\right)d_4 = 0, \quad (3.25)$$

$$-b_1 + c_1 + d_0 + H_2d_1 + (H_1 + H_3)d_2 + (H_2 + H_4)d_3 + (H_3 + H_5)d_4 = 0, \quad (3.26)$$

$$\begin{aligned} -b_2 + 0.5c_2 + 1.5H_2d_0 + 1.5H_3d_1 + 1.5H_4d_2 + \left(\frac{H_1}{2} + 1.5H_5\right)d_3 \\ + \left(\frac{H_2}{2} + 1.5H_6\right)d_4 = 0, \end{aligned} \quad (3.27)$$

$$\begin{aligned} a_1 - b_3 + 0.5c_3 + \left(-\frac{H_1}{2} + 2H_3\right)d_0 + \left(-\frac{H_2}{2} + 2H_4\right)d_1 + \left(-\frac{H_3}{2} + 2H_5\right)d_2 \\ + \left(-\frac{H_4}{2} + 2H_6\right)d_3 + \left(-\frac{H_5}{2} + 2H_7 + \frac{H_1}{2}\right)d_4 = 0, \end{aligned} \quad (3.28)$$

$$\begin{aligned} 2a_2 - b_4 + 0.5c_4 + (-H_2 + 2.5H_4)d_0 + (-H_3 + 2.5H_5)d_1 + (-H_4 + 2.5H_6)d_2 \\ + (-H_5 + 2.5H_7)d_3 + (-H_6 + 2.5H_8)d_4 = 0, \end{aligned} \quad (3.29)$$



$$\begin{aligned}
3a_3 - b_5 + 0.5c_5 + \left(-\frac{3H_3}{2} + 3H_5\right)d_0 + \left(-\frac{3H_4}{2} + 3H_6\right)d_1 + \left(-\frac{3H_5}{2} + 3H_7\right)d_2 \\
+ \left(-\frac{3H_6}{2} + 3H_8\right)d_3 + \left(-\frac{3H_7}{2} + 3H_9\right)d_4 = 0,
\end{aligned} \tag{3.30}$$

$$\begin{aligned}
-\left(\frac{3}{M} + \frac{\mu_2}{\mu_1}\right)a_3 + c_3 - 1.25c_5 + \frac{H_3}{2}d_0 + \frac{H_4}{2}d_1 + \frac{H_5}{2}d_2 \\
+ \frac{H_6}{2}d_3 + \left(\frac{H_7}{2} + H_1\right)d_4 = 0,
\end{aligned} \tag{3.31}$$

$$\begin{aligned}
-\left(\frac{2}{M} + \frac{\mu_2}{\mu_1}\right)a_2 + 0.75c_2 - c_4 + \frac{H_2}{2}d_0 + \frac{H_3}{2}d_1 + \frac{H_4}{2}d_2 \\
+ \left(\frac{H_5}{2} + \frac{H_1}{4}\right)d_3 + \left(\frac{H_6}{2} + \frac{H_2}{4}\right)d_4 = 0,
\end{aligned} \tag{3.32}$$

$$\begin{aligned}
-\left(\frac{1}{M} + \frac{\mu_2}{\mu_1}\right)a_1 + 0.5c_1 - 0.75c_3 + \frac{H_1}{2}d_0 + \frac{H_2}{2}d_1 + \frac{H_3}{2}d_2 + \frac{H_4}{2}d_3 \\
+ \left(\frac{H_5}{2} + \frac{3H_1}{4}\right)d_4 = 0,
\end{aligned} \tag{3.33}$$

$$\begin{aligned}
-0.75c_0 + 0.5c_2 - 0.25H_1d_1 - 0.25H_2d_2 + (0.5H_1 - 0.25H_3)d_3 \\
+ (0.5H_2 - 0.25H_4)d_4 = 0,
\end{aligned} \tag{3.34}$$





$$\begin{aligned}
& -\left(\frac{1}{M} + \frac{\mu_2}{2\mu_1}\right)b_1 - 0.25c_1 + \frac{H_1}{2}d_0 + \frac{H_2}{2}d_1 + \left(-\frac{H_1}{4} + \frac{H_3}{2}\right)d_2 \\
& + \left(-\frac{H_2}{4} + \frac{H_4}{2}\right)d_3 + \left(-\frac{H_3}{4} + \frac{H_5}{2}\right)d_4 = \mu_2\varepsilon_1,
\end{aligned} \tag{3.35}$$

$$\begin{aligned}
& -\left(\frac{2}{M} + \frac{\mu_2}{2\mu_1}\right)b_2 - 0.5c_2 + 0.75H_2d_0 + 0.75H_3d_1 + 0.75H_4d_2 \\
& + \left(-\frac{H_1}{2} + 0.75H_5\right)d_3 + \left(-\frac{H_2}{2} + 0.75H_6\right)d_4 = 0,
\end{aligned} \tag{3.36}$$

$$\begin{aligned}
& \left(\frac{3}{M} + \frac{\mu_2}{2\mu_1}\right)a_1 - \left(\frac{3}{M} + \frac{\mu_2}{2\mu_1}\right)b_3 - 0.5c_3 + \left(-\frac{H_1}{4} + H_3\right)d_0 + \left(-\frac{H_2}{4} + H_4\right)d_1 \\
& + \left(-\frac{H_3}{4} + H_5\right)d_2 + \left(-\frac{H_4}{4} + H_6\right)d_3 + \left(-\frac{H_5}{4} + H_7 - \frac{H_1}{2}\right)d_4 = 0,
\end{aligned} \tag{3.37}$$

$$\begin{aligned}
& \left(\frac{8}{M} + \frac{\mu_2}{\mu_1}\right)a_2 - \left(\frac{4}{M} + \frac{\mu_2}{2\mu_1}\right)b_4 - 0.5c_4 + \left(-\frac{H_2}{2} + 1.25H_4\right)d_0 \\
& + \left(-\frac{H_3}{2} + 1.25H_5\right)d_1 + \left(-\frac{H_4}{2} + 1.25H_6\right)d_2 + \left(-\frac{H_5}{2} + 1.25H_7\right)d_3 \\
& + \left(-\frac{H_6}{2} + 1.25H_8\right)d_4 = 0,
\end{aligned} \tag{3.38}$$

and



$$\begin{aligned}
& \left( \frac{15}{M} + 1.5 \frac{\mu_2}{\mu_1} \right) a_3 - \left( \frac{5}{M} + \frac{\mu_2}{2\mu_1} \right) b_5 - 0.5c_5 + \left( -\frac{3H_3}{4} + \frac{3H_5}{2} \right) d_0 \\
& + \left( -\frac{3H_4}{4} + \frac{3H_6}{2} \right) d_1 + \left( -\frac{3H_5}{4} + \frac{3H_7}{2} \right) d_2 + \left( -\frac{3H_6}{4} + \frac{3H_8}{2} \right) d_3 \\
& + \left( -\frac{3H_7}{4} + \frac{3H_9}{2} \right) d_4 = 0.
\end{aligned} \tag{3.39}$$

### 3.5.2 Case 2: Interface parameter $m = 3n$

Secondly, we consider the case where the imperfect inclusion–matrix interface is represented by the condition where the normal interface parameter is three times the tangential interface parameter ( $m = 3n$ ). By definition of the spring-type imperfect interface in (2.3), the normal interface parameter  $m$  is directly proportional to Young's modulus while the tangential interface parameter  $n$ , is also directly proportional to the shear modulus. Generally, the ratio of Young's modulus to shear modulus is approximately equal to three and is the reason for considering the case,  $m = 3n$ , known as the *elastic interphase layer*. Again, we derive a solution to the set of equations in a manner that takes into account the various degrees of imperfection by introducing a second non-dimensional parameter,  $L = nR/\mu_2$ . Similar to the case of  $m = n$ , a very small value of  $L$  ( $L = 0.01$ ) corresponds to a completely debonded inclusion and values of  $L$  between 1 and 100 represent imperfect bonding. In this study, we choose a value of  $L=1$  to represent imperfect bonding and a large value of  $L$  (eg.  $L > 100$ ) corresponds to the case of perfect bonding between the matrix and inclusion.



In this case, given that  $m = 3n$  we can again compute  $F$  and  $G$ .

From  $F = \frac{m+n}{4R}$  we obtain  $F = \frac{n}{R}$  and from  $G = R\left(\frac{m-n}{4}\right)$  we obtain  $G = \frac{nR}{2}$ .

In this example, the first eight equations (3.23) to (3.30) from the traction continuity condition remain unchanged. Substituting  $F$  and  $G$  above into (3.11) – (3.19) from the general form of the set of algebraic equations for the displacement discontinuity condition leads to the following reduced-form of algebraic equations

$$\begin{aligned} & -\left(\frac{3}{L} + 3.5\frac{\mu_2}{\mu_1}\right)a_3 + \frac{\mu_2}{2\mu_1}b_5 + 2c_3 - 2c_5 + \left(\frac{7H_3}{4} - 1.5H_5\right)d_0 + \left(\frac{7H_4}{4} - 1.5H_6\right)d_1 \\ & + \left(\frac{7H_5}{4} - 1.5H_7\right)d_2 + \left(\frac{7H_6}{4} - 1.5H_8\right)d_3 + \left(\frac{7H_7}{4} - 1.5H_9 + H_1\right)d_4 = 0, \end{aligned} \quad (3.40)$$

$$\begin{aligned} & -\left(\frac{2}{L} + 3\frac{\mu_2}{\mu_1}\right)a_2 + \frac{\mu_2}{2\mu_1}b_4 + 1.5c_2 - 1.5c_4 + (1.5H_2 - 1.25H_4)d_0 \\ & + (1.5H_3 - 1.25H_5)d_1 + (1.5H_4 - 1.25H_6)d_2 + (1.5H_5 - 1.25H_7 + 0.5H_1)d_3 \\ & + (1.5H_6 - 1.25H_8 + 0.5H_2)d_4 = 0, \end{aligned} \quad (3.41)$$

$$\begin{aligned} & -\left(\frac{1}{L} + 2.5\frac{\mu_2}{\mu_1}\right)a_1 + 0.5\frac{\mu_2}{\mu_1}b_3 + c_1 - c_3 + (1.25H_1 - H_3)d_0 + (1.25H_2 - H_4)d_1 \\ & + (1.25H_3 - H_5)d_2 + (1.25H_4 - H_6)d_3 + (1.25H_5 - H_7 - H_1)d_4 = 0, \end{aligned} \quad (3.42)$$



$$\begin{aligned}
& -0.5\frac{\mu_2}{\mu_1}b_2 - 1.5c_0 + 0.5c_2 + 0.75H_2d_0 + (0.75H_3 - 0.5H_1)d_1 \\
& + (0.75H_4 - 0.5H_2)d_2 + (0.75H_5 - 0.5H_3 + 0.5H_1)d_3 \\
& + (0.75H_6 - 0.5H_4 + 0.5H_2)d_4 = 0,
\end{aligned} \tag{3.43}$$

$$\begin{aligned}
& -\left(\frac{1}{L} + 1.5\frac{\mu_2}{\mu_1}\right)b_1 - 0.75c_1 + 1.5H_1d_0 + 1.5H_2d_1 + (1.5H_3 - 0.75H_1)d_2 \\
& + (1.5H_4 - 0.75H_2)d_3 + (1.5H_5 - 0.75H_3)d_4 = \mu_2\epsilon_1,
\end{aligned} \tag{3.44}$$

$$\begin{aligned}
& -\left(\frac{2}{L} + \frac{\mu_2}{\mu_1}\right)b_2 - 0.75c_0 - 0.5c_2 + 1.5H_2d_0 + (1.5H_3 - 0.25H_1)d_1 \\
& + (1.5H_4 - 0.25H_2)d_2 + (1.5H_5 - 0.25H_3 - 0.5H_1)d_3 \\
& + (1.5H_6 - 0.25H_4 - 0.5H_2)d_4 = 0,
\end{aligned} \tag{3.45}$$

$$\begin{aligned}
& \left(\frac{3}{L} + 2\frac{\mu_2}{\mu_1}\right)a_1 - \left(\frac{3}{L} + \frac{\mu_2}{\mu_1}\right)b_3 - 0.5c_1 - 0.25c_3 + (2H_3 - H_1)d_0 + (2H_4 - H_2)d_1 \\
& + (2H_5 - H_3)d_2 + (2H_6 - H_4)d_3 + (2H_7 - H_5 - 0.25H_1)d_4 = 0,
\end{aligned} \tag{3.46}$$

$$\begin{aligned}
& \left(\frac{8}{L} + 3\frac{\mu_2}{\mu_1}\right)a_2 - \left(\frac{4}{L} + \frac{\mu_2}{\mu_1}\right)b_4 - 0.75c_2 + (2.5H_4 - 1.5H_2)d_0 \\
& + (2.5H_5 - 1.5H_3)d_1 + (2.5H_6 - 1.5H_4)d_2 + (2.5H_7 - 1.5H_5 - 0.25H_1)d_3 \\
& + (2.5H_8 - 1.5H_6 - 0.25H_2)d_4 = 0,
\end{aligned} \tag{3.47}$$





and

$$\begin{aligned}
& \left( \frac{15}{L} + 4 \frac{\mu_2}{\mu_1} \right) a_3 - \left( \frac{5}{L} + \frac{\mu_2}{\mu_1} \right) b_5 - c_3 + 0.25c_5 + (3H_5 - 2H_3)d_0 \\
& + (3H_6 - 2H_4)d_1 + (3H_7 - 2H_5)d_2 + (3H_8 - 2H_6)d_3 \\
& + (3H_9 - 2H_7 - 0.5H_1)d_4 = 0.
\end{aligned} \tag{3.48}$$

Hence, in the case of  $m = 3n$ , to determine the unknown coefficients the seventeen equations to be considered are (3.23) – (3.30) and (3.40) – (3.48).

### 3.5.3 Algebraic equations for mechanical load

All the above equations for  $m = n$  and  $m = 3n$ , were derived with the applied load represented as a purely thermal load. If the above set of algebraic equations for a given interface parameter is written in a matrix form as  $[A]\{x\} = \{b\}$ , then, in the case of a mechanical load, the coefficient matrix  $[A]$  remains unchanged. Under a uniaxial tensile loading condition, the load vector for the case of  $m = n$  in matrix form is found to be

$$\{b\}^T = \left[ 0 \ 0 \ \frac{\sigma^\infty}{2} \ \frac{\sigma^\infty}{2} \ 0 \ 0 \ 0 \ 0 \ 0 \ 0 \ \frac{\sigma^\infty}{2} \left( \frac{1}{M} - \frac{\mu_2}{2\mu_1} \right) \ 0 \ \frac{\sigma^\infty}{2} \left( \frac{1}{M} - \frac{\mu_2}{4\mu_1} \right) \ 0 \ 0 \ 0 \ 0 \right].$$

At this stage, by equating powers of  $z$ , a set of seventeen equations ((3.23) – (3.39) for  $m = n$  and (3.23) – (3.30) and (3.40) – (3.48) for  $m = 3n$ ) have been derived. However, in this form, these equations cannot be solved to obtain a solution because the number of unknowns exceeds the number of equations. In order to be able to determine the unknown coefficients  $a_k, b_k, c_k$  and  $d_k$  uniquely, two additional equations are required. These two auxiliary equations will be derived in Chapter 4.



# CHAPTER 4

## 4 Numerical Procedure and Results

### 4.1 Introduction

The first part of this chapter deals with the numerical procedure used to solve the coupled linear algebraic equations in order to determine the stress intensity factor at the crack tips. This first requires the determination of the unknown coefficients  $a_k, b_k, c_k$  and  $d_k$  such that they satisfy all the derived equations for a given crack-inclusion geometry and material properties of the inclusion and matrix.

As observed in Chapter 3, after comparing powers of  $z$ , one of the equations from the traction continuity condition was automatically satisfied and hence a total of 17 instead of the anticipated 18 equations ( $2n+2$ , where  $n=4$  in this case) was obtained. The 17 linear algebraic equations obtained had 19 unknown namely  $a_1, a_2, a_3, b_1, b_2, b_3, b_4, b_5, c_0, c_1, c_2, c_3, c_4, c_5, d_0, d_1, d_2, d_3$  and  $d_4$ . Since the number of equations is two less than the number of unknown coefficients, it is clear that the set of equations cannot be solved uniquely for the unknown coefficients. To deal with this problem, two auxiliary equations are derived. These two equations are obtained from the implicit definition of the function  $Y(z)$  in (2.21) at the two crack end points  $a$  and  $b$ . This leads to the expressions



$$Y(a) = \sum_{k=0}^4 d_k a^k = d_0 + d_1 a + d_2 a^2 + d_3 a^3 + d_4 a^4 = 0, \quad (4.1)$$

and

$$Y(b) = \sum_{k=0}^4 d_k b^k = d_0 + d_1 b + d_2 b^2 + d_3 b^3 + d_4 b^4 = 0. \quad (4.2)$$

With the addition of (4.1) and (4.2), the final form of the coefficient matrix  $[A]$ , of the system of linear algebraic equations becomes an invertible (19x19)-square matrix. In this form, for a specified load vector  $\{b\}$  (thermal or mechanical), we solve the system  $\{x\} = [A]^{-1} \{b\}$  using MATLAB to obtain the solution vector  $\{x\}$ , of unknown coefficients. Appendix C shows three examples of the values of the unknown coefficients calculated for selected interface parameters, shear modulus ratio and crack positions.

## 4.2 Stress Intensity Factor

Understanding the behavior of load-carrying solid materials used in engineering applications in the presence of metallurgical flaws and stress concentrations is important to the proper design of the component and to the safety assessment of the structure in service. It is known that flaws and cracks are inherent in most if not all structures and if left unattended, they can lead to failure of devices by fracture before their intended lifetime. It should be noted that the development of the general theory of fracture mechanics was given considerable impetus by the local stress criterion propounded in 1913 by a Professor of Naval Architecture, C. E. Inglis. He published stress analysis for an elliptical hole in an infinite linear elastic plate subjected to a uniform equal-biaxial



tension and showed that the stress in the neighborhood of the tips of the crack could be much greater than elsewhere in the material.

In this study we find formulas for stresses in the immediate neighborhood of the crack tip of a radial crack located inside an inclusion. In this respect, the stress intensity factor is used as a means of characterizing the elastic stress distribution near the crack tip. In general, for any loaded system, three possible modes of deformation (mode I, II and III), which may appear alone or in arbitrary combination, can be observed. However, in this study, only the Mode I (crack-opening) stress intensity factor,  $K_I$  (which is regarded as the most significant) is considered, since mode II stress intensity factor,  $K_{II}$  in this type of application is usually very small and almost constant [7]. Further, it is assumed that the critical value of the stress intensity factor is a property which may be used to determine the direction of crack growth in the fiber or the maximum permissible thermal or mechanical stress for a given interior radial crack size. It must be noted that all computations are performed under the assumption of no crack growth at the crack tips. This implies that the stress intensity factor at the crack tips,  $K_I$  is always smaller than the critical stress intensity factor,  $K_{IC}$  ( $K_I < K_{IC}$ ).

Again, using the cartesian form of (2.1) we can write

$$\sigma_{xx} + \sigma_{yy} = 2\phi'_2(z) + 2\overline{\phi'_2(z)}, \quad (4.3)$$

$$\sigma_{xx} - i\sigma_{xy} = \phi'_2(z) + \overline{\phi'_2(z)} - z\phi''_2(z) - \overline{\psi'_2(z)}. \quad (4.4)$$

Taking the conjugate of (4.4) and substituting into (4.3) we get,

$$\sigma_{yy} - i\sigma_{xy} = \phi'_2(z) + \overline{\phi'_2(z)} + z\overline{\phi''_2(z)} + \overline{\psi'_2(z)}. \quad (4.5)$$

From (4.4) and (4.5) we can write the following,





$$\begin{aligned}
\sigma_{xx} &= \operatorname{Re} \left[ \phi_2'(z) + \overline{\phi_2'(z)} - z \overline{\phi_2''(z)} - \overline{\psi_2'(z)} \right], \\
\sigma_{yy} &= \operatorname{Re} \left[ \phi_2'(z) + \overline{\phi_2'(z)} + z \overline{\phi_2''(z)} + \overline{\psi_2'(z)} \right], \\
\sigma_{xy} &= \operatorname{Im} \left[ \phi_2'(z) + \overline{\phi_2'(z)} - z \overline{\phi_2''(z)} - \overline{\psi_2'(z)} \right].
\end{aligned} \tag{4.6}$$

In view of (2.24) we can write,

$$\overline{\psi_2'(z)} = \phi_2'(\bar{z}) - \phi_2'(\bar{z}) + \bar{z} \overline{\phi_2''(z)} + X'(\bar{z}). \tag{4.7}$$

Finally, the stresses inside the inclusion can be expressed in the form

$$\begin{aligned}
\sigma_{xx} &= \operatorname{Re} \left[ \phi_2'(z) - \phi_2'(\bar{z}) + 2\overline{\phi_2'(z)} + (\bar{z} - z) \overline{\phi_2''(z)} + X'(\bar{z}) \right], \\
\sigma_{yy} &= \operatorname{Re} \left[ \phi_2'(z) + \phi_2'(\bar{z}) + (z - \bar{z}) \overline{\phi_2''(z)} - X'(\bar{z}) \right], \\
\sigma_{xy} &= \operatorname{Im} \left[ \phi_2'(z) - \phi_2'(\bar{z}) + 2\overline{\phi_2'(z)} + (\bar{z} - z) \overline{\phi_2''(z)} + X'(\bar{z}) \right].
\end{aligned} \tag{4.8}$$

From (2.23) we obtain,

$$\phi_2'(z) = \frac{(a+b-2z)Y(z)}{4(z-a)^{\frac{3}{2}}(z-b)^{\frac{3}{2}}} + \frac{Y'(z)}{2(z-a)^{\frac{1}{2}}(z-b)^{\frac{1}{2}}} + \frac{X'(z)}{2}, \tag{4.9}$$

and

$$\begin{aligned}
\phi_2''(z) &= \frac{-Y(z)}{2(z-a)^{\frac{3}{2}}(z-b)^{\frac{3}{2}}} + \frac{3(a+b-2z)^2 Y(z)}{8(z-a)^{\frac{5}{2}}(z-b)^{\frac{5}{2}}} + \frac{(a+b-2z)Y'(z)}{2(z-a)^{\frac{3}{2}}(z-b)^{\frac{3}{2}}} \\
&\quad + \frac{Y''(z)}{2(z-a)^{\frac{1}{2}}(z-b)^{\frac{1}{2}}} + \frac{X''(z)}{2}.
\end{aligned} \tag{4.10}$$

Since  $Y(z)$  is analytic inside the inclusion, the Taylor series expansions of  $Y(z)$  near each of the points  $z = a$  and  $z = b$  are given by



$$Y(z) = Y(a) + Y'(a)r_1e^{i\theta_1} + \frac{Y''(a)}{2}r_1^2e^{2i\theta_1} + \dots + \frac{Y^{(n)}(a)}{n!}r_1^ne^{ni\theta_1}, \quad (4.11)$$

$$Y(z) = Y(b) + Y'(b)r_2e^{i\theta_2} + \frac{Y''(b)}{2}r_2^2e^{2i\theta_2} + \dots + \frac{Y^{(n)}(b)}{n!}r_2^ne^{ni\theta_2}. \quad (4.12)$$

Using (4.8) – (4.12) explicit expressions for the stresses in the neighborhood of the crack tips (leading order terms only) can be derived for a given type of loading.

#### 4.2.2 Thermal load

For an inclusion with an interior crack embedded in an infinite matrix subjected to a two-dimensional eigenstrain, we obtain

for crack tip  $a$ , the stresses are given by:

$$\begin{aligned} \sigma_{xx} &= \frac{1}{\sqrt{2}r_1\sqrt{L}} \frac{1}{\mu_2\varepsilon_1} \left( \frac{3}{8} \sin \frac{\theta_1}{2} + \frac{1}{8} \sin \frac{5\theta_1}{2} \right) \{d_1 + 2d_2a + 3d_3a^2 + 4d_4a^3\}, \\ \sigma_{yy} &= -\frac{1}{\sqrt{2}r_1\sqrt{L}} \frac{1}{\mu_2\varepsilon_1} \left( \frac{5}{8} \sin \frac{\theta_1}{2} - \frac{1}{8} \sin \frac{5\theta_1}{2} \right) \{d_1 + 2d_2a + 3d_3a^2 + 4d_4a^3\}, \\ \sigma_{xy} &= \frac{1}{\sqrt{2}r_1\sqrt{L}} \frac{1}{\mu_2\varepsilon_1} \left( \frac{5}{8} \cos \frac{\theta_1}{2} - \frac{1}{8} \cos \frac{5\theta_1}{2} \right) \{d_1 + 2d_2a + 3d_3a^2 + 4d_4a^3\}. \end{aligned} \quad (4.13)$$

Similarly, the stresses near crack tip  $b$  are given by:

$$\begin{aligned} \sigma_{xx} &= \frac{1}{\sqrt{2}r_2\sqrt{L}} \frac{1}{\mu_2\varepsilon_1} \left( \frac{3}{8} \cos \frac{\theta_2}{2} + \frac{1}{8} \cos \frac{5\theta_2}{2} \right) \{d_1 + 2d_2b + 3d_3b^2 + 4d_4b^3\}, \\ \sigma_{yy} &= \frac{1}{\sqrt{2}r_2\sqrt{L}} \frac{1}{\mu_2\varepsilon_1} \left( \frac{5}{8} \cos \frac{\theta_2}{2} - \frac{1}{8} \cos \frac{5\theta_2}{2} \right) \{d_1 + 2d_2b + 3d_3b^2 + 4d_4b^3\}, \\ \sigma_{xy} &= -\frac{1}{\sqrt{2}r_2\sqrt{L}} \frac{1}{\mu_2\varepsilon_1} \left( \frac{1}{8} \sin \frac{\theta_2}{2} - \frac{1}{8} \sin \frac{5\theta_2}{2} \right) \{d_1 + 2d_2b + 3d_3b^2 + 4d_4b^3\}, \end{aligned} \quad (4.14)$$



where  $L = (b - a)/2$  is the half length of the crack. In each of the expressions for the stresses, the factors appearing in the brackets  $\{*\}$  represent the effect of the interface imperfection on the stress intensity factor. As mentioned earlier, by changing the interface parameter  $M$  or  $L$  we can calculate the stress intensity factors for various crack endpoints using (4.13) and (4.14). The results from the calculations are shown using the values of the normalized stress intensity factor of the crack tip (normalized using the stresses inside the inclusion) which is represented as  $-\frac{K_I(a)}{K_0}$  or  $-\frac{K_I(b)}{K_0}$ , where  $K_0 = \mu_2 \varepsilon_1 \sqrt{2r}$ , denotes the stress intensity factor of a crack in an infinite homogeneous matrix material under uniform volume expansion.

#### 4.2.2 Mechanical Load

For an inclusion with an interior crack embedded in an infinite matrix subjected to a uniaxial tensile force, by going through a similar derivation as that mentioned above, we obtain,

for crack tip  $a$ , the stresses are given by:

$$\begin{aligned}\sigma_{xx} &= \frac{1}{\sqrt{2r_1}\sqrt{L}} \frac{2}{\sigma^\infty} \left( \frac{3}{8} \sin \frac{\theta_1}{2} + \frac{1}{8} \sin \frac{5\theta_1}{2} \right) \{d_1 + 2d_2a + 3d_3a^2 + 4d_4a^3\}, \\ \sigma_{yy} &= -\frac{1}{\sqrt{2r_1}\sqrt{L}} \frac{2}{\sigma^\infty} \left( \frac{5}{8} \sin \frac{\theta_1}{2} - \frac{1}{8} \sin \frac{5\theta_1}{2} \right) \{d_1 + 2d_2a + 3d_3a^2 + 4d_4a^3\}, \\ \sigma_{xy} &= \frac{1}{\sqrt{2r_1}\sqrt{L}} \frac{2}{\sigma^\infty} \left( \frac{5}{8} \cos \frac{\theta_1}{2} - \frac{1}{8} \cos \frac{5\theta_1}{2} \right) \{d_1 + 2d_2a + 3d_3a^2 + 4d_4a^3\}.\end{aligned}\tag{4.15}$$



Similarly, the stresses near crack tip  $b$  are given by:

$$\begin{aligned}\sigma_{xx} &= \frac{1}{\sqrt{2} r_2 \sqrt{L}} \frac{2}{\sigma^\infty} \left( \frac{3}{8} \cos \frac{\theta_2}{2} + \frac{1}{8} \cos \frac{5\theta_2}{2} \right) \{d_1 + 2d_2 b + 3d_3 b^2 + 4d_4 b^3\}, \\ \sigma_{yy} &= \frac{1}{\sqrt{2} r_2 \sqrt{L}} \frac{2}{\sigma^\infty} \left( \frac{5}{8} \cos \frac{\theta_2}{2} - \frac{1}{8} \cos \frac{5\theta_2}{2} \right) \{d_1 + 2d_2 b + 3d_3 b^2 + 4d_4 b^3\}, \quad (4.16) \\ \sigma_{xy} &= -\frac{1}{\sqrt{2} r_2 \sqrt{L}} \frac{2}{\sigma^\infty} \left( \frac{1}{8} \sin \frac{\theta_2}{2} - \frac{1}{8} \sin \frac{5\theta_2}{2} \right) \{d_1 + 2d_2 b + 3d_3 b^2 + 4d_4 b^3\}.\end{aligned}$$

Similar to the case of thermal loading, only the crack opening mode (I) stress intensity factor  $K_I$  is calculated. The results from the calculations are shown using the values of the normalized stress intensity factor of the crack tip (normalized using the external stress) which is represented as  $\frac{K_I(a)}{K_0}$  or  $\frac{K_I(b)}{K_0}$ , where  $K_0 = \sigma^\infty \sqrt{2r}$ , denotes the stress intensity factor of a crack in an infinite homogeneous matrix material under uniaxial tensile stress.





## 4.3 Results

The values of the normalized stress intensity factor at the tips of a radial crack are presented in Figures and Tables for various crack-inclusion geometries, crack lengths and shear moduli ratio of inclusion-matrix. A specific example of a fixed crack half-length of  $R/4$  is considered and the position of this crack is varied as it gradually approaches the interface.

### 4.3.1 Thermal load

The normalized stress intensity factor represents the relative magnitude of the thermal stresses at the crack tips compared to that corresponding to the case of a homogeneous material. A negative value of the normalized stress intensity factor is an indication that the inclusion has a higher thermal expansion coefficient than the matrix. These negative values therefore imply that the surfaces of the radial crack are under compressive stresses.



#### 4.3.1.1 Case 1 : $m = n$

The results in Table 4.1 enable comparison of results for perfect interface and imperfect interface.

Crack points	$\frac{\mu_2}{\mu_1}$									
	0.1		0.5		1		2		10	
	I	P	I	P	I	P	I	P	I	P
$a = 0$ $b = \frac{R}{2}$	0.406	1.512	0.355	0.964	0.306	0.667	0.240	0.415	0.088	0.105
$a = \frac{R}{4}$ $b = \frac{3R}{4}$	0.427	1.441	0.374	0.944	0.324	0.667	0.255	0.425	0.096	0.112
$a = \frac{3R}{10}$ $b = \frac{4R}{5}$	0.431	1.427	0.378	0.940	0.327	0.667	0.259	0.427	0.097	0.114
$a = \frac{2R}{5}$ $b = \frac{9R}{10}$	0.434	1.398	0.381	0.932	0.331	0.667	0.262	0.431	0.100	0.117
$a = \frac{9R}{20}$ $b = \frac{19R}{20}$	0.430	1.390	0.378	0.930	0.328	0.667	0.260	0.431	0.099	0.117
$a = -\frac{R}{5}$ $b = \frac{R}{5}$	0.353	1.411	0.307	0.877	0.264	0.596	0.207	0.365	0.075	0.089

**Table 4.1** Normalized stress intensity factor for various positions of crack



The letter I stands for imperfect interface in which case  $M$  is taken as 1 and the letter  $P$  denotes a perfect interface, approximated by  $M > 100$ , in this case  $M = 10000$ . Table 4.1 shows the values of the normalized stress intensity factor at crack tip  $b$ ,  $-\frac{K_I(b)}{\mu_2 \varepsilon_1}$ , for six different interior crack positions and five shear moduli ratio. As can be seen from Table 4.1, there is a significant difference between the corresponding perfect and imperfect interface models. The results indicate that the perfect interface values are always greater than the corresponding imperfect interface values, in certain cases, by as much as 200 percent for soft inclusions,  $\frac{\mu_2}{\mu_1} < 1$ , and 150 percent for hard inclusions,  $\frac{\mu_2}{\mu_1} > 1$ .

Using a perfect interface model, it is known that if elastic mismatch between the inclusion and the matrix ( $\frac{\mu_2}{\mu_1} = 1$ ) is ignored, the stress intensity factors at both ends of the crack tips, for a given crack length, are equal under typical mechanical or thermal loading [16]. In fact, this stress intensity value is independent of the position of the crack in the inclusion as can be seen from the constant value of 0.667 obtained in the first five rows of column 7 in Table 4.1 for a crack half-length of  $R/4$ . The corresponding imperfect interface results in Table 4.1 and the results presented in Table 4.2 below show that  $K_I(a) \neq K_I(b)$  and  $K_I$  depends on the location of the crack.



Crack points	Perfect Interface	Imperfect Interface	
	$\frac{-K_I(a)}{\mu_2 \varepsilon_1} = \frac{-K_I(b)}{\mu_2 \varepsilon_1}$	$\frac{-K_I(a)}{\mu_2 \varepsilon_1}$	$\frac{-K_I(b)}{\mu_2 \varepsilon_1}$
$a = \frac{3R}{4}; b = \frac{3R}{4}$	0.667	0.309	0.324
$a = \frac{R}{5}; b = \frac{4R}{5}$	0.730	0.348	0.375
$a = -\frac{R}{5}; b = \frac{R}{5}$	0.596	0.264	0.264
$a = 0; b = \frac{R}{5}$	0.421	0.182	0.182

**Table 4.2** Normalized stress intensity factor with elastic mismatch ignored

In Figure 4.1, the effect of the interface imperfection on the stress intensity factor at crack tip  $b$  is studied for a fixed crack half-length of  $R/4$  as this tip approaches the interface. For a shear modulus ratio of  $\frac{\mu_2}{\mu_1} = 10$ , as the crack tip–interface distance  $d/R$  decreases, the stress intensity factor at crack tip  $b$  increases slightly for the imperfect interface parameter of  $M = 1$ . A relatively significant increase in stress intensity factor is observed for the perfect interface model as the crack-tip interface distance becomes small.

A graph similar to Figure 4.1 is shown in Figure 4.2 for a soft inclusion ( $\frac{\mu_2}{\mu_1} = 0.1$ ).

In this case, while the stress intensity factor increases as the crack-tip interface distance decreases for an imperfect interface model, the value decreases sharply for the perfect interface model.

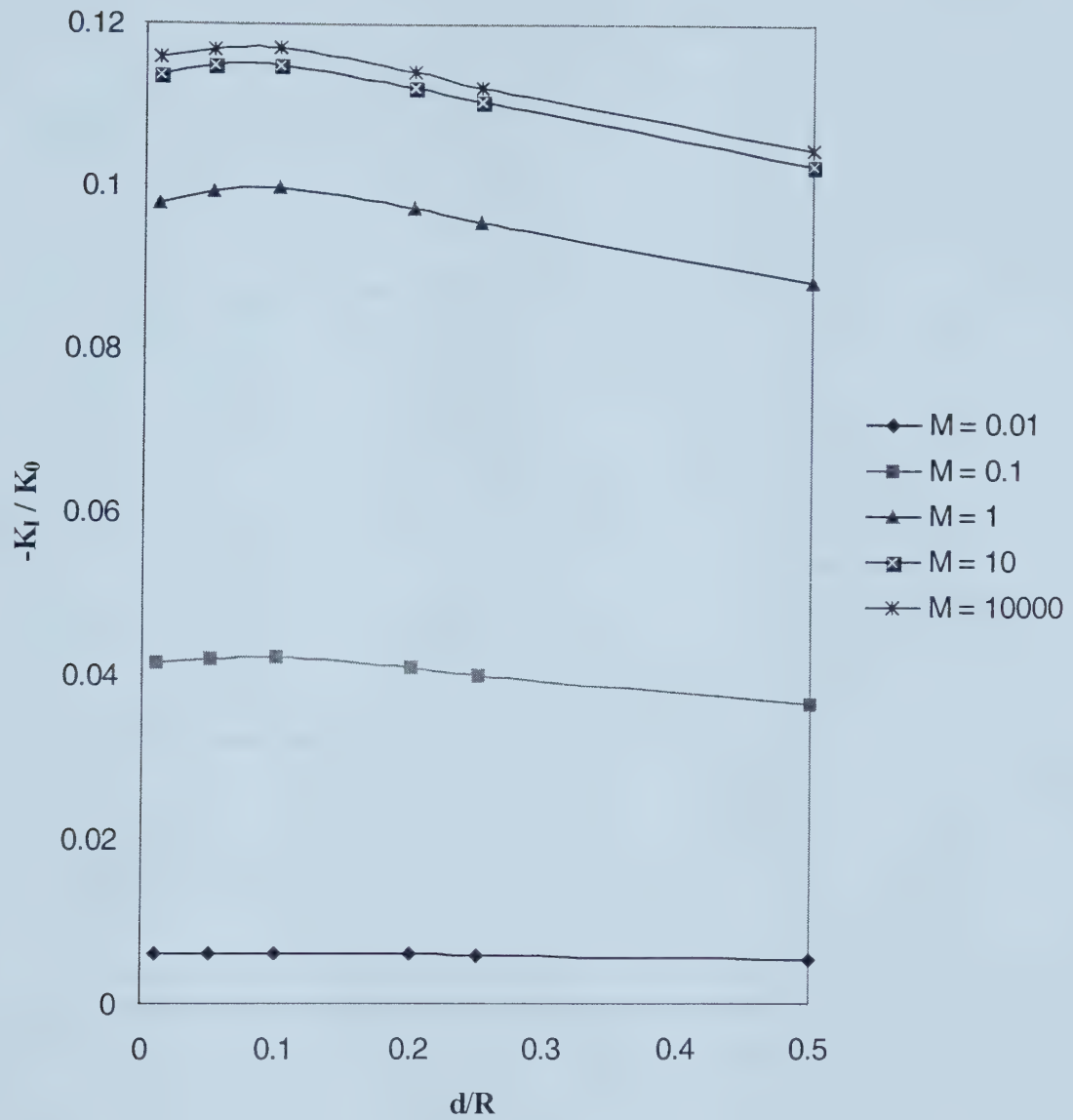




Figure 4.3 shows the dependency of the shear modulus ratio on the stress intensity factor for a given crack half-length of  $R/4$ . As the shear modulus ratio increases, the stress intensity factor at  $b$  decreases significantly. A similar conclusion is obtained for the stress intensity factor at crack tip  $a$ , although this is not as pronounced as that at crack tip  $b$ . This observation therefore suggests that where low stress intensity factor values are desired a hard inclusion would be preferable to a soft inclusion.

Figure 4.4 clearly exhibits the expected trend for the stress intensity factor at crack tip  $b$  with increasing crack length for three different cracks with crack tip  $a$  being fixed at the origin. As the crack length increases and approaches the interface, the stress intensity factor also increases accordingly.





**Figure 4.1** Dependency of Normalized stress intensity factor on crack tip–interface distance (Hard Inclusion)



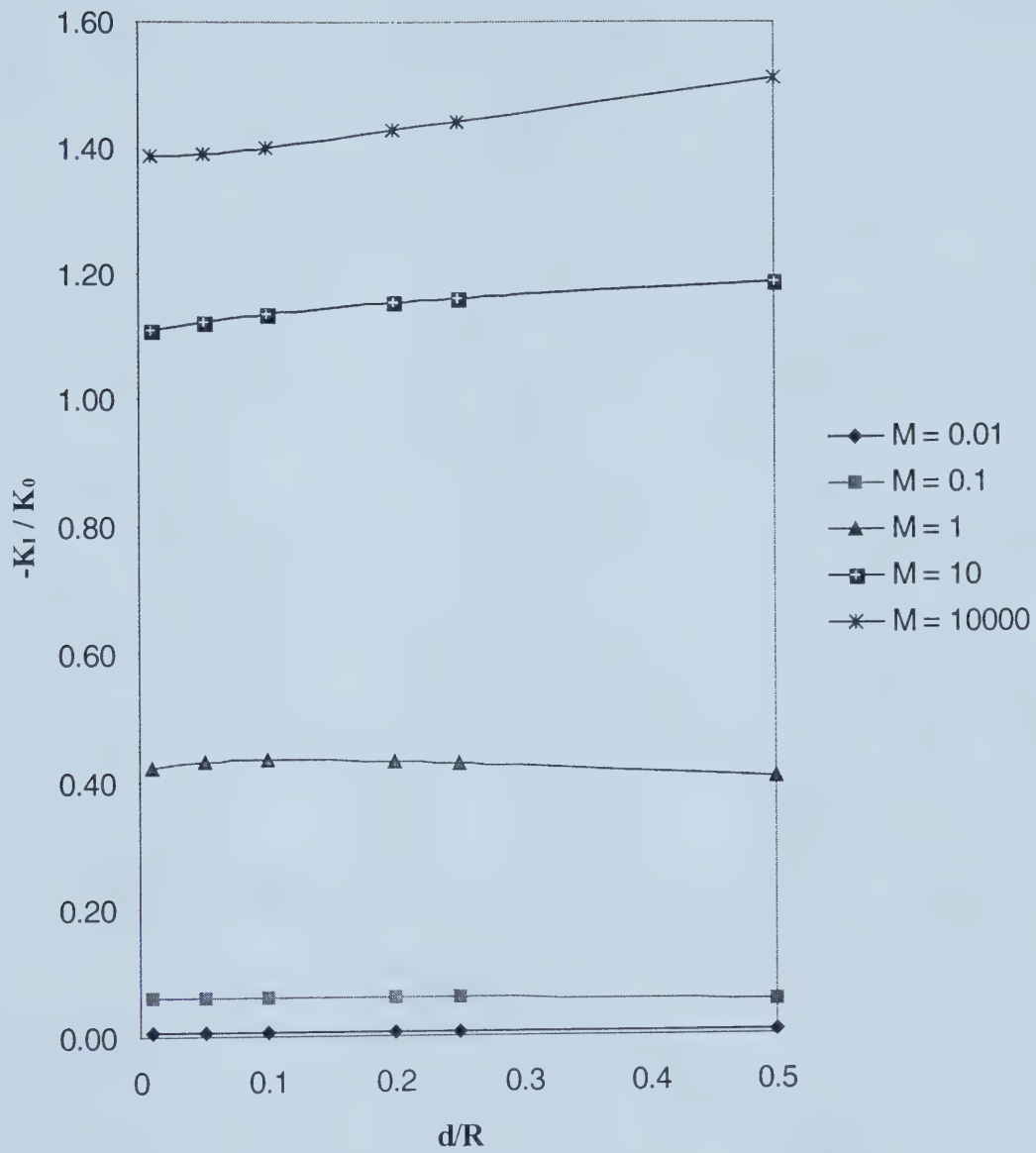


**Figure 4.2** Dependency of Normalized stress intensity factor on crack tip–interface distance (Soft Inclusion)



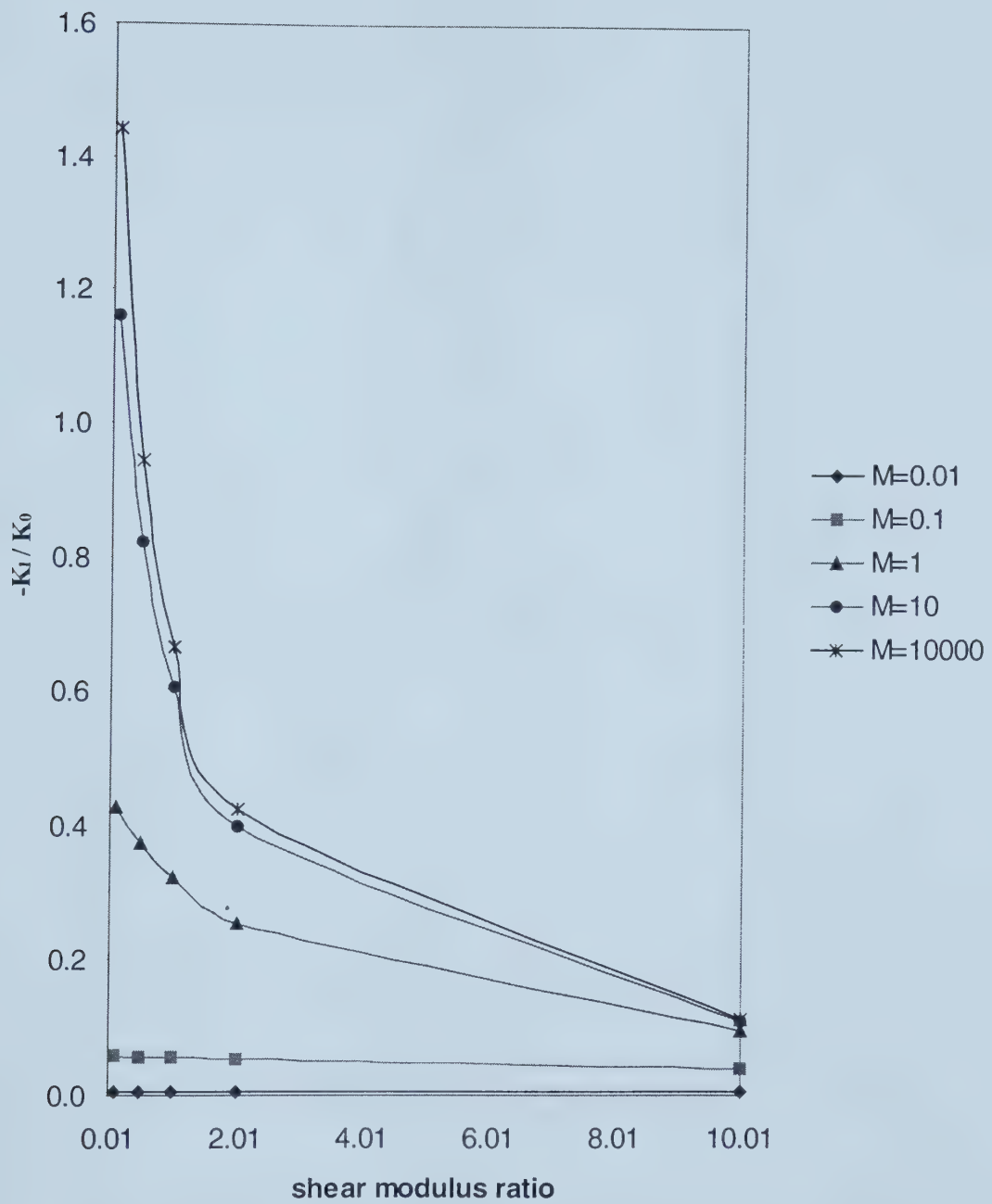


**Figure 4.3** The effect of shear modulus ratio on stress intensity factor





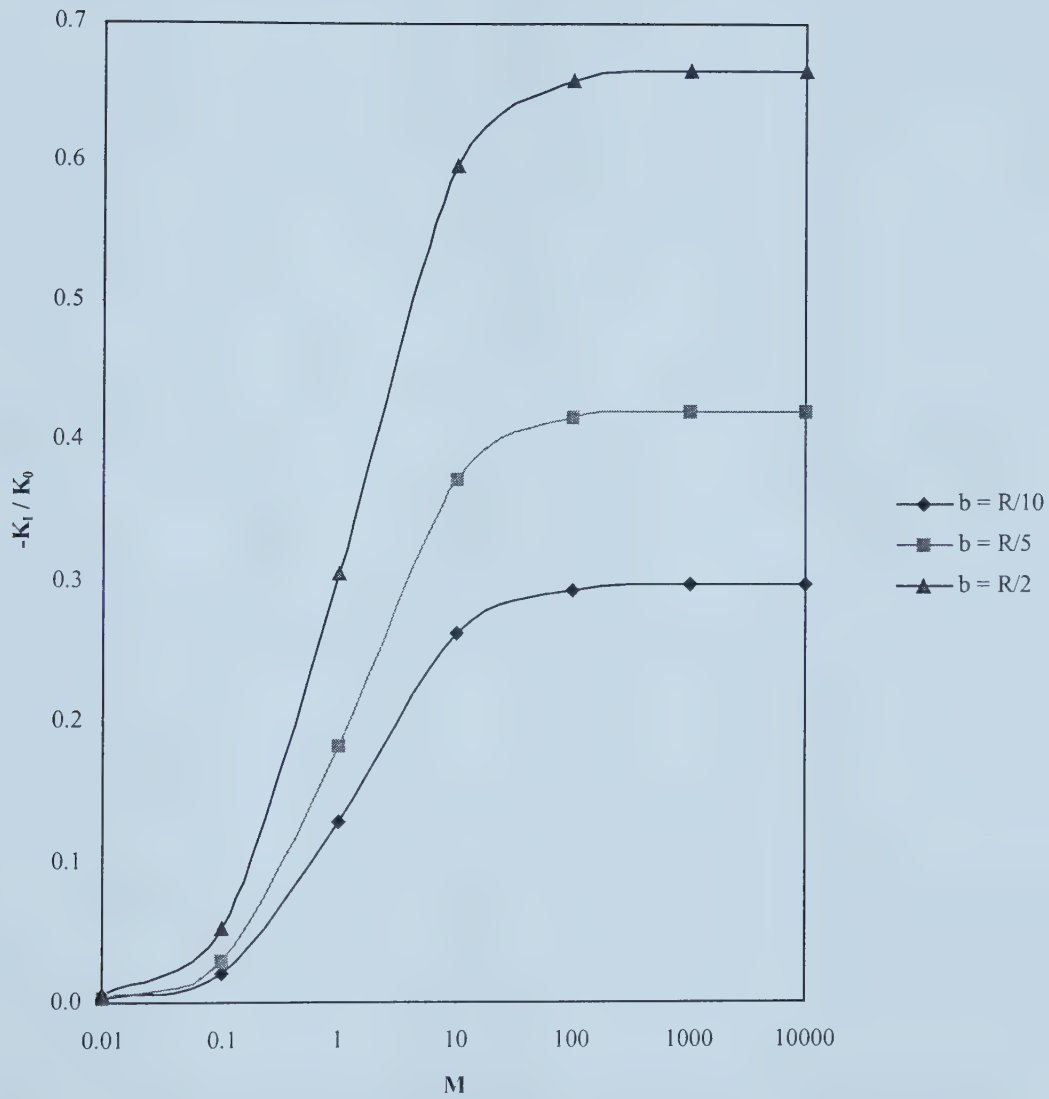


**Figure 4.4** Effect of interface imperfection on increasing crack length



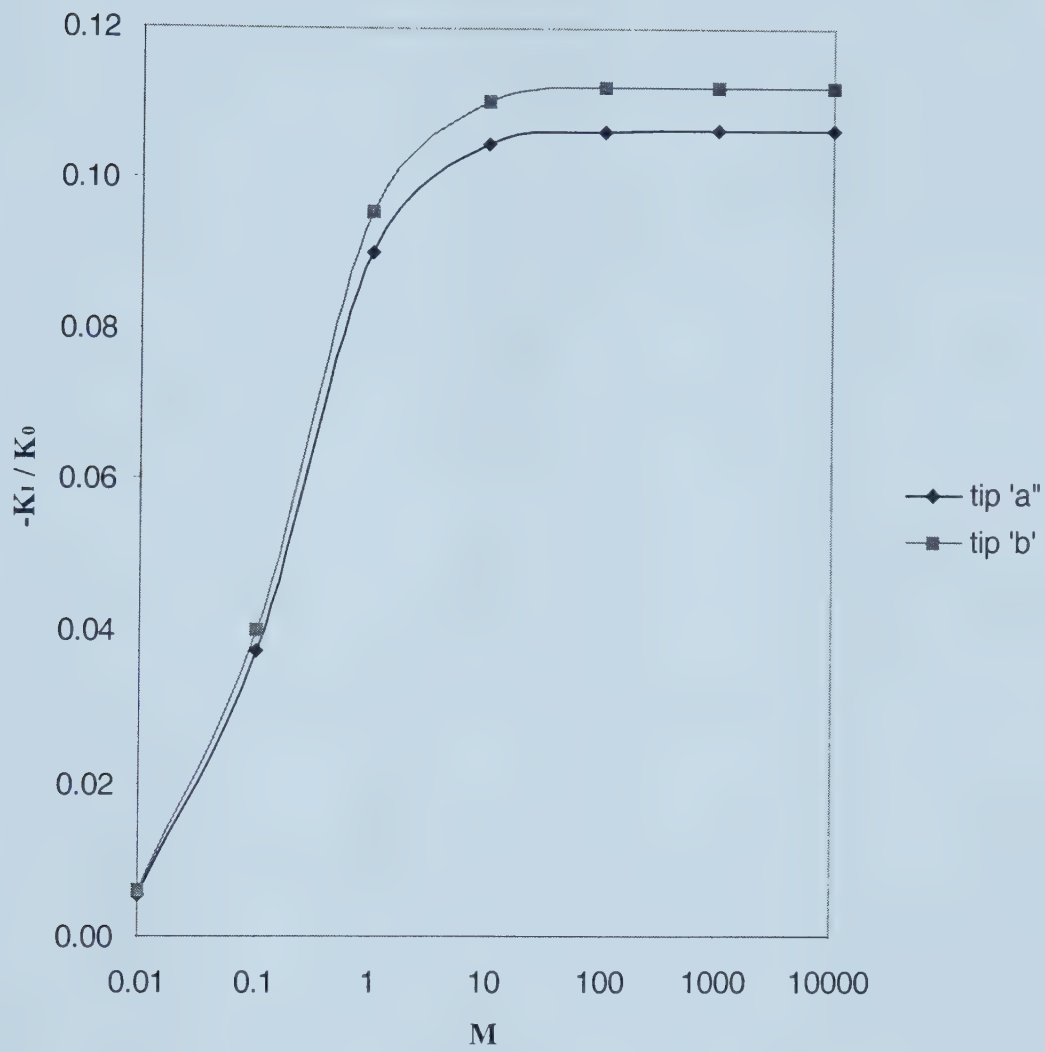


**Figure 4.5** Normalized stress intensity factor for a hard inclusion



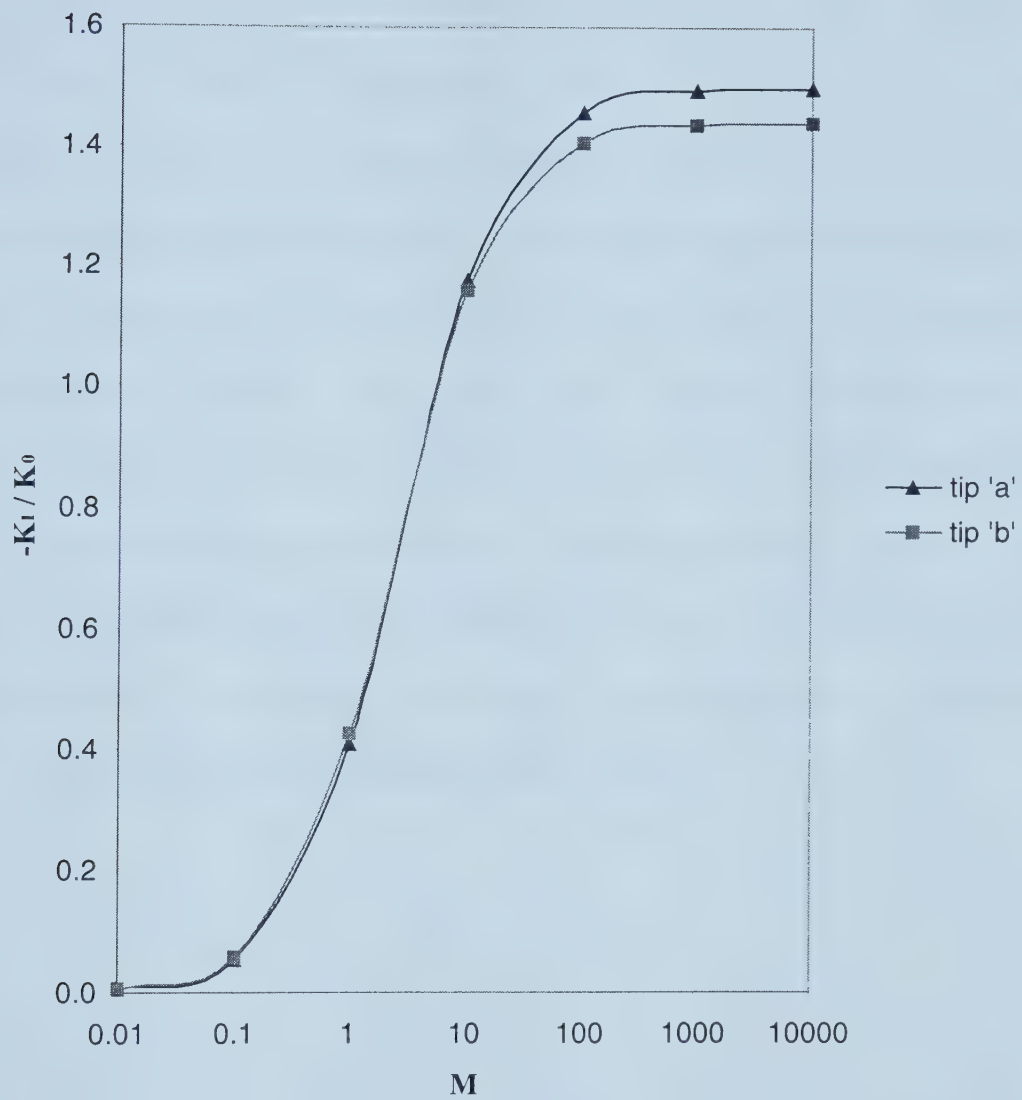


**Figure 4.6** Normalized stress intensity factor for a soft inclusion



To further illustrate the difference between the perfect and imperfect interface models graphically, results of the variation of the stress intensity factor at the two crack tips with interface imperfection parameter  $M$  for a hard inclusion ( $\mu_2/\mu_1 = 10$ ) and a soft inclusion ( $\mu_2/\mu_1 = 0.1$ ) are shown in Figures 4.5 and 4.6 respectively. In Figure 4.5 the stress intensity factor at crack tip  $b$  is always higher than that at  $a$  for both perfect and imperfect interface models. This implies that an existing crack in a hard inclusion has a higher likelihood of growing towards the interface than away from the interface. As shown in Figure 4.6, for a soft inclusion, the perfect interface model stress intensity factor at  $a$  is always greater than that at  $b$ , indicating a higher possibility of crack growth from  $a$  rather than  $b$ . This prediction is contrary to the corresponding result obtained from the imperfect interface model, which predicts higher stress intensity values at  $b$ , hence suggesting a crack growth towards the interface.





#### 4.3.1.2 Case 2 : $m = 3n$

Since the elastic interphase layer defined by  $m = 3n$  is similar to the case of the interface parameter  $m = n$ , it is not surprising that the general trend of the results for  $m = 3n$  is the same as the results for  $m = n$ . However, the stress intensity values for the case  $m = 3n$  are always lower than the corresponding values for  $m = n$ . For example, the decrease in the imperfect interface results for  $m = n$  and  $m = 3n$  for the symmetric crack of half-length  $R/5$  is about 50 percent for a soft inclusion ( $\mu_2/\mu_1 = 0.1$ ), 86 percent for a thermal inclusion ( $\mu_2/\mu_1 = 1$ ) and 168 percent for a hard inclusion ( $\mu_2/\mu_1 = 10$ ).

Crack points	$\frac{\mu_2}{\mu_1}$					
	0.1		1		10	
	I	P	I	P	I	P
$a = \frac{R}{4}$ $b = \frac{3R}{4}$	0.275	0.481	0.168	0.222	0.0355	0.037
$a = 0$ $b = \frac{R}{2}$	0.265	0.504	0.214	0.222	0.033	0.035
$a = \frac{2R}{5}$ $b = \frac{9R}{10}$	0.279	0.466	0.171	0.222	0.037	0.039
$a = -\frac{R}{5}$ $b = \frac{R}{5}$	0.235	0.470	0.140	0.199	0.028	0.030

**Table 4.3** Normalized stress intensity factor for various positions of crack



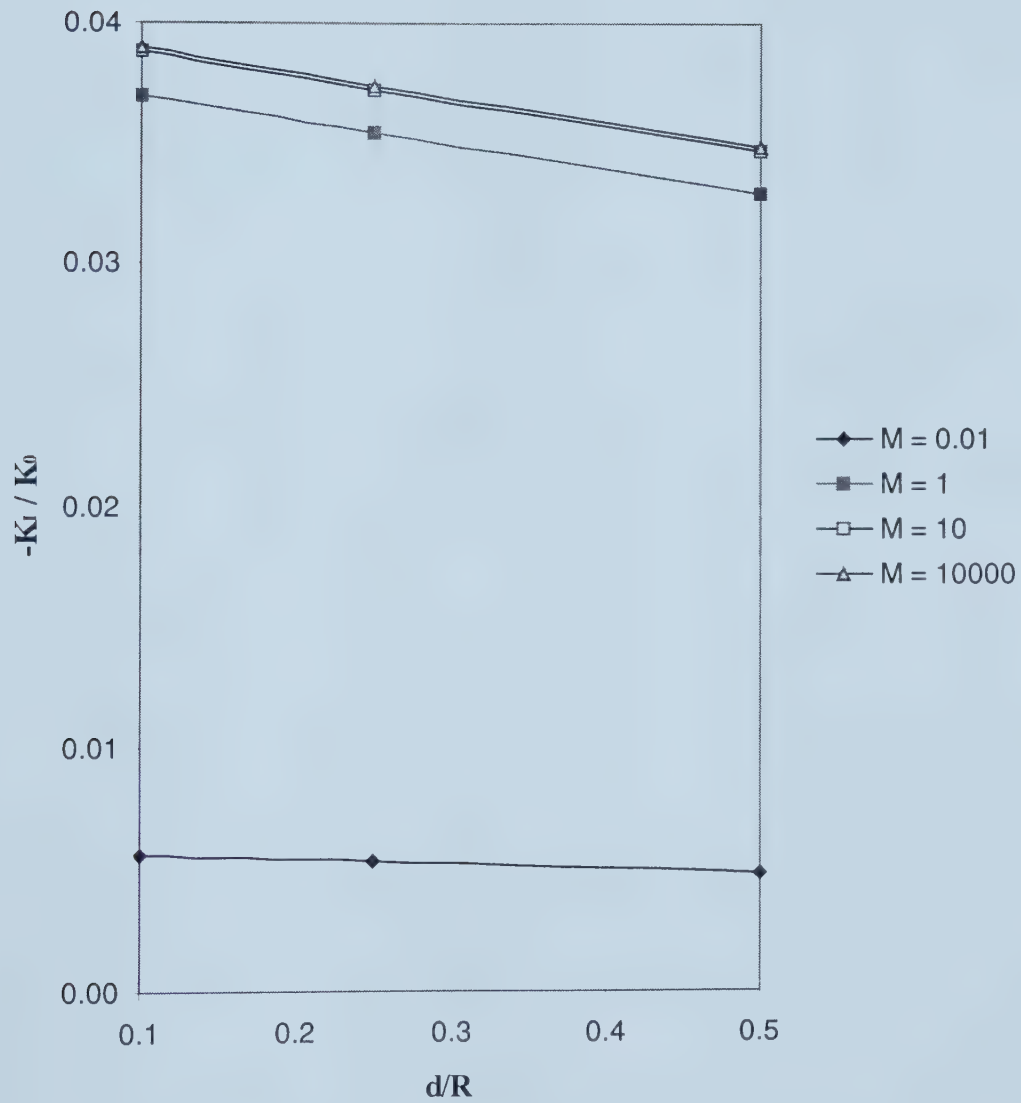


**Figure 4.7** Dependency of Normalized stress intensity factor on crack tip–interface distance (Hard Inclusion)



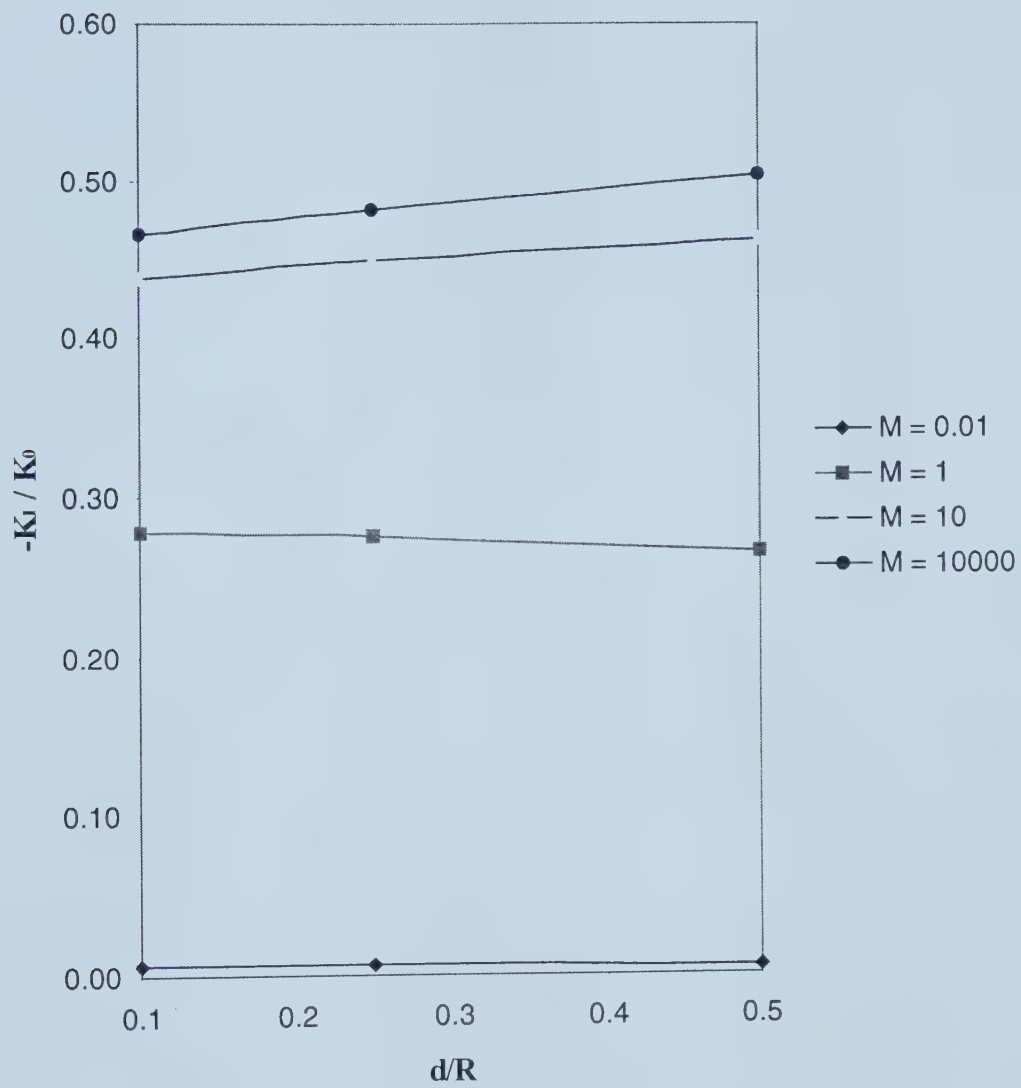


**Figure 4.8** Dependency of Normalized stress intensity factor on crack tip–interface distance (Soft Inclusion)



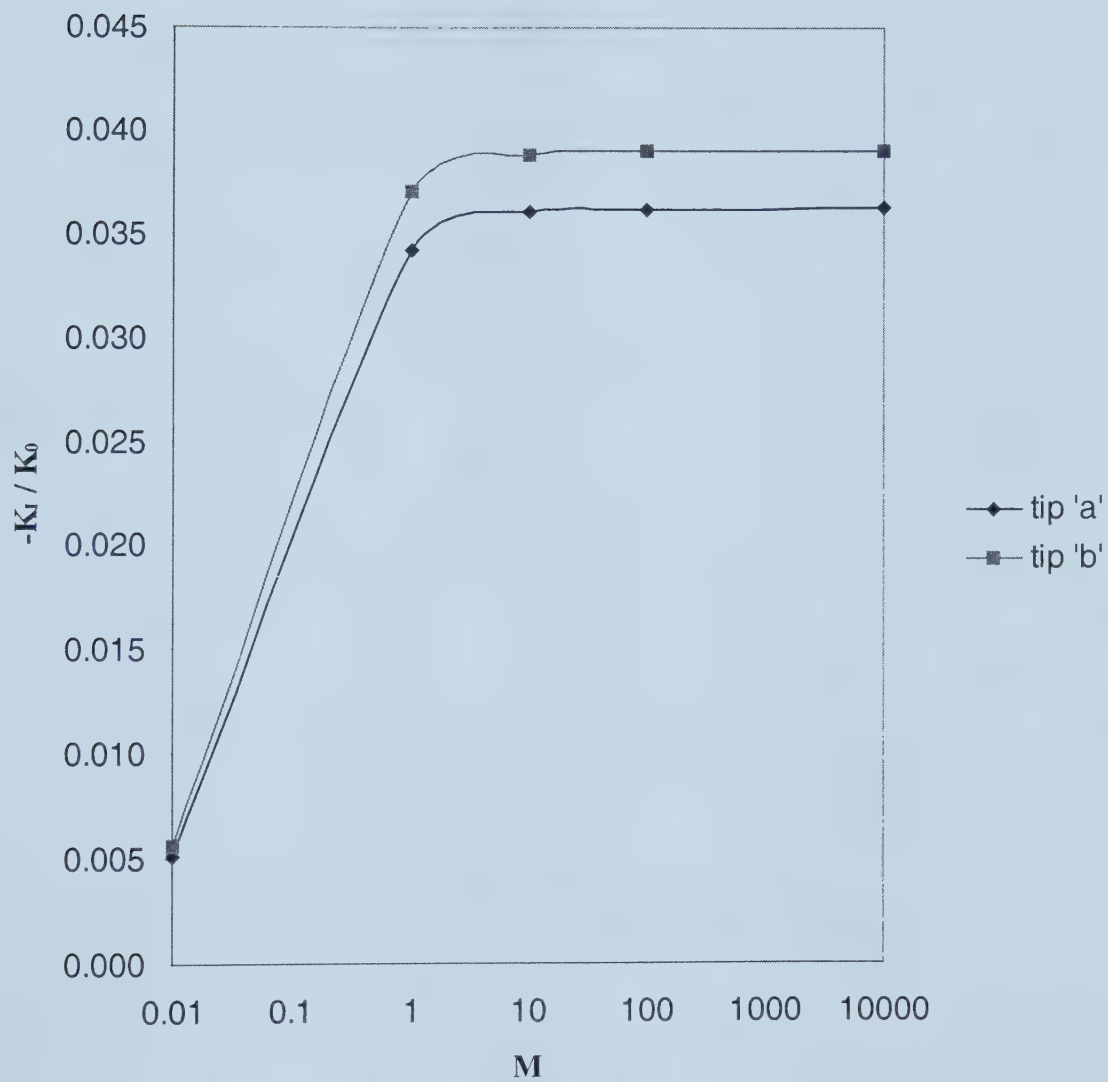


**Figure 4.9** Normalized stress intensity factor for a hard inclusion





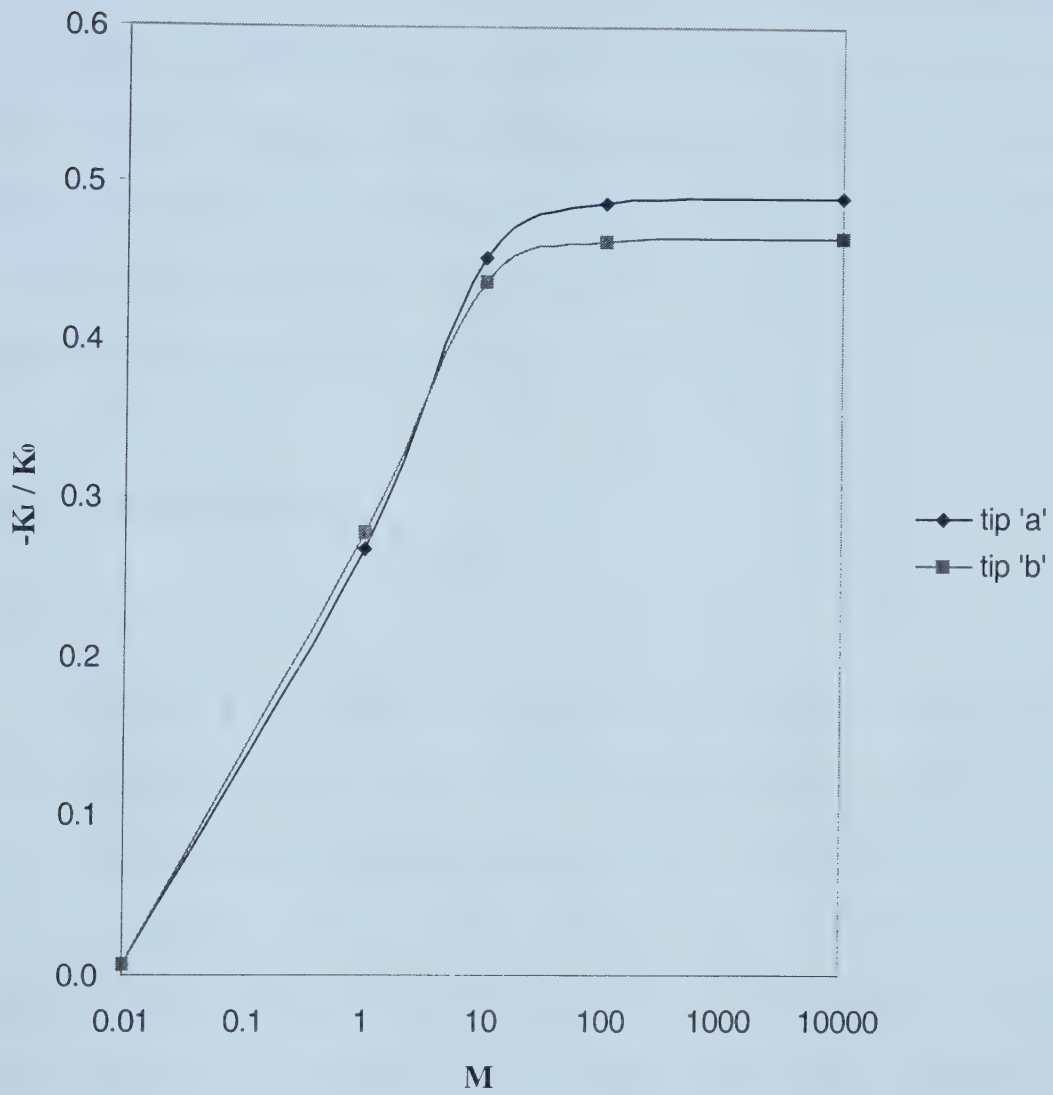


**Figure 4.10** Normalized stress intensity factor for a soft inclusion



The reason for the reduction in stress intensity factor values in Table 4.3 compared to Table 4.1 is due to the fact that the elastic interphase layer represents a much weaker inclusion-matrix bonding condition than  $m = n$ . As such, for any given load, a smaller amount of force is transmitted across the inclusion-matrix interface in the case of the elastic interphase layer. Although the pattern of results for  $m = n$  and  $m = 3n$  are the same, the difference in results between the perfect and imperfect interface models is much more pronounced for the elastic interphase layer.

### 4.3.2 Mechanical loading

#### 4.3.2.1 Case 1 : $m = n$

The pattern of the results of the stress intensity factor for uniaxial tensile stress shows significant similarity to that of uniform volume expansion. In Figure 4.11, for a hard inclusion, the stress intensity factor increases for both perfect and imperfect interface models as the crack tip-interface distance decreases. On the otherhand, for a soft inclusion as shown in Figure 4.12, the stress intensity factor decreases with decreasing crack tip-interface distance for the perfect interface model while it increases for an imperfect interface model. Figure 4.13 for a hard inclusion shows that the stress intensity factor at crack tip  $b$  is always greater than that at crack tip  $a$  for both perfect and imperfect interface models. A graphical representation of the stress intensity factor for a soft inclusion (as shown in Figure 4.14) shows that the stress intensity factor at crack tip  $a$  is greater than that at crack tip  $b$  for the perfect interface model.



Crack points	$\frac{\mu_2}{\mu_1}$									
	0.1		0.5		1		2		10	
	I	P	I	P	I	P	I	P	I	P
$a = \frac{R}{4}$ $b = \frac{3R}{4}$	0.168	0.432	0.701	1.416	1.165	2.000	1.750	2.550	2.991	3.369
$a = 0$ $b = \frac{R}{2}$	0.160	0.453	0.665	1.446	1.102	2.000	1.646	2.488	2.767	3.136
$a = \frac{2R}{5}$ $b = \frac{9R}{10}$	0.171	0.419	0.715	1.398	1.191	2.000	1.798	2.586	3.120	3.509
$a = -\frac{R}{5}$ $b = \frac{R}{5}$	0.139	0.423	0.576	1.315	0.952	1.789	1.416	2.187	2.354	2.678

**Table 4.4** Normalized stress intensity factor for various positions of crack



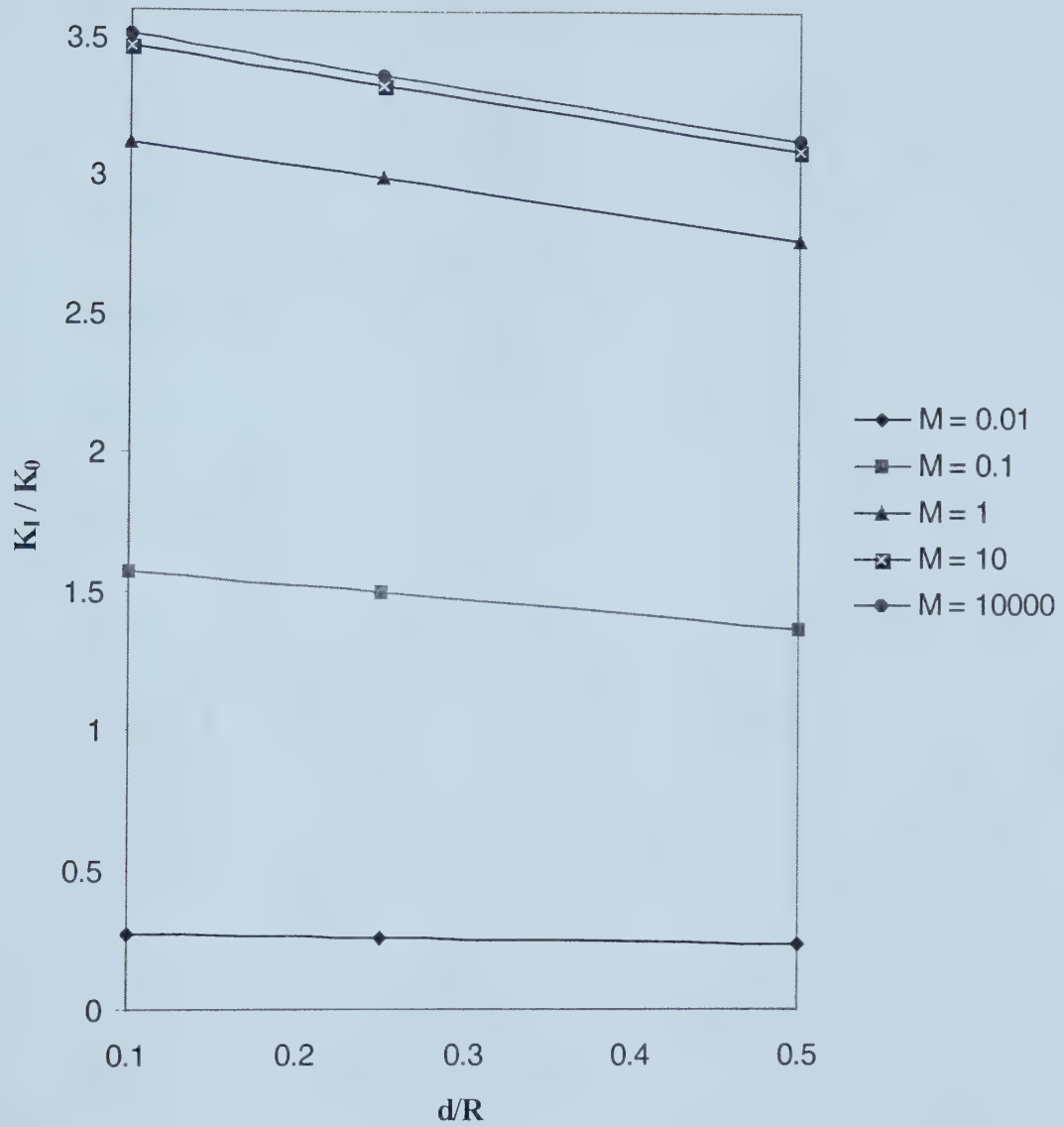


**Figure 4.11** Dependency of Normalized stress intensity factor on crack tip–interface distance (Hard Inclusion)





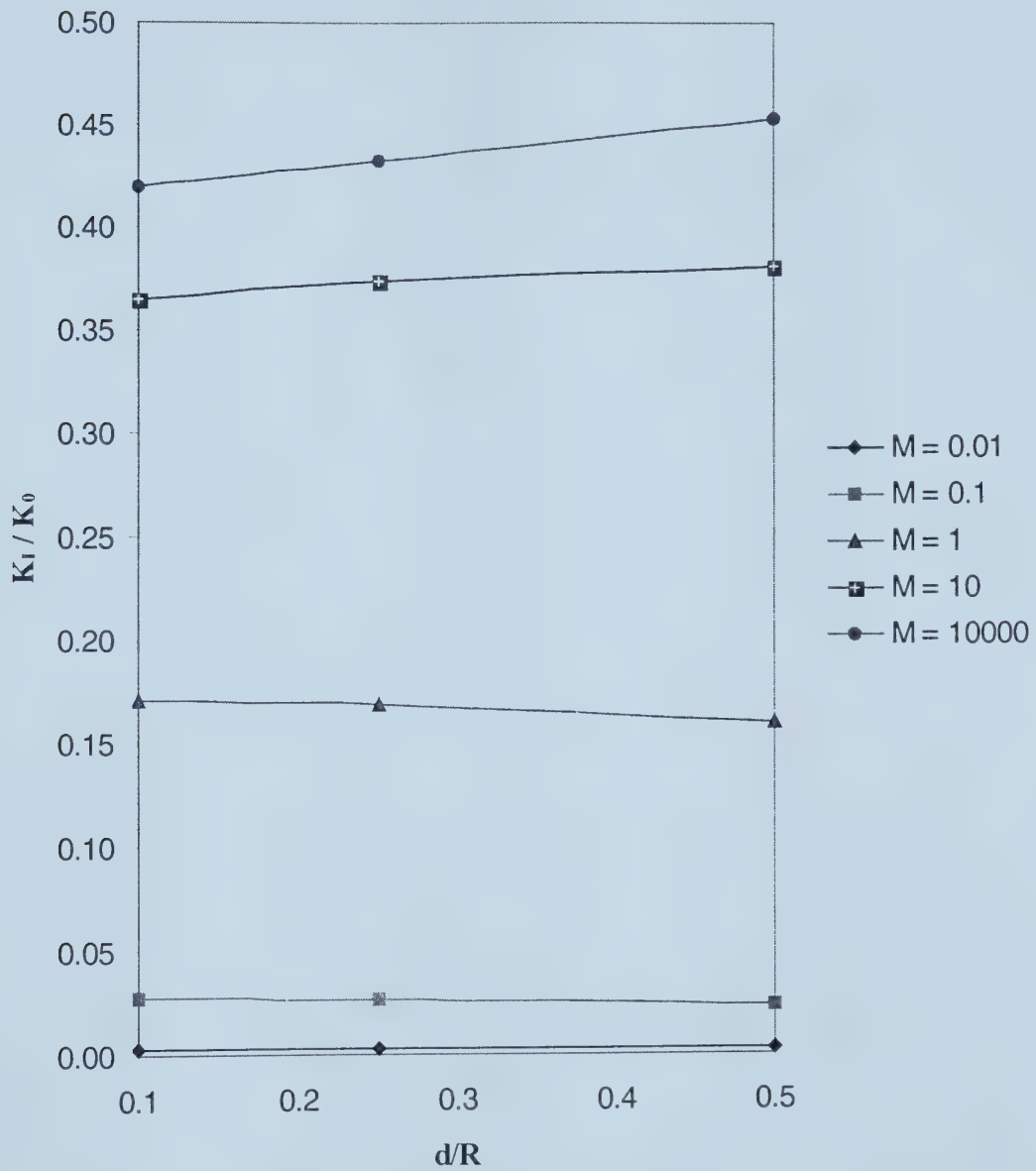


**Figure 4.12** Dependency of Normalized stress intensity factor on crack tip–interface distance (Soft Inclusion)



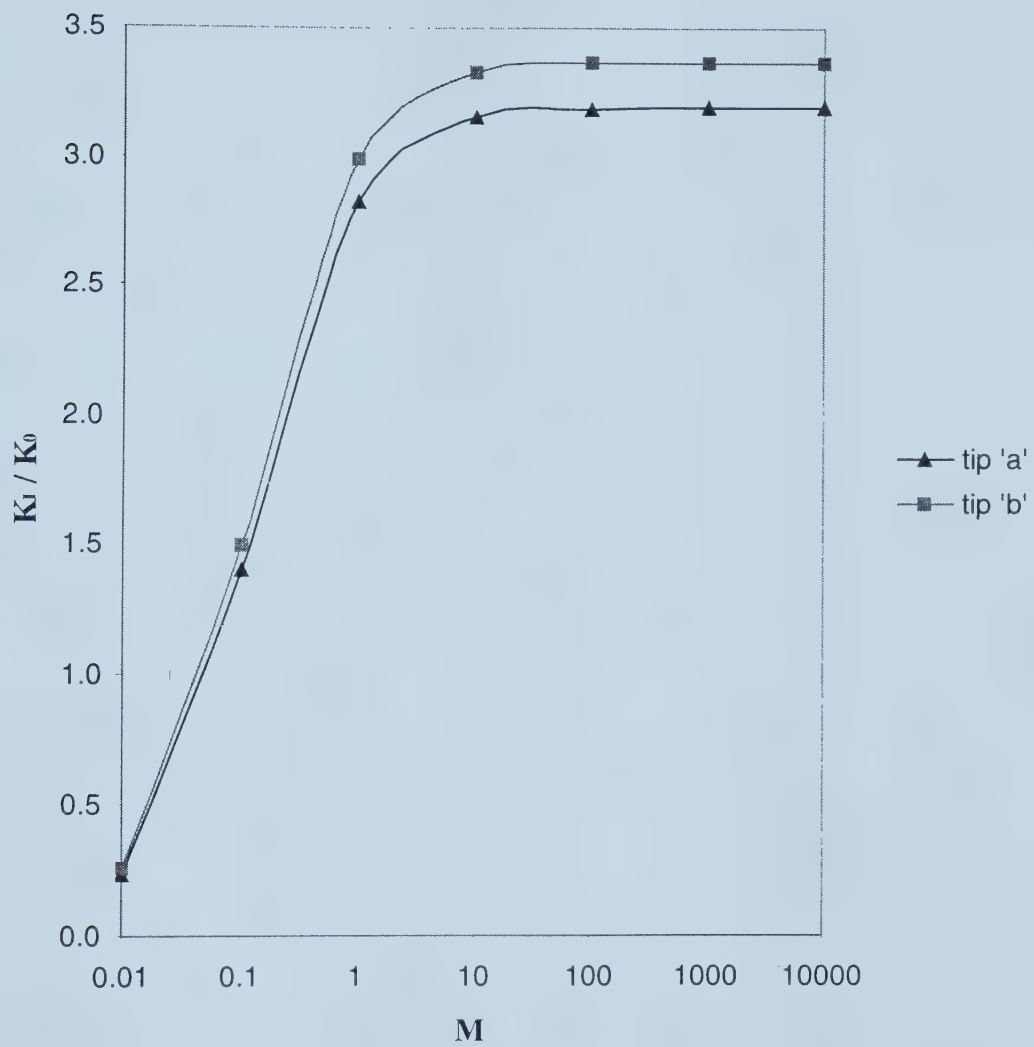


**Figure 4.13** Normalized stress intensity factor for a hard inclusion



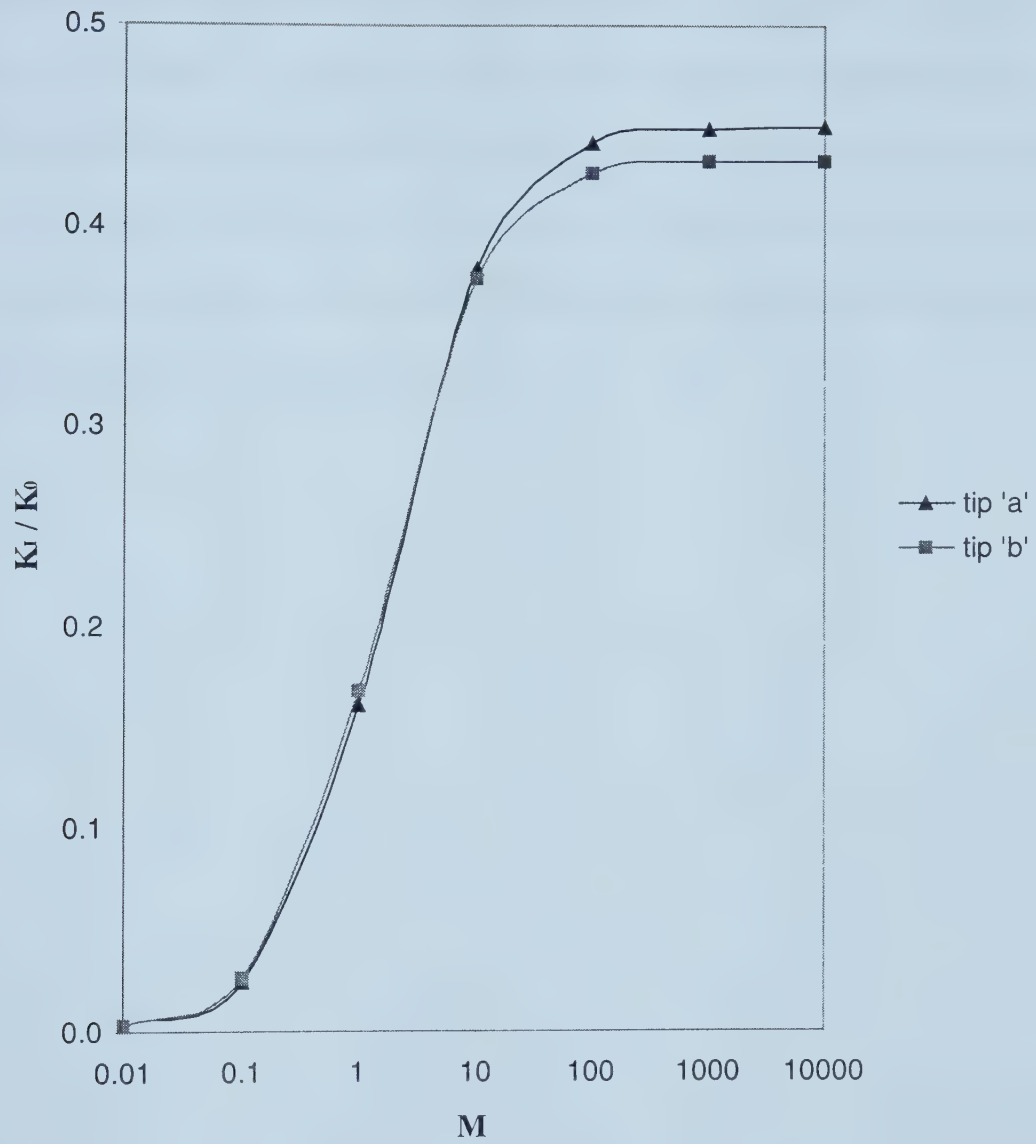


**Figure 4.14** Normalized stress intensity factor for a soft inclusion



The interaction between an interior radial crack and an imperfectly bonded inclusion has been determined using a semi-analytic method for different elastic material properties of inclusion and matrix as well as for various crack-inclusion geometries. The method is illustrated for a number of crack-inclusion geometries and shear moduli ratios to determine which inclusion-matrix combination, is more resistant to crack propagation. The results show clearly that the resistance to fiber-cracking of fiber-reinforced composites is dependent on the material properties of the constituents, the crack-inclusion geometry and, also on the fiber-matrix bond.





# CHAPTER 5

## 5 Conclusions and Future Work

### 5.1 Conclusions

In this study, a series method has been developed to analyze induced stresses within an inclusion containing an interior radial crack imperfectly bonded to the surrounding matrix due to the application of an eigenstrain or an external uniaxial tensile load. This was achieved by first of all formulating the appropriate single-inclusion problem of the interaction between an interior crack and an inclusion. Using the principles of linear elasticity and complex variable techniques, the dominant parameters (for example, stress potentials) and physical characteristics of the problem (for example, the crack face condition and interface conditions) were identified, isolated and analyzed. The magnitude of the elastic stress field in the vicinity of each of the crack tips - the stress intensity factor - is calculated by solving the governing boundary value problem and solving the ensuing set of algebraic equations numerically. An interpretation of the results was provided as illustrated in the Figures and Tables in Chapter 4. In order to verify the accuracy of the analytical and computational solution obtained in this study, we draw comparisons with corresponding cases documented in the literature where analytical results are available.

The results in Table 4.1, 4.3 and 4.4 show that, for the perfect interface model, for a hard inclusion, as the crack tip–interface distance decreases, the stress intensity factor increases, while for a soft inclusion, the stress intensity factor decreases as the crack



approaches the interface. On the other hand, for the imperfect interface model, the stress intensity factor for both hard and soft inclusions increases monotonically as the crack tip-interface distance decreases. Also, where elastic mismatch between the inclusion and matrix is ignored (thermal inclusion), the stress intensity factor increases as the crack tip approaches the interface, and is therefore not constant as suggested by the perfect interface model.

It is also noticeable from the results presented in Chapter 4 that values of the stress intensity factor for a given crack in the case of a soft inclusion are always greater than that of a corresponding hard inclusion. This conclusion is also obvious from Figure 4.3 where it can be seen that the stress intensity factor decreases with increasing shear modulus ratio. An explanation of this observation is that, under thermal or mechanical loading, the stress in the inclusion is generated as result of the constraint imposed by the matrix on the inclusion. Hence, it is expected that a stiff matrix will provide a higher resistive force on the fiber due to the load applied than will a soft matrix. This conclusion is evident in for example, Figures 4.1 – 4.3, where the stress intensity factors for  $M = 0.01$ , the case where the inclusion is largely unconstrained, are practically zero.

It has also been shown that using a perfect interface model instead of the more realistic imperfect interface model will lead to significant over - estimation of the stress intensity factor in excess of 100 percent for the hard inclusion and over 200 percent for the soft inclusion. The perfect interface model could also lead to an invalid prediction of the direction of crack growth, as illustrated in the case of thermal inclusions in Table 4.2 and soft inclusions in Figures 4.6, 4.11 and 4.14.



The results show that, generally, soft inclusions are much more susceptible to crack propagation than hard inclusions because of their relatively high stress intensity factors. Hence, if fiber-cracking is considered as a one of the major factors affecting the life-time of fiber-reinforced composite devices, it is recommended that, to reduce the risk of crack propagation, a fiber material with a high strength should be used.

The stress intensity factor at the crack tips, obtained from the present model but for a perfect interface show excellent agreement with the corresponding analytical results obtained in [16]. This suggests that the model used in this study can be used to efficiently predict the elastic stress field due to the interaction between an inclusion with an interior radial crack imperfectly bonded to the surrounding matrix.

The foregoing observations indicate conclusively that the analysis of the interaction between a fiber-crack and the interface imperfection is extremely important in an effort to understand and predict the strengthening mechanisms of fiber-reinforced composites. Therefore, the pronounced effect of the imperfect fiber-matrix bond on the stress intensity factor at the crack tip should not be ignored in such analyses.

It is known that failure by fracture in fiber-reinforced composites sometimes emanates from inherent cracks (due to manufacturing flaws or fatigue cracks) in the fiber. Therefore in the design of fiber-reinforced composites, it is important to have a good estimate of the disturbed stress state caused by the crack. An understanding of the micromechanics of the mode of this failure in the presence of the crack would be useful in improving the design of such devices. In such a design, the optimization criterion would be to maximize the strength and energy absorbing capabilities of the fiber and matrix to enhance reliability of the device while in service. The results presented in this



study could serve as a guide in the selection of fiber and matrix materials to ensure that the stress intensity factor is kept as small as possible to guarantee that failure does not occur within the intended lifetime.

## 5.2 Future Work

It has been shown that there are significant differences between the use of perfect and imperfect interface models describing the interaction between an interior crack and an inclusion. However, a much more comprehensive micromechanical model that takes into account the spatially nonuniform properties of the interphase layer (that is, pointwise variation of the properties of the interphase layer along its entire length) could be a worthwhile subject for future study. This is due to the fact that the interphase layer is often the product of processing conditions involved in the manufacture of composites and could therefore be regarded as an interaction zone with defects and stress concentrations. The interphase layer is therefore certainly *inhomogeneous*. This type of bonding condition is considered in [48] – [49]. In [48] it was shown that replacing the inhomogeneous interface by its homogeneous counterpart results in a relative error in the average mean stress of about 200 percent.

Kouris D. et al. [65] studied the interaction between two inclusions with perfect interface condition to determine how the interaction affects the local stress state of the fiber-matrix interface. In that paper, the Papkovitch-Neuber displacement formulation was used to account for the disturbance due to the presence of the other fiber and it was found that the distance between the fibers has a significant effect on the elastic stress field. This







observation suggests that using the single fiber solution may be quite inaccurate in predicting the local stress field. A proposed future work would be to study this problem for an imperfect bonding condition.



# References

- [1] Schwartz Mel M., Composite Materials Handbook, Second Edition, McGraw-Hill, Inc., 1992.
- [2] Kaw Autar K., Mechanics of Composite Materials, CRC Press LLC, 1997.
- [3] Eshelby J. D., "The Determination of the Elastic Field of an Ellipsoidal Inclusion and Related Problems," Proceedings of the Royal Society of London, **A241**, 1957, pp. 376 – 396.
- [4] Eshelby J. D., "The Elastic Field Outside an Ellipsoidal Inclusion," Proceedings of the Royal Society of London, **A 252**, 1959, pp. 561 – 569.
- [5] Aboudi J., "The Effective Moduli of Short-Fiber Composites," International Journal of Solids and Structures, **19**, 1983, pp. 693 – 707.
- [6] Sendekyj G. P., "Elastic Inclusion Problems in Plane Elastostatics," International Journal of Solids and Structures, **6**, 1970, pp. 1535 - 1543
- [7] Achenbach J. D. and Zhu H., "Radial matrix cracking and interphase failure in transversely loaded Fiber-Reinforced Composites," Mechanics of Materials, **11**, 1991, pp. 347 – 356.
- [8] Dundurs J. and Mura T., "Interaction between an Edge Dislocation and a Circular Inclusion," Journal of the Mechanics and Physics of Solids, **12**, 1964, pp. 177 – 189.
- [9] Müller W. H. and Schmauder S., "Stress intensity factors of r-Cracks in Fiber – Reinforced Composites under Thermal and Mechanical Loading," International Journal of Fracture, **59**, 1993, pp. 307 – 343.
- [10] Müller W. H. and Schmauder S., "On the behavior of r- and  $\vartheta$ - Cracks in Composite Materials under Thermal and Mechanical Loading," International Journal of Solids and Structures, **30**, 1993, pp. 1907 – 1918.
- [11] Dundurs J. and Sendekyj G. P., "Edge Dislocation inside a Circular Inclusion," Journal of the Mechanics and Physics of Solids, **13**, 1965, pp. 141 – 147.
- [12] Atkinson C., "The Interaction between a Crack and an Inclusion," International Journal of Engineering Science, **10**, 1972, pp. 127 – 136.
- [13] Anlas G. and Santare M. H., "Arbitrarily Oriented Crack inside an Elliptical Inclusion," ASME, Journal of Applied Mechanics, **60**, 1993, pp. 589 – 594.



- [14] Erdogan F., Gupta G. D. and Ratwani M., "Interaction between a Circular Inclusion and an Arbitrarily Oriented Crack," ASME, Journal of Applied Mechanics, **41**, 1974, pp. 1007 – 10013.
- [15] Tamate O., "The effect of a circular inclusion on the stresses around a line crack in a sheet under tension," International Journal of Fracture Mechanics, **4**, 1968, pp. 257 – 265.
- [16] Ru C. Q., "Stress Analysis of Thermal Inclusions With Interior Voids and Cracks," ASME, Journal of Electronic Packaging, **122**, 2000, pp. 192 - 199.
- [17] Liu Y., Ru C. Q., Schiavone P. and Mioduchowski A. "New Phenomena Concerning the Effect of Imperfect Bonding on Radial Matrix Cracking in Fiber Composites," International Journal of Engineering Science (accepted for publication).
- [18] Boniszewski T and Baker R. G., "Dislocations in Manganese Sulphide Inclusions in Steel," Acta Metallurgica, **11**, 1963, pp. 990 – 992.
- [19] Clegg W. J., Horsfall I., Mason J. F. and Edwards L., "The Tensile Deformation and Fracture of Al – "Saffil" Metal Matrix Composites," Acta Metallurgica, **36** No. 8, 1988, pp. 2151 – 2159.
- [20] Ru C. Q., "Effect of Interphase Layers on Thermal Stresses within an Elliptical Inclusion," Journal of Applied Physics, **84**, 1998, pp. 4872 - 4879.
- [21] Ru C. Q., "Interface Design of Neutral Elastic Inclusions," International Journal of Solids and Structures, **35**, 1998, pp. 559 - 572.
- [22] Mikata Y. and Taya M. "Stress Field in a coated Continuous Fiber Composite Subjected to Thermo – Mechanical Loading," Journal of Composite Materials, **19**, 1985, pp. 554 - 578.
- [23] Cherkaoui M., Sabar H. and Berveiller M., "Micromechanical approach of the Coated Inclusion problem and applications to Composite Materials," ASME, Journal of Eng. Mater. Tech., **116**, 1994, pp. 274 - 278.
- [24] Bigoni D., Serkov S. K., Valentini M. and Movchan A. B., "Asymptotic Model of Dilute Composites with Imperfectly Bonded Inclusions," International Journal of Solids and Structures, **35**, 1998, pp. 3239 – 3258.
- [25] Lipton R. and Vernescu B., "Variational Methods, Size Effects and Extremal Microstructures for Elastic Composites with Imperfect Interface," Mathematical Models and Methods in Applied Sciences, **5**, 1995, pp. 1139 – 1173



- [26] Qui Y. P. and Weng G. J., "Elastic Moduli of Thickly Coated Particle and Fiber – Reinforced Composites," ASME Journal of Applied Mechanics, **58**, 1991, pp. 388 – 398.
- [27] Walpole L., "A Coated Inclusion in an Elastic Medium," Mathematical Proceedings of the Cambridge Philosophical Society, **83**, 1978, pp. 495 – 506.
- [28] Broutman L. J. and Agarwal B. D., "A Theoretical Study of the Effect on an Interfacial Layer on the Properties of Composites", Polymer Engineering Science, **14**, 1974, pp. 581 – 588.
- [29] Maurer F. J., Simha R. and Jain R. K., "On the Elastic Moduli of Particulate Composites: Interlayer versus Molecular model", Composites Interfaces, H. Ishida et al., ed., North – Holland, 1986, pp. 367 – 374.
- [30] Sideridis E., "The In – Plane Shear Modulus of Fiber Reinforced Composites as Defined by the Concept of Interphase", Composite Science and Technology, **31**, 1988, pp. 35 – 53.
- [31] Theocaris P. S., Sideridis E. P. and Papanicolaou G. C., "The Elastic Longitudinal Modulus and Poisson's Ratio of fiber Composites", Journal of Reinforced Plastics and Composites, **4**, 1985, pp. 396 – 418.
- [32] Benveniste Y., Dvorak G. J. and Chen T., "Stress fields in Composites with Coated Inclusions," Mechanics of Materials, **7**, 1989, pp. 305 – 317.
- [33] Owen D. R. and Lyness J. F., "Investigation of Bond Failure in Fiber Reinforced Materials by the Finite Element Method", Fiber Science and Technology, **5**, 1972, pp. 129 – 141.
- [34] Robertson D. D. and Mall S., "Fiber-Matrix Interphase Effects upon Transverse Behavior in Metal-Matrix Composites", Journal of Composites Technology and Research, JCTRER, **14**, 1992, pp. 3 – 11.
- [35] Hashin Z., "Thermoelastic effect of fiber reinforced composites with imperfect interface," Mechanics of Materials, **8**, 1990, pp. 333 – 348.
- [36] Hashin Z., "The Spherical Inclusion with Imperfect Interface," ASME, Journal of Applied Mechanics, **58**, 1991, pp. 444 – 449.
- [37] Gao Z., "A circular inclusion with imperfect interface: Eshelby's Tensor and Related Problems," ASME, Journal of Applied Mechanics, **62**, 1995, pp. 860 – 866.





- [38] Achenbach J. D. and Zhu H., "Effect of Interfacial Zone on Mechanical Behavior and Failure of Fiber-Reinforced Composites," *Journal of the Mechanics and Physics of Solids*, **37**, No. 3, 1989, pp. 381 – 393.
- [39] Lene F. and Leguillon D., "Homogenized Constitutive Law for a Partially Cohesive Composite Material", *International Journal of Solids and Structures*, **18**, 1982, pp. 443 – 458.
- [40] Steif P. S. and Hoysan S. F., "An Energy Method for Calculating the Stiffness of Aligned Short-Fiber Composites", *Mechanics of Materials*, **6**, 1987, pp. 197 – 210.
- [41] Aboudi J., "Damage in Composites – Modeling of Imperfect Bonding", *Composite Science and Technology*, **28**, 1987, pp. 103 – 128.
- [42] Gosz M., Moran B. and Achenbach J. D., "Load-Dependent Constitutive Response of Fiber Composites with Compliant Interphases," *Journal of the Mechanics and Physics of Solids*, **40**, No. 8, 1992, pp. 1789 – 1803.
- [43] Benveniste Y., "The Effective Mechanical Behaviour of Composite Materials with Imperfect Contact between the Constituents," *Mechanics of Materials*, **4**, 1985, pp. 197 – 208.
- [44] Zhong Z. and Meguid S. A., "On the eigenstrain problem of a spherical inclusion with an imperfect bonded interface," *ASME, Journal of Applied Mechanics*, **63**, 1996, pp. 877 – 883.
- [45] Amenyah W., Schiavone P., Ru C. Q. and Mioduchowski A. "Interior Cracking of a Circular Inclusion with Imperfect Interface Under Thermal Loading," *Mathematics and Mechanics of Solids* (accepted for publication).
- [46] Jasuik I. and Tong Y., "The Effect of Interface on the Elastic Stiffness of Composites," *Mechanics of Composite Materials and Structures*, Reddy J. N. et al, ed., *ASME AMD*, **100**, 1989, pp. 49 – 54.
- [47] Muskhelishvili N. I., "Some basic problems of the mathematical theory of elasticity," 1963, P. Noordhoff Ltd., Netherlands.
- [48] Sudak L., Ru C. Q, Schiavone P. and Mioduchowski A., "A Circular Inclusion with Inhomogeneously Imperfect Interface in Plane Elasticity," *Journal of Elasticity*, **55**, 1999, pp. 19 - 41
- [49] Ru C. Q. and Schiavone P., "A Circular Inclusion with Circumferentially Inhomogeneous Interface in Antiplane Shear," *Proceedings of the Royal Society of London*, **A453**, 1997, pp. 2551 – 2572.



- [50] Jayaraman K., Reifsnider K. L. and Swain R. E., "Elastic and Thermal Effects in the Interphase: Part I. Comments on Characterization Methods," *Journal of Composites, Technology and Research, JCTRER*, **15**, No. 1, 1993, pp. 3 – 13.
- [51] Jayaraman K., Reifsnider K. L. and Swain R. E., "Elastic and Thermal Effects in the Interphase: Part II. Comments on Modeling Studies," *Journal of Composites, Technology and Research, JCTRER*, **15**, No. 1, 1993, pp. 14 – 22.
- [52] Swain R. E., Reifsnider K. L., Jayaraman K. and El-Zein M., "Interface/Interphase Concepts in Composite Material Systems," *Journal of Thermoplastic Composites*, **3**, 1990, pp. 13 – 23.
- [53] Karihaloo B. L. and Viswanathan K., "Elastic Field of a Partially Debonded Elliptic Inhomogeneity in an Elastic Matrix (Plane-Stain)," *ASME Journal of Applied Mechanics*, **52**, 1985, pp. 835 – 840.
- [54] Karihaloo B. L. and Viswanathan K., "Elastic Field of an Elliptic Inhomogeneity with Debonding over an Arc (Antiplane strain)," *ASME Journal of Applied Mechanics*, **52**, 1985, pp. 91 – 97.
- [55] Kato M, Niwa H., Yagi H., and Tsuchikawa H., " Stress distribution in an Aluminum interconnect of very large scale integration," *Journal of Applied Physics*, **68**, 1990, pp. 328 – 333.
- [56] Hashin Z., " Analysis of Composite Materials – A Survey," *ASME, Journal of Applied Mechanics*, **50**, 1983, pp. 481 – 505.
- [57] Verpoest I., Desaegeer M., and Ivens J., "The influence of the Fiber-Matrix Interface on Damage Development in Composite Materials," *Proceedings of the Colloquim on Interfaces in Materials*, Brussels, Dec. 1988.
- [58] Goto K. and Kagawa Y., "Crack–Fiber Interaction and Interfacial Failure Models in Fiber–Reinforced Ceramics," *Material Science and Engineering*, **A176**, 1994, pp. 357 – 361.
- [59] Churchill R. V. and Brown J. W., "Complex Variables and Applications," Fourth Edition, McGraw-Hill, Inc., 1984.
- [60] Chung D. D., *Carbon Fiber Composites*, Butterworth-Heinemann, 1994.
- [61] Jasiuk I., Chen J. and Thorpe M. F., "Elastic Moduli of Composites With Rigid Sliding Inclusions," *Journal of the Mechanics and Physics of Solids*, **40**, 1992, pp. 373 – 391.



- [62] Drzal L. T., "Composite Interphase Characterization," SAMPE Journal, **19**, 1983, pp. 7 – 13.
- [63] Mura T. and Furuhashi R., "The Elastic Inclusion With a Sliding Interface," ASME, Journal of Applied Mechanics, **51**, 1984, pp. 308 – 310.
- [64] Xiao Z. M. and Chen B. J., "On the Interaction between an Edge Dislocation and a Coated Inclusion," International Journal of Solids and Structures, **38**, 2001, pp. 2533 – 2548.
- [65] Kouris D. and Tsuchida E., "On the Elastic Interaction between two Fibers in a Continuous Fiber Composite under Thermal Loading," Mechanics of Materials, **12**, 1991, pp. 131 – 146.
- [66] Shen H., Schiavone P, Ru C. Q. and Mioduchowski A., "An Elliptic Inclusion with Imperfect Interface in Antiplane Shear," International Journal of Solids and Structures, **37**, 2000, pp. 4557 – 4575.
- [67] Shen H., Schiavone P, Ru C. Q. and Mioduchowski A., "Analysis of Internal Stress in an Elliptic Inclusion with Imperfect Interface in Plane Elasticity," Mathematics and Mechanics of Solids **5**, 2000, pp. 501 - 521.
- [68] Shen H., Schiavone P, Ru C. Q. and Mioduchowski A., "Interfacial Thermal Stress Analysis of an Elliptic Inclusion with a Compliant Interphase Layer in Plane Elasticity," International Journal of Solids and Structures (To appear).



# APPENDIX A

## Detailed derivation of some of the relevant equations

### 1. Equation (2.6)

$$\begin{aligned}
 \sigma_{rr} - i\sigma_{r\theta} &= m[[u_r]] - mu_r^0 - i(n[[u_\theta]] - nu_\theta^0), \\
 &= m(u_r^1 - u_r^2) - mu_r^0 - i[n(u_\theta^1 - u_\theta^2) - nu_\theta^0], \\
 &= mu_r^1 - mu_r^2 - mu_r^0 - inu_\theta^1 + inu_\theta^2 + inu_\theta^0, \\
 &= \frac{mu_r^1}{2} + \frac{mu_r^1}{2} - \frac{mu_r^2}{2} - \frac{mu_r^2}{2} - \frac{inu_\theta^1}{2} - \frac{inu_\theta^1}{2} + \frac{inu_\theta^2}{2} + \frac{inu_\theta^2}{2} \\
 &\quad + \frac{nu_r^1}{2} - \frac{nu_r^1}{2} + \frac{nu_r^2}{2} - \frac{nu_r^2}{2} + \frac{imu_\theta^1}{2} - \frac{imu_\theta^1}{2} + \frac{imu_\theta^2}{2} - \frac{imu_\theta^2}{2} \\
 &\quad - [mu_r^0 - inu_\theta^0], \\
 &= \left(\frac{m+n}{2}\right)u_r^1 + \left(\frac{m-n}{2}\right)u_r^1 - \left(\frac{m-n}{2}\right)u_r^2 - \left(\frac{m+n}{2}\right)u_r^2 + \left(\frac{m-n}{2}\right)iu_\theta^1 \\
 &\quad - \left(\frac{m+n}{2}\right)iu_\theta^1 + \left(\frac{m+n}{2}\right)iu_\theta^2 - \left(\frac{m+n}{2}\right)iu_\theta^2 - [mu_r^0 - inu_\theta^0], \\
 &= \left(\frac{m+n}{2}\right)[u_r^1 - u_r^2 - iu_\theta^1 + iu_\theta^2] + \left(\frac{m-n}{2}\right)[u_r^1 - u_r^2 + iu_\theta^1 - iu_\theta^2] \\
 &\quad - [mu_r^0 - inu_\theta^0].
 \end{aligned}$$

Hence, we obtain,

$$\begin{aligned}
 (\sigma_{rr} - i\sigma_{r\theta})_1 &= \left(\frac{m+n}{2}\right)[(u_r^1 - iu_\theta^1) - (u_r^2 - iu_\theta^2)] + \left(\frac{m-n}{2}\right)[(u_r^1 + iu_\theta^1) - (u_r^2 + iu_\theta^2)] \\
 &\quad - [mu_r^0 - inu_\theta^0], \quad z \in \Gamma.
 \end{aligned} \tag{2.6}$$





## 2. Equation (2.7)

From the results [13] we can write the displacement due to eigenstrain as

$$u_r^0 = R(\varepsilon_x^0 \cos^2 \theta + \varepsilon_y^0 \sin^2 \theta + \varepsilon_{xy}^0 \sin 2\theta), \quad u_\theta^0 = R\left(\frac{\varepsilon_y^0 - \varepsilon_x^0}{2} \sin 2\theta + \varepsilon_{xy}^0 \cos 2\theta\right).$$

Using Trigonometric half – angle formulae, the above can be written as

$$u_r^0 = R\left(\frac{\varepsilon_x^0 + \varepsilon_x^0 \cos 2\theta}{2} + \frac{\varepsilon_y^0 - \varepsilon_y^0 \cos 2\theta}{2} + \varepsilon_{xy}^0 \sin 2\theta\right),$$

$$= R\varepsilon_1 + R\varepsilon_2 \cos 2\theta + R\varepsilon_3 \sin 2\theta,$$

$$u_\theta^0 = R\varepsilon_3 \cos 2\theta - R\varepsilon_2 \sin 2\theta,$$

$$\text{where } \varepsilon_1 = \frac{\varepsilon_x^0 + \varepsilon_y^0}{2}, \quad \varepsilon_2 = \frac{\varepsilon_x^0 - \varepsilon_y^0}{2}, \quad \varepsilon_3 = \varepsilon_{xy}^0.$$

Substituting into the square bracket term of (2.6) we obtain,

$$\begin{aligned} [mu_r^0 - inu_\theta^0] &= mR\varepsilon_1 + mR\varepsilon_2 \cos 2\theta + mR\varepsilon_3 \sin 2\theta - inR\varepsilon_3 \cos 2\theta + inR\varepsilon_2 \sin 2\theta, \\ &= \frac{mR\varepsilon_2}{2} \cos 2\theta + \frac{mR\varepsilon_2}{2} \cos 2\theta - \frac{imR\varepsilon_2}{2} \sin 2\theta + \frac{imR\varepsilon_2}{2} \sin 2\theta \\ &\quad + \frac{imR\varepsilon_3}{2} \cos 2\theta - \frac{imR\varepsilon_3}{2} \cos 2\theta + \frac{mR\varepsilon_3}{2} \sin 2\theta + \frac{mR\varepsilon_3}{2} \sin 2\theta \\ &\quad + \frac{inR\varepsilon_2}{2} \sin 2\theta + \frac{inR\varepsilon_2}{2} \sin 2\theta - \frac{inR\varepsilon_3}{2} \cos 2\theta - \frac{inR\varepsilon_3}{2} \cos 2\theta \\ &\quad + \frac{nR\varepsilon_3}{2} \sin 2\theta - \frac{mR\varepsilon_3}{2} \sin 2\theta + \frac{n\varepsilon_3}{2} \cos 2\theta - \frac{n\varepsilon_3}{2} \cos 2\theta \\ &\quad + mR\varepsilon_1, \end{aligned}$$



$$\begin{aligned}
&= R\left(\frac{m+n}{2}\right)\varepsilon_2 \cos 2\theta + R\left(\frac{m-n}{2}\right)\varepsilon_2 \cos 2\theta + R\left(\frac{m-n}{2}\right)\varepsilon_3 \sin 2\theta \\
&+ R\left(\frac{m+n}{2}\right)\varepsilon_3 \sin 2\theta - R\left(\frac{m-n}{2}\right)i\varepsilon_2 \sin 2\theta + R\left(\frac{m+n}{2}\right)i\varepsilon_2 \sin 2\theta \\
&+ R\left(\frac{m-n}{2}\right)\varepsilon_3 \cos 2\theta - R\left(\frac{m+n}{2}\right)\varepsilon_3 \cos 2\theta + mR\varepsilon_1,
\end{aligned}$$

$$\begin{aligned}
[mu_r^0 - inu_\theta^0] &= mR\varepsilon_1 + R\left(\frac{m+n}{2}\right)\{(\varepsilon_2 - i\varepsilon_3) \cos 2\theta + i(\varepsilon_2 - i\varepsilon_3) \sin 2\theta\} \\
&+ R\left(\frac{m-n}{2}\right)\{(\varepsilon_2 + i\varepsilon_3) \cos 2\theta - i(\varepsilon_2 + i\varepsilon_3) \sin 2\theta\}, \\
&= mR\varepsilon_1 + R\left(\frac{m+n}{2}\right)(\varepsilon_2 - i\varepsilon_3)e^{2i\theta} + R\left(\frac{m-n}{2}\right)(\varepsilon_2 + i\varepsilon_3)e^{-2i\theta}.
\end{aligned}$$

Using  $z = Re^{i\theta}$ , the term in the square bracket in (2.6) can be written in a convenient form as

$$[mu_r^0 - inu_\theta^0] = mR\varepsilon_1 + \left(\frac{m+n}{2R}\right)(\varepsilon_2 - i\varepsilon_3)z^2 + \left(\frac{m-n}{2z}\right)R^3(\varepsilon_2 + i\varepsilon_3), \quad z \in \Gamma. \quad (2.7)$$

### 3. Equation (2.8)

Using (2.1) and substituting  $z = Re^{i\theta}$  we can write,

$$u_r^1 + iu_\theta^1 = \frac{R}{2\mu_1 z} [k_1 \phi_1(z) - z\overline{\phi_1'(z)} - \overline{\psi_1(z)}],$$

$$u_r^2 + iu_\theta^2 = \frac{R}{2\mu_2 z} [k_2 \phi_2(z) - z\overline{\phi_2'(z)} - \overline{\psi_2(z)}].$$

Taking the conjugate of the above we obtain,



$$u_r^1 - iu_\theta^1 = \frac{z}{2\mu_1 R} \left[ k_1 \overline{\phi_1(z)} - \overline{z} \phi_1'(z) - \psi_1(z) \right],$$

$$u_r^2 - iu_\theta^2 = \frac{z}{2\mu_2 R} \left[ k_2 \overline{\phi_2(z)} - \overline{z} \phi_2'(z) - \psi_2(z) \right].$$

We now rewrite the left-hand-side of (2.6) using (2.1) and also substituting the two expressions above, we obtain,

$$\begin{aligned} \phi_1'(z) + \overline{\phi_1'}\left(\frac{R^2}{z}\right) - z\phi_1''(z) - \frac{z^2}{R^2}\psi_1'(z) = & \left( \frac{m+n}{2} \right) \left\{ \begin{aligned} & \frac{z}{2\mu_1 R} \left[ k_1 \overline{\phi_1}\left(\frac{R^2}{z}\right) - \overline{z} \phi_1'(z) - \psi_1(z) \right] - \\ & \frac{z}{2\mu_2 R} \left[ k_2 \overline{\phi_2}\left(\frac{R^2}{z}\right) - \overline{z} \phi_2'(z) - \psi_2(z) \right] \end{aligned} \right\} \\ & + \left( \frac{m-n}{2} \right) \left\{ \begin{aligned} & \frac{R}{2\mu_1 z} \left[ k_1 \phi_1(z) - z \overline{\phi_1'}\left(\frac{R^2}{z}\right) - \overline{\psi_1}\left(\frac{R^2}{z}\right) \right] - \\ & \frac{R}{2\mu_2 z} \left[ k_2 \phi_2(z) - z \overline{\phi_2'}\left(\frac{R^2}{z}\right) - \overline{\psi_2}\left(\frac{R^2}{z}\right) \right] \end{aligned} \right\} \\ & - [m u_r^0 - i n u_\theta^0]. \end{aligned}$$

The square bracket term in the above equation is written using (2.7) and finally we obtain,



$$\begin{aligned}
\phi_1'(z) + \overline{\phi_1'}\left(\frac{R^2}{z}\right) - z\phi_1''(z) - \frac{z^2}{R^2}\psi_1'(z) &= \left(\frac{m+n}{4R}\right) \left\{ \begin{aligned} &\frac{z}{\mu_1} k_1 \overline{\phi_1'}\left(\frac{R^2}{z}\right) - \frac{R^2}{\mu_1} \phi_1'(z) - \frac{z}{\mu_1} \psi_1'(z) \\ &-\frac{z}{\mu_2} k_2 \overline{\phi_2'}\left(\frac{R^2}{z}\right) + \frac{R^2}{\mu_2} \phi_2'(z) + \frac{z}{\mu_2} \psi_2'(z) \end{aligned} \right\} \\
&+ R\left(\frac{m-n}{4}\right) \left\{ \begin{aligned} &\frac{1}{\mu_1 z} k_1 \phi_1(z) - \frac{1}{\mu_1} \overline{\phi_1'}\left(\frac{R^2}{z}\right) - \frac{1}{\mu_1 z} \overline{\psi_1'}\left(\frac{R^2}{z}\right) \\ &-\frac{1}{\mu_2 z} k_2 \phi_2(z) + \frac{1}{\mu_2} \overline{\phi_2'}\left(\frac{R^2}{z}\right) + \frac{1}{\mu_2 z} \overline{\psi_2'}\left(\frac{R^2}{z}\right) \end{aligned} \right\} \\
&- mR\mathcal{E}_1 - \left(\frac{m+n}{2R}\right)(\mathcal{E}_2 - i\mathcal{E}_3)z^2
\end{aligned} \tag{2.8}$$

$$-\left(\frac{m-n}{2z^2}\right)R^3(\mathcal{E}_2 + i\mathcal{E}_3), \quad z \in \Gamma.$$

#### 4. Derivation of the complex potentials $\phi_2(z)$ and $\psi_2(z)$

Given that

$$\phi_2(z) = \frac{Y(z)}{2\sqrt{(z-a)(z-b)}} + \frac{X(z)}{2},$$

$$Y(z) = \sum_{k=0}^{\infty} d_k z^k = d_0 + d_1 z + d_2 z^2 + d_3 z^3 + d_4 z^4 + d_5 z^5 + \dots, \quad z \in C,$$





$$\frac{Y(z)}{2\sqrt{(z-a)(z-b)}} = (d_0 + d_1z + d_2z^2 + d_3z^3 + d_4z^4 + d_5z^5 + \dots)^*$$

$$\left( \frac{H_1}{z} + \frac{H_2}{z^2} + \frac{H_3}{z^3} + \frac{H_4}{z^4} + \frac{H_5}{z^5} + \frac{H_6}{z^6} + \frac{H_7}{z^7} + \frac{H_8}{z^8} + \frac{H_9}{z^9} + \frac{H_{10}}{z^{10}} + \dots \right),$$

we obtain,

$$\begin{aligned} \phi_2(z) = & H_1d_5z^4 + (H_2d_5 + H_1d_4)z^3 \\ & + (H_3d_5 + H_2d_4 + H_1d_3)z^2 + (H_4d_5 + H_3d_4 + H_2d_3 + H_1d_2)z \\ & + (H_5d_5 + H_4d_4 + H_3d_3 + H_2d_2 + H_1d_1) \\ & + (H_6d_5 + H_5d_4 + H_4d_3 + H_3d_2 + H_2d_1 + H_1d_0)\frac{1}{z} \\ & + (H_7d_5 + H_6d_4 + H_5d_3 + H_4d_2 + H_3d_1 + H_2d_0)\frac{1}{z^2} \\ & + (H_8d_5 + H_7d_4 + H_6d_3 + H_5d_2 + H_4d_1 + H_3d_0)\frac{1}{z^3} \\ & + (H_9d_5 + H_8d_4 + H_7d_3 + H_6d_2 + H_5d_1 + H_4d_0)\frac{1}{z^4} \\ & + (H_{10}d_5 + H_9d_4 + H_8d_3 + H_7d_2 + H_6d_1 + H_5d_0)\frac{1}{z^5} \\ & + (H_{11}d_5 + H_{10}d_4 + H_9d_3 + H_8d_2 + H_7d_1 + H_6d_0)\frac{1}{z^6} \\ & + (H_{12}d_5 + H_{11}d_4 + H_{10}d_3 + H_9d_2 + H_8d_1 + H_7d_0)\frac{1}{z^7}. \end{aligned}$$

Also we can write,



$$\frac{X(z)}{2} = \frac{1}{2} \sum_{k=0}^{\infty} c_k z^k = \frac{c_0}{2} + \frac{c_1 z}{2} + \frac{c_2 z^2}{2} + \frac{c_3 z^3}{2} + \frac{c_4 z^4}{2} + \frac{c_5 z^5}{2} + \dots, \quad z \in C,$$

which leads to

$$\begin{aligned} \phi_2(z) = & \frac{c_5}{2} z^5 + \frac{1}{2} (c_4 + H_1 d_5) z^4 + \frac{1}{2} (c_3 + H_2 d_5 + H_1 d_4) z^3 \\ & + \frac{1}{2} (c_2 + H_3 d_5 + H_2 d_4 + H_1 d_3) z^2 + \frac{1}{2} (c_1 + H_4 d_5 + H_3 d_4 + H_2 d_3 + H_1 d_2) z \\ & + \frac{1}{2} (c_0 + H_5 d_5 + H_4 d_4 + H_3 d_3 + H_2 d_2 + H_1 d_1) \\ & + \frac{1}{2} (H_6 d_5 + H_5 d_4 + H_4 d_3 + H_3 d_2 + H_2 d_1 + H_1 d_0) \frac{1}{z} \\ & + \frac{1}{2} (H_7 d_5 + H_6 d_4 + H_5 d_3 + H_4 d_2 + H_3 d_1 + H_2 d_0) \frac{1}{z^2} \\ & + \frac{1}{2} (H_8 d_5 + H_7 d_4 + H_6 d_3 + H_5 d_2 + H_4 d_1 + H_3 d_0) \frac{1}{z^3} \\ & + \frac{1}{2} (H_9 d_5 + H_8 d_4 + H_7 d_3 + H_6 d_2 + H_5 d_1 + H_4 d_0) \frac{1}{z^4} \\ & + \frac{1}{2} (H_{10} d_5 + H_9 d_4 + H_8 d_3 + H_7 d_2 + H_6 d_1 + H_5 d_0) \frac{1}{z^5} \\ & + \frac{1}{2} (H_{11} d_5 + H_{10} d_4 + H_9 d_3 + H_8 d_2 + H_7 d_1 + H_6 d_0) \frac{1}{z^6} \\ & + \frac{1}{2} (H_{12} d_5 + H_{11} d_4 + H_{10} d_3 + H_9 d_2 + H_8 d_1 + H_7 d_0) \frac{1}{z^7}. \end{aligned} \tag{2.27}$$

We know  $\psi_2(z) = \overline{\phi_2}(z) - z\phi_2'(z) - \overline{X}(z)$ ,



$$\begin{aligned}
\overline{\phi}_2(z) = & \frac{\overline{c}_5}{2} z^5 + \frac{1}{2} (\overline{c}_4 + H_1 \overline{d}_5) z^4 + \frac{1}{2} (\overline{c}_3 + H_2 \overline{d}_5 + H_1 \overline{d}_4) z^3 \\
& + \frac{1}{2} (\overline{c}_2 + H_3 \overline{d}_5 + H_2 \overline{d}_4 + H_1 \overline{d}_3) z^2 + \frac{1}{2} (\overline{c}_1 + H_4 \overline{d}_5 + H_3 \overline{d}_4 + H_2 \overline{d}_3 + H_1 \overline{d}_2) z \\
& + \frac{1}{2} (\overline{c}_0 + H_5 \overline{d}_5 + H_4 \overline{d}_4 + H_3 \overline{d}_3 + H_2 \overline{d}_2 + H_1 \overline{d}_1) \\
& + \frac{1}{2} (H_6 \overline{d}_5 + H_5 \overline{d}_4 + H_4 \overline{d}_3 + H_3 \overline{d}_2 + H_2 \overline{d}_1 + H_1 d_0) \frac{1}{z} \\
& + \frac{1}{2} (H_7 \overline{d}_5 + H_6 \overline{d}_4 + H_5 \overline{d}_3 + H_4 \overline{d}_2 + H_3 \overline{d}_1 + H_2 d_0) \frac{1}{z^2} \\
& + \frac{1}{2} (H_8 \overline{d}_5 + H_7 \overline{d}_4 + H_6 \overline{d}_3 + H_5 \overline{d}_2 + H_4 \overline{d}_1 + H_3 d_0) \frac{1}{z^3} \\
& + \frac{1}{2} (H_9 \overline{d}_5 + H_8 \overline{d}_4 + H_7 \overline{d}_3 + H_6 \overline{d}_2 + H_5 \overline{d}_1 + H_4 d_0) \frac{1}{z^4} \\
& + \frac{1}{2} (H_{10} \overline{d}_5 + H_9 \overline{d}_4 + H_8 \overline{d}_3 + H_7 \overline{d}_2 + H_6 \overline{d}_1 + H_5 d_0) \frac{1}{z^5} \\
& + \frac{1}{2} (H_{11} \overline{d}_5 + H_{10} \overline{d}_4 + H_9 \overline{d}_3 + H_8 \overline{d}_2 + H_7 \overline{d}_1 + H_6 d_0) \frac{1}{z^6} \\
& + \frac{1}{2} (H_{12} \overline{d}_5 + H_{11} \overline{d}_4 + H_{10} \overline{d}_3 + H_9 \overline{d}_2 + H_8 \overline{d}_1 + H_7 d_0) \frac{1}{z^7},
\end{aligned}$$



$$\begin{aligned}
\phi_2'(z) = & \frac{5c_5}{2}z^4 + 2(c_4 + H_1d_5)z^3 + \frac{3}{2}(c_3 + H_2d_5 + H_1d_4)z^2 \\
& + (c_2 + H_3d_5 + H_2d_4 + H_1d_3)z + \frac{1}{2}(c_1 + H_4d_5 + H_3d_4 + H_2d_3 + H_1d_2) \\
& - \frac{1}{2}(H_6d_5 + H_5d_4 + H_4d_3 + H_3d_2 + H_2d_1 + H_1d_0)\frac{1}{z^2} \\
& - (H_7d_5 + H_6d_4 + H_5d_3 + H_4d_2 + H_3d_1 + H_2d_0)\frac{1}{z^3} \\
& - \frac{3}{2}(H_8d_5 + H_7d_4 + H_6d_3 + H_5d_2 + H_4d_1 + H_3d_0)\frac{1}{z^4} \\
& - 2(H_9d_5 + H_8d_4 + H_7d_3 + H_6d_2 + H_5d_1 + H_4d_0)\frac{1}{z^5} \\
& - \frac{5}{2}(H_{10}d_5 + H_9d_4 + H_8d_3 + H_7d_2 + H_6d_1 + H_5d_0)\frac{1}{z^6} \\
& - 3(H_{11}d_5 + H_{10}d_4 + H_9d_3 + H_8d_2 + H_7d_1 + H_6d_0)\frac{1}{z^7} \\
& - \frac{7}{2}(H_{12}d_5 + H_{11}d_4 + H_{10}d_3 + H_9d_2 + H_8d_1 + H_7d_0)\frac{1}{z^8}.
\end{aligned}$$

Using the above expansion we can write,





$$\begin{aligned}
-z\phi'_2(z) = & -\frac{5c_5}{2}z^5 - 2(c_4 + H_1d_5)z^4 - \frac{3}{2}(c_3 + H_2d_5 + H_1d_4)z^3 \\
& - (c_2 + H_3d_5 + H_2d_4 + H_1d_3)z^2 - \frac{1}{2}(c_1 + H_4d_5 + H_3d_4 + H_2d_3 + H_1d_2)z \\
& + \frac{1}{2}(H_6d_5 + H_5d_4 + H_4d_3 + H_3d_2 + H_2d_1 + H_1d_0)\frac{1}{z} \\
& + (H_7d_5 + H_6d_4 + H_5d_3 + H_4d_2 + H_3d_1 + H_2d_0)\frac{1}{z^2} \\
& + \frac{3}{2}(H_8d_5 + H_7d_4 + H_6d_3 + H_5d_2 + H_4d_1 + H_3d_0)\frac{1}{z^3} \\
& + 2(H_9d_5 + H_8d_4 + H_7d_3 + H_6d_2 + H_5d_1 + H_4d_0)\frac{1}{z^4} \\
& + \frac{5}{2}(H_{10}d_5 + H_9d_4 + H_8d_3 + H_7d_2 + H_6d_1 + H_5d_0)\frac{1}{z^5} \\
& + 3(H_{11}d_5 + H_{10}d_4 + H_9d_3 + H_8d_2 + H_7d_1 + H_6d_0)\frac{1}{z^6} \\
& + \frac{7}{2}(H_{12}d_5 + H_{11}d_4 + H_{10}d_3 + H_9d_2 + H_8d_1 + H_7d_0)\frac{1}{z^7}, \\
-\overline{X}(z) = & c_0 - c_1z - c_2z^2 - c_3z^3 - c_4z^4 - c_5z^5 - \dots .
\end{aligned}$$

Substituting the above into  $\psi_2(z) = \overline{\phi_2}(z) - z\phi'_2(z) - \overline{X}(z)$ , we obtain,



$$\begin{aligned}
\psi_2 = & -\frac{1}{2}(\overline{c_5} + 5c_5)z^5 - \frac{1}{2}(\overline{c_4} - H_1\overline{d_5} + 4c_4 + 4H_1d_5)z^4 \\
& - \frac{1}{2}(\overline{c_3} - H_2\overline{d_5} - H_1\overline{d_4} + 3c_3 + 3H_2d_5 + 3H_1d_4)z^3 \\
& + \left( -\frac{\overline{c_2}}{2} + \frac{H_3\overline{d_5}}{2} + \frac{H_2\overline{d_4}}{2} + \frac{H_1\overline{d_3}}{2} - c_2 - H_3d_5 - H_2d_4 - H_1d_3 \right) z^2 \\
& + \left( -\frac{\overline{c_1}}{2} + \frac{H_4\overline{d_5}}{2} + \frac{H_3\overline{d_4}}{2} + \frac{H_2\overline{d_3}}{2} + \frac{H_1\overline{d_2}}{2} - \frac{c_1}{2} - \frac{H_4d_5}{2} - \frac{H_3d_4}{2} - \frac{H_2d_3}{2} - \frac{H_1d_2}{2} \right) z \\
& + \left( -\frac{c_0}{2} + \frac{H_5\overline{d_5}}{2} + \frac{H_4\overline{d_4}}{2} + \frac{H_3\overline{d_3}}{2} + \frac{H_2\overline{d_2}}{2} + \frac{H_1\overline{d_1}}{2} \right) \\
& + \left( \frac{H_6\overline{d_5}}{2} + \frac{H_5\overline{d_4}}{2} + \frac{H_4\overline{d_3}}{2} + \frac{H_3\overline{d_2}}{2} + \frac{H_2\overline{d_1}}{2} + \frac{H_1d_0}{2} + \frac{H_6d_5}{2} + \frac{H_5d_4}{2} + \frac{H_4d_3}{2} \right. \\
& \quad \left. + \frac{H_3d_2}{2} + \frac{H_2d_1}{2} + \frac{H_1d_0}{2} \right) \frac{1}{z} \\
& + \left( \frac{H_7\overline{d_5}}{2} + \frac{H_6\overline{d_4}}{2} + \frac{H_5\overline{d_3}}{2} + \frac{H_4\overline{d_2}}{2} + \frac{H_3\overline{d_1}}{2} + \frac{H_2d_0}{2} + H_7d_5 + H_6d_4 + H_5d_3 \right. \\
& \quad \left. + H_4d_2 + H_3d_1 + H_2d_0 \right) \frac{1}{z^2} \\
& + \left( \frac{H_8\overline{d_5}}{2} + \frac{H_7\overline{d_4}}{2} + \frac{H_6\overline{d_3}}{2} + \frac{H_5\overline{d_2}}{2} + \frac{H_4\overline{d_1}}{2} + \frac{H_3d_0}{2} + \frac{3H_8d_5}{2} + \frac{3H_7d_4}{2} + \frac{3H_6d_3}{2} \right. \\
& \quad \left. + \frac{3H_5d_2}{2} + \frac{3H_4d_1}{2} + \frac{3H_3d_0}{2} \right) \frac{1}{z^3}
\end{aligned}$$



$$\begin{aligned}
& + \left( \frac{H_9 \overline{d}_5}{2} + \frac{H_8 \overline{d}_4}{2} + \frac{H_7 \overline{d}_3}{2} + \frac{H_6 \overline{d}_2}{2} + \frac{H_5 \overline{d}_1}{2} + \frac{H_4 d_0}{2} + 2H_9 d_5 + 2H_8 d_4 + 2H_7 d_3 \right. \\
& \quad \left. + 2H_6 d_2 + 2H_5 d_1 + 2H_4 d_0 \right) \frac{1}{z^4} \\
& + \left( \frac{H_{10} \overline{d}_5}{2} + \frac{H_9 \overline{d}_4}{2} + \frac{H_8 \overline{d}_3}{2} + \frac{H_7 \overline{d}_2}{2} + \frac{H_6 \overline{d}_1}{2} + \frac{H_5 d_0}{2} + \frac{5H_{10} d_5}{2} + \frac{5H_9 d_4}{2} + \frac{5H_8 d_3}{2} \right. \\
& \quad \left. + \frac{5H_7 d_2}{2} + \frac{5H_6 d_1}{2} + \frac{5H_5 d_0}{2} \right) \frac{1}{z^5} \\
& + \left( \frac{H_{11} \overline{d}_5}{2} + \frac{H_{10} \overline{d}_4}{2} + \frac{H_9 \overline{d}_3}{2} + \frac{H_8 \overline{d}_2}{2} + \frac{H_7 \overline{d}_1}{2} + \frac{H_6 d_0}{2} + 3H_{11} d_5 + 3H_{10} d_4 + 3H_9 d_3 \right. \\
& \quad \left. + 3H_8 d_2 + 3H_7 d_1 + 3H_6 d_0 \right) \frac{1}{z^6} \\
& \hspace{15em} (2.28) \\
& + \left( \frac{H_{12} \overline{d}_5}{2} + \frac{H_{11} \overline{d}_4}{2} + \frac{H_{10} \overline{d}_3}{2} + \frac{H_9 \overline{d}_2}{2} + \frac{H_8 \overline{d}_1}{2} + \frac{H_7 d_0}{2} + \frac{7H_{12} d_5}{2} + \frac{7H_{11} d_4}{2} + \frac{7H_{10} d_3}{2} \right. \\
& \quad \left. + \frac{7H_9 d_2}{2} + \frac{7H_8 d_1}{2} + \frac{7H_7 d_0}{2} \right) \frac{1}{z^7}.
\end{aligned}$$



# APPENDIX B

## Continuation of detailed derivation of relevant equations

### 1. Equation (3.1)

$$\text{From (2.9) } \phi_1(z) = Az + \sum_{k=1}^{\infty} a_k z^{-k}, \quad \psi_1(z) = Bz + \sum_{k=1}^{\infty} b_k z^{-k}, \quad z \in S_1,$$

we can obtain the following,

$$\phi_1(z) = Az + \frac{a_1}{z} + \frac{a_2}{z^2} + \frac{a_3}{z^3} + \frac{a_4}{z^4} + \frac{a_5}{z^5},$$

$$\psi_1(z) = Bz + \frac{b_1}{z} + \frac{b_2}{z^2} + \frac{b_3}{z^3} + \frac{b_4}{z^4} + \frac{b_5}{z^5},$$

$$\phi_1'(z) = A - \frac{a_1}{z^2} - \frac{2a_2}{z^3} - \frac{3a_3}{z^4} - \frac{4a_4}{z^5} - \frac{5a_5}{z^6},$$

$$\phi_1'\left(\frac{R^2}{z}\right) = A - \frac{a_1 z^2}{R^4} - \frac{2a_2 z^3}{R^6} - \frac{3a_3 z^4}{R^8} - \frac{4a_4 z^5}{R^{10}} - \frac{5a_5 z^6}{R^{12}},$$

$$\overline{\phi_1'}\left(\frac{R^2}{z}\right) = A - \frac{\overline{a_1} z^2}{R^4} - \frac{2\overline{a_2} z^3}{R^6} - \frac{3\overline{a_3} z^4}{R^8} - \frac{4\overline{a_4} z^5}{R^{10}} - \frac{5\overline{a_5} z^6}{R^{12}},$$

$$-z\phi_1''(z) = -\frac{2a_1}{z^2} - \frac{6a_2}{z^3} - \frac{12a_3}{z^4} - \frac{20a_4}{z^5} - \frac{30a_5}{z^6},$$

$$\psi_1'(z) = B - \frac{b_1}{z^2} - \frac{2b_2}{z^3} - \frac{3b_3}{z^4} - \frac{4b_4}{z^5} - \frac{5b_5}{z^6},$$

and,

$$-\frac{z^2}{R^2} \psi_1'(z) = -\frac{Bz^2}{R^2} + \frac{b_1}{R^2} + \frac{2b_2}{R^2 z} + \frac{3b_3}{R^2 z^2} + \frac{4b_4}{R^2 z^3} + \frac{5b_5}{R^2 z^4}.$$

Hence, upon substitution the above into the left-hand-side of (2.4) we obtain,





$$\begin{aligned}
\phi_1'(z) + \overline{\phi_1'}\left(\frac{R^2}{z}\right) - z\phi_1''(z) - \frac{z^2}{R^2}\psi_1'(z) = & -\frac{5\overline{a_5}}{R^{12}}z^6 - \frac{4\overline{a_4}}{R^{10}}z^5 - \frac{3\overline{a_3}}{R^8}z^4 - \frac{2\overline{a_2}}{R^6}z^3 \\
& - \left(\frac{\overline{a_1}}{R^4} + \frac{B}{R^2}\right)z^2 + 2A + \frac{b_1}{R^2} + \frac{2b_2}{R^2}\frac{1}{z} + 3\left(\frac{b_3}{R^2} - a_1\right)\frac{1}{z^2} \quad (3.1) \\
& + 4\left(\frac{b_4}{R^2} - 2a_2\right)\frac{1}{z^3} + 5\left(\frac{b_5}{R^2} - 3a_3\right)\frac{1}{z^4} - 24a_4\frac{1}{z^5}.
\end{aligned}$$

## 2. Equation (3.2)

In order to derive (3.2) the following expansions were obtained:

$$\begin{aligned}
\overline{\phi_1'}\left(\frac{R^2}{z}\right) = & \frac{5}{2}R^8\overline{c_5}\frac{1}{z^4} + 2R^6(\overline{c_4} + H_1\overline{d_5})\frac{1}{z^3} + \frac{3R^4}{2}(\overline{c_3} + H_2\overline{d_5} + H_1\overline{d_4})\frac{1}{z^2} \\
& + R^2(\overline{c_2} + H_3\overline{d_5} + H_2\overline{d_4} + H_1\overline{d_3})\frac{1}{z} + \frac{1}{2}(\overline{c_1} + H_4\overline{d_5} + H_3\overline{d_4} + H_2\overline{d_3} + H_1\overline{d_2}) \\
& - \frac{1}{2R^4}(H_6\overline{d_5} + H_5\overline{d_4} + H_4\overline{d_3} + H_3\overline{d_2} + H_2\overline{d_1} + H_1d_0)z^2 \\
& - \frac{1}{R^6}(H_7\overline{d_5} + H_6\overline{d_4} + H_5\overline{d_3} + H_4\overline{d_2} + H_3\overline{d_1} + H_2d_0)z^3 \\
& - \frac{3}{2R^8}(H_8\overline{d_5} + H_7\overline{d_4} + H_6\overline{d_3} + H_5\overline{d_2} + H_4\overline{d_1} + H_3d_0)z^4 \\
& - \frac{2}{R^{10}}(H_9\overline{d_5} + H_8\overline{d_4} + H_7\overline{d_3} + H_6\overline{d_2} + H_5\overline{d_1} + H_4d_0)z^5 \\
& - \frac{5}{2R^{12}}(H_{10}d_5 + H_9d_4 + H_8d_3 + H_7d_2 + H_6d_1 + H_5d_0),
\end{aligned}$$



$$-z\phi''(z) = -10c_5z^4 - 6(c_4 + H_1d_5)z^3 - 3(c_3 + H_2d_5 + H_1d_4)z^2$$

$$-(c_2 + H_3d_5 + H_2d_4 + H_1d_3)z$$

$$-(H_6d_5 + H_5d_4 + H_4d_3 + H_3d_2 + H_2d_1 + H_1d_0)\frac{1}{z^2}$$

$$-3(H_7d_5 + H_6d_4 + H_5d_3 + H_4d_2 + H_3d_1 + H_2d_0)\frac{1}{z^3}$$

$$-6(H_8d_5 + H_7d_4 + H_6d_3 + H_5d_2 + H_4d_1 + H_3d_0)\frac{1}{z^4},$$

$$-\frac{z^2}{R^2}\psi_1'(z) = \frac{5}{2R^2}(\overline{c_5} + 5c_5)z^6 + \frac{2}{R^2}(\overline{c_4} - H_1\overline{d_5} + 4c_4 + 4H_1d_5)z^5$$

$$+ \frac{3}{2R^2}(\overline{c_3} - H_2\overline{d_5} - H_1\overline{d_4} + 3c_3 + 3H_2d_5 + 3H_1d_4)z^4$$

$$- \frac{2}{R^2} \left( -\frac{\overline{c_2}}{2} + \frac{H_3\overline{d_5}}{2} + \frac{H_2\overline{d_4}}{2} + \frac{H_1\overline{d_3}}{2} - c_2 - H_3d_5 - H_2d_4 - H_1d_3 \right) z^3$$

$$- \frac{1}{R^2} \left( \begin{array}{c} -\frac{\overline{c_1}}{2} + \frac{H_4\overline{d_5}}{2} + \frac{H_3\overline{d_4}}{2} + \frac{H_2\overline{d_3}}{2} + \frac{H_1\overline{d_2}}{2} \\ -\frac{c_1}{2} - \frac{H_4d_5}{2} - \frac{H_3d_4}{2} - \frac{H_2d_3}{2} - \frac{H_1d_2}{2} \end{array} \right) z^2$$

$$+ \frac{1}{R^2} \left( \begin{array}{c} \frac{H_6\overline{d_5}}{2} + \frac{H_5\overline{d_4}}{2} + \frac{H_4\overline{d_3}}{2} + \frac{H_3\overline{d_2}}{2} + \frac{H_2\overline{d_1}}{2} + \frac{H_1\overline{d_0}}{2} \\ \frac{H_6d_5}{2} + \frac{H_5d_4}{2} + \frac{H_4d_3}{2} + \frac{H_3d_2}{2} + \frac{H_2d_1}{2} + \frac{H_1d_0}{2} \end{array} \right)$$



$$\begin{aligned}
& + \frac{2}{R^2} \left( \frac{H_7 \overline{d_5}}{2} + \frac{H_6 \overline{d_4}}{2} + \frac{H_5 \overline{d_3}}{2} + \frac{H_4 \overline{d_2}}{2} + \frac{H_3 \overline{d_1}}{2} + \frac{H_2 \overline{d_0}}{2} \right) \frac{1}{z} \\
& + \frac{3}{R^2} \left( \frac{H_8 \overline{d_5}}{2} + \frac{H_7 \overline{d_4}}{2} + \frac{H_6 \overline{d_3}}{2} + \frac{H_5 \overline{d_2}}{2} + \frac{H_4 \overline{d_1}}{2} + \frac{H_3 \overline{d_0}}{2} \right) \frac{1}{z^2} \\
& + \frac{4}{R^2} \left( \frac{H_9 \overline{d_5}}{2} + \frac{H_8 \overline{d_4}}{2} + \frac{H_7 \overline{d_3}}{2} + \frac{H_6 \overline{d_2}}{2} + \frac{H_5 \overline{d_1}}{2} + \frac{H_4 \overline{d_0}}{2} \right) \frac{1}{z^3} \\
& + \frac{5}{R^2} \left( \frac{H_{10} \overline{d_5}}{2} + \frac{H_9 \overline{d_4}}{2} + \frac{H_8 \overline{d_3}}{2} + \frac{H_7 \overline{d_2}}{2} + \frac{H_6 \overline{d_1}}{2} + \frac{H_5 \overline{d_0}}{2} \right) \frac{1}{z^4},
\end{aligned}$$

$$\frac{zk_1}{\mu_1} \overline{\phi_1} \left( \frac{R^2}{z} \right) = \frac{Fk_1 A R^2}{\mu_1} + \frac{Fk_1 \overline{a_1}}{\mu_1 R^2} z^2 + \frac{Fk_1 \overline{a_2}}{\mu_1 R^4} z^3 + \frac{Fk_1 \overline{a_3}}{\mu_1 R^6} z^4 + \frac{Fk_1 \overline{a_4}}{\mu_1 R^8} z^5,$$

$$-\frac{R^2}{\mu_1} \phi_1'(z) = -\frac{F A R^2}{\mu_1} + \frac{F a_1 R^2}{\mu_1} \frac{1}{z^2} + \frac{2 F a_2 R^2}{\mu_1} \frac{1}{z^3} + \frac{3 F a_3 R^2}{\mu_1} \frac{1}{z^4} + \frac{4 F a_4 R^2}{\mu_1} \frac{1}{z^5},$$



$$-\frac{z}{\mu_1}\psi_1(z)=-\frac{FB}{\mu_1}z^2-\frac{Fb_1}{\mu_1}-\frac{Fb_2}{\mu_1}\frac{1}{z}-\frac{Fb_3}{\mu_1}\frac{1}{z^2}-\frac{Fb_4}{\mu_1}\frac{1}{z^3}-\frac{Fb_5}{\mu_1}\frac{1}{z^4},$$

$$\begin{aligned} -\frac{zk_2}{\mu_2}\overline{\phi_2}\left(\frac{R^2}{z}\right) &= -\frac{Fk_2R^{10}\overline{c_5}}{2\mu_2}\frac{1}{z^4}-\frac{Fk_2R^8}{2\mu_2}\left(\overline{c_4}+H_1\overline{d_5}\right)\frac{1}{z^3} \\ &\quad -\frac{Fk_2R^6}{2\mu_2}\left(\overline{c_3}+H_2\overline{d_5}+H_1\overline{d_4}\right)\frac{1}{z^2}-\frac{Fk_2R^4}{2\mu_2}\left(\overline{c_2}+H_3\overline{d_5}+H_2\overline{d_4}+H_1\overline{d_3}\right)\frac{1}{z} \\ &\quad -\frac{Fk_2R^2}{2\mu_2}\left(\overline{c_1}+H_4\overline{d_5}+H_3\overline{d_4}+H_2\overline{d_3}+H_1\overline{d_2}\right) \\ &\quad -\frac{Fk_2}{2\mu_2}\left(\overline{c_0}+H_5\overline{d_5}+H_4\overline{d_4}+H_3\overline{d_3}+H_2\overline{d_2}+H_1\overline{d_1}\right)z \\ &\quad -\frac{Fk_2}{2\mu_2R^2}\left(H_6\overline{d_5}+H_5\overline{d_4}+H_4\overline{d_3}+H_3\overline{d_2}+H_2\overline{d_1}+H_1d_0\right)z^2 \\ &\quad -\frac{Fk_2}{2\mu_2R^4}\left(H_7\overline{d_5}+H_6\overline{d_4}+H_5\overline{d_3}+H_4\overline{d_2}+H_3\overline{d_1}+H_2d_0\right)z^3 \\ &\quad -\frac{Fk_2}{2\mu_2R^6}\left(H_8\overline{d_5}+H_7\overline{d_4}+H_6\overline{d_3}+H_5\overline{d_2}+H_4\overline{d_1}+H_3d_0\right)z^4, \end{aligned}$$





$$\begin{aligned}
\frac{R^2}{\mu_2} \phi'_2(z) = & \frac{5FR^2 c_5}{2\mu_2} z^4 + \frac{2FR^2}{\mu_2} (c_4 + H_1 d_5) z^3 + \frac{3FR^2}{2\mu_2} (c_3 + H_2 d_5 + H_1 d_4) z^2 \\
& + \frac{FR^2}{\mu_2} (c_2 + H_3 d_5 + H_2 d_4 + H_1 d_3) z + \frac{FR^2}{2\mu_2} (c_1 + H_4 d_5 + H_3 d_4 + H_2 d_3 + H_1 d_2) \\
& - \frac{FR^2}{2\mu_2} (H_6 d_5 + H_5 d_4 + H_4 d_3 + H_3 d_2 + H_2 d_1 + H_1 d_0) \frac{1}{z^2} \\
& - \frac{FR^2}{\mu_2} (H_7 d_5 + H_6 d_4 + H_5 d_3 + H_4 d_2 + H_3 d_1 + H_2 d_0) \frac{1}{z^3} \\
& - \frac{3FR^2}{2\mu_2} (H_8 d_5 + H_7 d_4 + H_6 d_3 + H_5 d_2 + H_4 d_1 + H_3 d_0) \frac{1}{z^4},
\end{aligned}$$

$$\begin{aligned}
\frac{z}{\mu_2} \psi_2(z) = & -\frac{F}{2\mu_2} \left( -\frac{\overline{c_3}}{2} - H_2 \overline{d_5} - H_1 \overline{d_4} + 3c_3 + 3H_2 d_5 + 3H_1 d_4 \right) z^4 \\
& + \frac{F}{\mu_2} \left( -\frac{\overline{c_2}}{2} + \frac{H_3 \overline{d_5}}{2} + \frac{H_2 \overline{d_4}}{2} + \frac{H_1 \overline{d_3}}{2} - \frac{c_2}{2} - H_3 d_5 - H_2 d_4 - H_1 d_3 \right) z^3 \\
& + \frac{F}{\mu_2} \left( -\frac{\overline{c_1}}{2} + \frac{H_4 \overline{d_5}}{2} + \frac{H_3 \overline{d_4}}{2} + \frac{H_2 \overline{d_3}}{2} + \frac{H_1 \overline{d_2}}{2} \right. \\
& \left. - \frac{c_1}{2} - \frac{H_4 d_5}{2} - \frac{H_3 d_4}{2} - \frac{H_2 d_3}{2} - \frac{H_1 d_2}{2} \right) z^2 \\
& + \frac{F}{\mu_2} \left( -\frac{\overline{c_0}}{2} + \frac{H_5 \overline{d_5}}{2} + \frac{H_4 \overline{d_4}}{2} + \frac{H_3 \overline{d_3}}{2} + \frac{H_2 \overline{d_2}}{2} + \frac{H_1 \overline{d_1}}{2} \right) z \\
& + \frac{F}{\mu_2} \left( \frac{H_6 \overline{d_5}}{2} + \frac{H_5 \overline{d_4}}{2} + \frac{H_4 \overline{d_3}}{2} + \frac{H_3 \overline{d_2}}{2} + \frac{H_2 \overline{d_1}}{2} + \frac{H_1 \overline{d_0}}{2} \right. \\
& \left. + \frac{H_6 d_5}{2} + \frac{H_5 d_4}{2} + \frac{H_4 d_3}{2} + \frac{H_3 d_2}{2} + \frac{H_2 d_1}{2} + \frac{H_1 d_0}{2} \right)
\end{aligned}$$



$$\begin{aligned}
& + \frac{F}{\mu_2} \left( \frac{H_7 \overline{d_5}}{2} + \frac{H_6 \overline{d_4}}{2} + \frac{H_5 \overline{d_3}}{2} + \frac{H_4 \overline{d_2}}{2} + \frac{H_3 \overline{d_1}}{2} + \frac{H_2 d_0}{2} \right. \\
& \quad \left. + H_7 d_5 + H_6 d_4 + H_5 d_3 + H_4 d_2 + H_3 d_1 + H_2 d_0 \right) \frac{1}{z} \\
& + \frac{F}{\mu_2} \left( \frac{H_8 \overline{d_5}}{2} + \frac{H_7 \overline{d_4}}{2} + \frac{H_6 \overline{d_3}}{2} + \frac{H_5 \overline{d_2}}{2} + \frac{H_4 \overline{d_1}}{2} + \frac{H_3 d_0}{2} \right. \\
& \quad \left. + \frac{3H_8 d_5}{2} + \frac{3H_7 d_4}{2} + \frac{3H_6 d_3}{2} + \frac{3H_5 d_2}{2} + \frac{3H_4 d_1}{2} + \frac{3H_3 d_0}{2} \right) \frac{1}{z^2} \\
& + \frac{F}{\mu_2} \left( \frac{H_9 \overline{d_5}}{2} + \frac{H_8 \overline{d_4}}{2} + \frac{H_7 \overline{d_3}}{2} + \frac{H_6 \overline{d_2}}{2} + \frac{H_5 \overline{d_1}}{2} + \frac{H_4 d_0}{2} \right. \\
& \quad \left. + 2H_9 d_5 + 2H_8 d_4 + 2H_7 d_3 + 2H_6 d_2 + 2H_5 d_1 + 2H_4 d_0 \right) \frac{1}{z^3} \\
& + \frac{F}{\mu_2} \left( \frac{H_{10} \overline{d_5}}{2} + \frac{H_9 \overline{d_4}}{2} + \frac{H_8 \overline{d_3}}{2} + \frac{H_7 \overline{d_2}}{2} + \frac{H_6 \overline{d_1}}{2} + \frac{H_5 d_0}{2} \right. \\
& \quad \left. + \frac{5H_{10} d_5}{2} + \frac{5H_9 d_4}{2} + \frac{5H_8 d_3}{2} + \frac{5H_7 d_2}{2} + \frac{5H_6 d_1}{2} + \frac{5H_5 d_0}{2} \right) \frac{1}{z^4},
\end{aligned}$$

$$\frac{k_1}{\mu_1 z} \phi_1(z) = \frac{Gk_1 A}{\mu_1} + \frac{Gk_1 a_1}{\mu_1} \frac{1}{z^2} + \frac{Gk_1 a_2}{\mu_1} \frac{1}{z^3} + \frac{Gk_1 a_3}{\mu_1} \frac{1}{z^4} + \frac{Gk_1 a_4}{\mu_1} \frac{1}{z^5},$$

$$-\frac{1}{\mu_1} \overline{\phi_1'} \left( \frac{R^2}{z} \right) = -\frac{GA}{\mu_1} + \frac{Ga_1}{\mu_1 R^4} z^2 + \frac{2Ga_2}{\mu_1 R^6} z^3 + \frac{3Ga_3}{\mu_1 R^8} z^4 + \frac{4Ga_4}{\mu_1 R^{10}} z^5,$$

$$-\frac{1}{\mu_1 z} \overline{\psi_1} \left( \frac{R^2}{z} \right) = -\frac{G\overline{B}R^2}{\mu_1} \frac{1}{z^2} - \frac{G\overline{b_1}}{\mu_1 R^2} - \frac{G\overline{b_2}}{\mu_1 R^4} z - \frac{G\overline{b_3}}{\mu_1 R^6} z^2 - \frac{G\overline{b_4}}{\mu_1 R^8} z^3 - \frac{G\overline{b_5}}{\mu_1 R^{10}} z^4,$$



$$\begin{aligned}
-\frac{k_2}{\mu_2 z} \phi_2(z) = & -\frac{Gk_2 c_5}{2\mu_2} z^3 - \frac{Gk_2}{2\mu_2} (c_3 + H_1 d_5) z^3 - \frac{Gk_2}{2\mu_2} (c_3 + H_2 d_5 + H_1 d_4) z^2 \\
& - \frac{Gk_2}{2\mu_2} (c_2 + H_3 d_5 + H_2 d_4 + H_1 d_3) z \\
& - \frac{Gk_2}{2\mu_2} (c_1 + H_4 d_5 + H_3 d_4 + H_2 d_3 + H_1 d_2) \\
& - \frac{Gk_2}{2\mu_2} (c_0 + H_5 d_5 + H_4 d_4 + H_3 d_3 + H_2 d_2 + H_1 d_1) \frac{1}{z} \\
& - \frac{Gk_2}{2\mu_2} (H_6 d_5 + H_5 d_4 + H_4 d_3 + H_3 d_2 + H_2 d_1 + H_1 d_0) \frac{1}{z^2} \\
& - \frac{Gk_2}{2\mu_2} (H_7 d_5 + H_6 d_4 + H_5 d_3 + H_4 d_2 + H_3 d_1 + H_2 d_0) \frac{1}{z^3} \\
& - \frac{Gk_2}{2\mu_2} (H_8 d_5 + H_7 d_4 + H_6 d_3 + H_5 d_2 + H_4 d_1 + H_3 d_0) \frac{1}{z^4},
\end{aligned}$$



$$\begin{aligned}
\frac{1}{\mu_2} \overline{\phi_2'} \left( \frac{R^2}{z} \right) &= \frac{5GR^8 \overline{c_5}}{2\mu_2} \frac{1}{z^4} + \frac{2GR^6}{\mu_2} (\overline{c_4} + H_1 \overline{d_5}) \frac{1}{z^3} + \frac{3GR^4}{2\mu_2} (\overline{c_3} + H_2 \overline{d_5} + H_1 \overline{d_4}) \frac{1}{z^2} \\
&+ \frac{GR^2}{\mu_2} (\overline{c_2} + H_3 \overline{d_5} + H_2 \overline{d_4} + H_1 \overline{d_3}) \frac{1}{z} \\
&+ \frac{G}{2\mu_2} (\overline{c_1} + H_4 \overline{d_5} + H_3 \overline{d_4} + H_2 \overline{d_3} + H_1 \overline{d_2}) \\
&- \frac{G}{2\mu_2 R^4} (H_6 \overline{d_5} + H_5 \overline{d_4} + H_4 \overline{d_3} + H_3 \overline{d_2} + H_2 \overline{d_1} + H_1 d_0) z^2 \\
&- \frac{G}{\mu_2 R^6} (H_7 \overline{d_5} + H_6 \overline{d_4} + H_5 \overline{d_3} + H_4 \overline{d_2} + H_3 \overline{d_1} + H_2 d_0) z^3 \\
&- \frac{3G}{2\mu_2 R^8} (H_8 \overline{d_5} + H_7 \overline{d_4} + H_6 \overline{d_3} + H_5 \overline{d_2} + H_4 \overline{d_1} + H_3 d_0) z^4,
\end{aligned}$$

and





$$\begin{aligned}
\frac{1}{\mu_2 z} \overline{\psi}_2 \left( \frac{R^2}{z} \right) = & -\frac{GR^6}{2\mu_2} \left( c_3 - H_2 d_5 - H_1 d_4 + 3\overline{c}_3 + 3H_2 \overline{d}_5 + 3H_1 \overline{d}_4 \right) \frac{1}{z^4} \\
& + \frac{GR^4}{\mu_2} \left( \begin{array}{c} -\frac{c_2}{2} + \frac{H_3 d_5}{2} + \frac{H_2 d_4}{2} + \frac{H_1 d_3}{2} \\ -\overline{c}_2 - H_3 \overline{d}_5 - H_2 \overline{d}_4 - H_1 \overline{d}_3 \end{array} \right) \frac{1}{z^3} \\
& + \frac{GR^2}{\mu_2} \left( \begin{array}{c} -\frac{c_1}{2} + \frac{H_4 d_5}{2} + \frac{H_3 d_4}{2} + \frac{H_2 d_3}{2} + \frac{H_1 d_2}{2} \\ -\frac{\overline{c}_1}{2} - \frac{H_4 \overline{d}_5}{2} - \frac{H_3 \overline{d}_4}{2} - \frac{H_2 \overline{d}_3}{2} - \frac{H_1 \overline{d}_2}{2} \end{array} \right) \frac{1}{z^2} \\
& + \frac{G}{\mu_2} \left( -\frac{c_0}{2} + \frac{H_5 d_5}{2} + \frac{H_4 d_4}{2} + \frac{H_3 d_3}{2} + \frac{H_2 d_2}{2} + \frac{H_1 d_1}{2} \right) \frac{1}{z} \\
& + \frac{G}{\mu_2 R^2} \left( \begin{array}{c} \frac{H_6 d_5}{2} + \frac{H_5 d_4}{2} + \frac{H_4 d_3}{2} + \frac{H_3 d_2}{2} + \frac{H_2 d_1}{2} + \frac{H_1 d_0}{2} \\ + \frac{H_6 \overline{d}_5}{2} + \frac{H_5 \overline{d}_4}{2} + \frac{H_4 \overline{d}_3}{2} + \frac{H_3 \overline{d}_2}{2} + \frac{H_2 \overline{d}_1}{2} + \frac{H_1 d_0}{2} \end{array} \right) \\
& + \frac{G}{\mu_2 R^4} \left( \begin{array}{c} \frac{H_7 d_5}{2} + \frac{H_6 d_4}{2} + \frac{H_5 d_3}{2} + \frac{H_4 d_2}{2} + \frac{H_3 d_1}{2} + \frac{H_2 d_0}{2} \\ H_7 \overline{d}_5 + H_6 \overline{d}_4 + H_5 \overline{d}_3 + H_4 \overline{d}_2 + H_3 \overline{d}_1 + H_2 d_0 \end{array} \right) z \\
& + \frac{G}{\mu_2 R^6} \left( \begin{array}{c} \frac{H_8 d_5}{2} + \frac{H_7 d_4}{2} + \frac{H_6 d_3}{2} + \frac{H_5 d_2}{2} + \frac{H_4 d_1}{2} + \frac{H_3 d_0}{2} \\ \frac{3H_8 \overline{d}_5}{2} + \frac{3H_7 \overline{d}_4}{2} + \frac{3H_6 \overline{d}_3}{2} + \frac{3H_5 \overline{d}_2}{2} + \frac{3H_4 \overline{d}_1}{2} + \frac{3H_3 d_0}{2} + \end{array} \right) z^2
\end{aligned}$$



$$\begin{aligned}
& + \frac{G}{\mu_2 R^8} \left( \frac{H_9 d_5}{2} + \frac{H_8 d_4}{2} + \frac{H_7 d_3}{2} + \frac{H_6 d_2}{2} + \frac{H_5 d_1}{2} + \frac{H_4 d_0}{2} \right. \\
& \quad \left. 2H_9 \overline{d_5} + 2H_8 \overline{d_4} + 2H_7 \overline{d_3} + 2H_6 \overline{d_2} + 2H_5 \overline{d_1} + 2H_4 d_0 \right) z^3 \\
& + \frac{G}{\mu_2 R^{10}} \left( \frac{H_{10} d_5}{2} + \frac{H_9 d_4}{2} + \frac{H_8 d_3}{2} + \frac{H_7 d_2}{2} + \frac{H_6 d_1}{2} + \frac{H_5 d_0}{2} \right. \\
& \quad \left. \frac{5H_{10} \overline{d_5}}{2} + \frac{5H_9 \overline{d_4}}{2} + \frac{5H_8 \overline{d_3}}{2} + \frac{5H_7 \overline{d_2}}{2} + \frac{5H_6 \overline{d_1}}{2} + \frac{5H_5 d_0}{2} + \right) z^4 .
\end{aligned}$$



# Appendix C

## **Determination of unknown coefficients**



a = R/4      b = 3R/4      m = n      shear modulus ratio = 0.5      Thermal load

	M = 0.01	M = 0.1	M = 1	M = 10	M = 100	M = 1000	M = 10000	M=Infinity
a1	0.0000	0.0024	0.00857	0.03499	0.04348	0.04450	0.04460	0.04461
a2	0.0000	0.00006	0.00287	0.01605	0.02152	0.02222	0.02229	0.02230
a3	0.0000	0.00002	0.00114	0.00787	0.01131	0.01178	0.01183	0.01183
b1	-0.00995	-0.09499	-0.65524	-1.60248	-1.87463	-1.90706	-1.91036	-1.91073
b2	0.0000	0.00019	0.00793	0.03984	0.05185	0.05333	0.05349	0.05350
b3	0.0000	0.00024	0.00884	0.03655	0.04557	0.04666	0.04677	0.04678
b4	0.0000	0.00011	0.00490	0.02608	0.03423	0.03524	0.03534	0.03535
b5	0.0000	0.00006	0.00273	0.01745	0.02428	0.02516	0.02525	0.02526
c0	-0.00224	-0.02100	-0.13017	-0.27207	-0.30534	-0.30912	-0.30950	-0.30954
c1	0.00014	0.00116	0.00134	-0.00949	-0.01328	-0.01373	-0.01378	-0.01379
c2	0.00056	0.00499	0.02045	-0.00214	-0.01979	-0.02224	-0.02250	-0.02253
c3	0.00033	0.00305	0.01526	0.00393	-0.01175	-0.01419	-0.01444	-0.01447
c4	0.00009	0.00086	0.00416	0.00119	-0.00248	-0.00303	-0.00309	-0.00309
c5	0.00010	0.00095	0.00494	0.00195	-0.00304	-0.00383	-0.00391	-0.00392
d0	-0.00208	-0.01979	-0.13191	-0.30808	-0.35599	-0.36161	-0.36219	-0.36225
d1	0.01088	0.10336	0.69466	1.64359	1.90645	1.93748	1.94064	1.94099
d2	-0.00989	-0.09460	-0.65944	-1.64660	-1.93814	-1.97313	-1.97670	-1.97709
d3	-0.00093	-0.00825	-0.03084	0.00680	0.02949	0.03242	0.03272	0.03275
d4	-0.00036	-0.00329	-0.01627	-0.00403	0.01236	0.01490	0.01517	0.01519
Y(a)	0.0000	0.0000	0.0000	0.0000	0.0000	0.0000	0.0000	0.0000
Y(b)	0.0000	0.00001	0.00006	0.00002	-0.00005	-0.00006	-0.00006	-0.00006
[a]	0.00573	0.05431	0.35814	0.82132	0.94368	0.95792	0.95937	0.95953
[b]	-0.00614	-0.05801	-0.37399	-0.82163	-0.93013	-0.94237	-0.94361	-0.94375
$-K_f(a)$								
$\mu_1 \varepsilon_1$	0.00573	0.05431	0.35814	0.82132	0.94368	0.95792	0.95937	0.95953
$-K_f(b)$								
$\mu_1 \varepsilon_1$	0.00614	0.05801	0.37399	0.82163	0.93013	0.94237	0.94361	0.94375





$a = 0$	$b = R/2$	$m = 3n$	shear modulus ratio = 10	Thermal load		
	$L = 0.01$	$L = 1$	$L = 10$	$L = 100$	$L = 10000$	$L = \text{Infinity}$
a1	0.00000	0.00015	0.00015	0.00015	0.00015	0.00015
a2	0.00000	0.00004	0.00004	0.00004	0.00004	0.00004
a3	0.00000	0.00001	0.00001	0.00001	0.00001	0.00001
b1	-0.00863	-0.05943	-0.06279	-0.06314	-0.06318	-0.06318
b2	0.00000	0.00016	0.00020	0.00020	0.00020	0.00020
b3	0.00000	0.00001	-0.00003	-0.00003	-0.00003	-0.00003
b4	0.00000	0.00001	-0.00002	-0.00002	-0.00002	-0.00002
b5	0.00000	0.00001	-0.00001	-0.00001	-0.00001	-0.00001
c0	-0.00084	-0.00609	-0.00651	-0.00655	-0.00656	-0.00656
c1	0.00045	0.00256	0.00260	0.00260	0.00260	0.00260
c2	0.00037	0.00204	0.00203	0.00202	0.00202	0.00202
c3	-0.00006	-0.00032	-0.00034	-0.00034	-0.00034	-0.00034
c4	0.00011	0.00061	0.00059	0.00059	0.00059	0.00059
c5	0.00005	0.00029	0.00028	0.00028	0.00028	0.00028
d0	0.00000	0.00000	0.00000	0.00000	0.00000	0.00000
d1	0.00475	0.03235	0.03411	0.03429	0.03431	0.03431
d2	-0.00925	-0.06326	-0.06677	-0.06714	-0.06718	-0.06718
d3	-0.00066	-0.00362	-0.00361	-0.00361	-0.00360	-0.00360
d4	0.00027	0.00145	0.00145	0.00145	0.00145	0.00145
Y(a)	0.00000	0.00000	0.00000	0.00000	0.00000	0.00000
Y(b)	0.00000	0.00000	0.00000	0.00000	0.00000	0.00000
[a]	0.00475	0.03235	0.03411	0.03429	0.03431	0.03431
[b]	-0.00485	-0.03290	-0.03465	-0.03483	-0.03485	-0.03485
$-K_1(a)$						
$\mu_1 \varepsilon_1$	0.00475	0.03235	0.03411	0.03429	0.03431	0.03431
$-K_1(b)$						
$\mu_1 \varepsilon_1$	0.00485	0.03290	0.03465	0.03483	0.03485	0.03485



$a = R/4$        $b = 3R/4$        $m = n$       shear modulus ratio =1      Uniaxial tensile load

	<b>M = 0.01</b>	<b>M = 0.1</b>	<b>M = 1</b>	<b>M = 10</b>	<b>M = 100</b>	<b>M = 1000</b>	<b>M = 10000</b>	<b>M=Infinity</b>
<b>a1</b>	-0.98523	-0.87005	-0.41067	-0.08976	-0.03743	-0.03186	-0.03130	-0.03124
<b>a2</b>	0.00000	-0.00013	-0.00382	-0.01285	-0.01531	-0.01560	-0.01563	-0.01563
<b>a3</b>	0.00000	-0.00005	-0.00158	-0.00645	-0.00808	-0.00828	-0.00830	-0.00830
<b>b1</b>	-0.99256	-0.93075	-0.58668	-0.16898	-0.07440	-0.06372	-0.06263	-0.06251
<b>b2</b>	0.00000	-0.00039	-0.01147	-0.03853	-0.04593	-0.04679	-0.04687	-0.04688
<b>b3</b>	-0.98523	-0.87006	-0.41107	-0.09132	-0.03934	-0.03382	-0.03326	-0.03320
<b>b4</b>	0.00000	-0.00022	-0.00641	-0.01978	-0.02284	-0.02316	-0.02320	-0.02320
<b>b5</b>	0.00000	-0.00012	-0.00370	-0.01338	-0.01592	-0.01619	-0.01622	-0.01622
<b>c0</b>	0.00500	0.04415	0.20349	0.31440	0.33138	0.33314	0.33332	0.33334
<b>c1</b>	-0.01510	-0.13289	-0.60468	-0.93838	-0.99347	-0.99934	-0.99993	-1.00000
<b>c2</b>	-0.00124	-0.01049	-0.03359	-0.01314	-0.00163	-0.00015	0.00000	0.00001
<b>c3</b>	-0.00074	-0.00642	-0.02424	-0.01251	-0.00170	-0.00018	-0.00002	0.00000
<b>c4</b>	-0.00021	-0.00180	-0.00660	-0.00314	-0.00040	-0.00003	0.00001	0.00001
<b>c5</b>	-0.00023	-0.00199	-0.00778	-0.00424	-0.00059	-0.00006	-0.00001	0.00000
<b>d0</b>	0.00466	0.04160	0.20492	0.34556	0.37182	0.37468	0.37497	0.37500
<b>d1</b>	-0.02429	-0.21732	-1.07848	-1.83735	-1.98234	-1.99821	-1.99981	-1.99999
<b>d2</b>	0.02210	0.19889	1.02068	1.81545	1.97962	1.99793	1.99978	1.99999
<b>d3</b>	0.00208	0.01736	0.05124	0.01686	0.00198	0.00020	0.00002	0.00000
<b>d4</b>	0.00080	0.00692	0.02586	0.01313	0.00178	0.00018	0.00002	0.00000
<b>Y(a)</b>	0.00000	0.00000	0.00000	0.00000	0.00000	0.00000	0.00000	0.00000
<b>Y(b)</b>	0.00000	-0.00003	-0.00010	-0.00005	-0.00001	0.00000	0.00000	0.00000
<b>[a]</b>	-0.01280	-0.11419	-0.55691	-0.92565	-0.99205	-0.99919	-0.99991	-0.99999
<b>[b]</b>	0.01372	0.12199	0.58266	0.93643	0.99344	0.99934	0.99993	0.99999
$\frac{K_I(a)}{\sigma^*}$	0.02560	0.22837	1.11383	1.85129	1.98410	1.99839	1.99983	1.99999
$\frac{K_I(b)}{\sigma^*}$	0.02744	0.24397	1.16531	1.87285	1.98687	1.99867	1.99985	1.99998

















University of Alberta Library



0 1620 1264 7556

**B45425**